UNIVERSITY OF OKLAHOMA

GRADUATE COLLEGE

MODELING RATES AND ENERGETICS OF ANAEROBIC HYDROCARBON BIODEGRADATION

A DISSERTATION

SUBMITTED TO THE GRADUATE FACULTY

in partial fulfillment of the requirements for the

Degree of

DOCTOR OF PHILOSOPHY

By

KEISHA KOHLER BEASLEY
Norman, Oklahoma
2012

MODELING RATES AND ENERGETICS OF ANAEROBIC HYDROCARBON BIODEGRADATION

A DISSERTATION APPROVED FOR THE
SCHOOL OF CIVIL ENGINEERING AND ENVIRONMENTAL SCIENCE

BY

_____
Dr. Mark A. Nanny, Chair

_____
Dr. Elizabeth C. Butler

_____
Dr. Kathleen E. Duncan

_____
Dr. David A. Sabatini

_____
Dr. Joseph M. Suflita

Acknowledgements

I would like to thank my research advisor Dr. Mark Nanny for his support and guidance throughout my doctoral program at the University of Oklahoma. In addition I would like to thank the members of my doctoral committee: Dr. Elizabeth Butler, Dr. Kathleen Duncan, Dr. David Sabatini, and Dr. Joseph Suflita, for serving on my committee and providing thoughtful advice. I am also thankful for to the University of Oklahoma and the financial support that was provided by a Department of Education Graduate Assistance in Areas of National Need Fellowship (Award No. P200A030155) through the School of Civil Engineering and Environmental Science.

A considerable amount of my laboratory work was conducted in Dr. Joseph Suflita's Lab. I am grateful to Dr. Suflita for the opportunity to train and work in his lab. In addition, I would like to thank Dr. Irene Davidova, Dr. Lisa Gieg, and Dr. Tori Parisi for teaching me so much about microbiology and for their friendship and support. I was also fortunate to be able to work with Dr. Roger Prince of ExxonMobil Biomedical Sciences Inc. and I thank him for offering his time and expertise.

Tutelage from many chemists was particularly critical to my completing my work in Computational Chemistry. Dr. James Kubicki, Dr. Ralph Wheeler, Dr. Scott Boesch, Dr. James Kubicki, and Dr. Paul Cook offered their time in discussing and teaching me topics in Computational and Biochemistry for which I am grateful.

Some of the computing for this project was performed at the OU Supercomputing Center for Education and Research (OSCER) at the University of Oklahoma. Dr. Henry Neeman, Brandon George, David Akin, Josh Alexander and Dr. Charles Rice were especially helpful in getting Computational Chemistry software running on the University of Oklahoma supercomputer.

The assistance I received in the writing of this dissertation was tremendous. I thank everyone who reviewed my draft documents and presentations, including Chris Nanny, Julianna Osuna, Sharin Wolfe, Moira Ozias, and Lindsey Allgood. I am also appreciative of the support offered by my graduate student writing group and the OU Writing Center.

Thank you to my family and friends for offering moral support, bringing food to my family, proof reading my dissertation, and doing anything they could think of to help. Specifically, I thank my mother, Suzanne, for traveling to be here with me and caring for my children. My husband, Will, I thank for his help with graphics, statistics, encouragement, patience and love. And, thank you to my children, Maya and William, for their presence and inspiration.

Table of Contents

List of Tables vi
List of Figures vi
Abstract ix

Chapter 1. Introduction
Background – General Information 1
Research Questions and Goals 18
Literature Cited 22

Chapter 2. Polarizability and Spin Density Correlate with the Relative Anaerobic Biodegradability of Alkylaromatic Hydrocarbons
Abstract 33
Introduction 34
Materials and Methods 38
Results 41
Discussion 44
Acknowledgements 49
Literature Cited 49

Chapter 3. A Potential Energy Surface for Anaerobic Oxidation of Methane via Fumarate Addition
Abstract 54
Introduction 55
Methods 61
Results 63
Discussion 69
Acknowledgements 75
Literature Cited 75

Chapter 4. The Application of Density Functional Theory (DFT) Calculations to Anaerobic Hydrocarbon Biodegradation Research: Suggestions for Future Research
Abstract 83
Introduction 83
Proposed Research 85
Proposed Methods 86
Significance 89
Literature Cited 91

Appendix A. Biodegradation Rate Determination by Direct Analysis of Sacrificed Microcosms
Abstract 94
Introduction 95
Materials and Methods 98
Results and Discussion 100

Literature Cited 109

Appendix B: Definitions of Computational Methods Used or Proposed for Use in this Dissertation
Summary 112
Literature Cited 114

Appendix C: A General Schematic and Details of Computational Chemistry Calculation Methods
Literature Cited 117

List of Tables

Chapter 1
Table 1.1 Pure and enrichment culture analyses in which fumarate addition metabolites were detected 15
Table 1.2 Field evidence of fumarate addition metabolites 17

Chapter 2
Table 2.1 Calculated Electronic Properties of the Seventeen Alkylbenzene Radical Intermediates and Their Corresponding Percent Biodegradation 42

Appendix B
Table B.1 Definitions of Computational Methods Used or Proposed for Use in this Dissertation 112

Appendix C
Table C.1 Strategy for locating transition state structures 115
Table C.2 Computational chemistry software and their uses 115
Table C.3 Specific details of how each calculation type was performed in this dissertation. Further information about options can be found in Foresman and Frisch, 1993 117

List of Figures

Chapter 1
Figure 1.1 U.S. primary energy consumption by fuel 1980-2035 (quadrillion Btu per year) (Source: Annual Energy Outlook 2012 Early Release Overview; U.S. Energy Information Administration, U.S. Department of Energy: Washington, D.C., January 23, 2012; page 7) 3
Figure 1.2 Primary Energy Consumption by Source and Sector, 2010 4
Figure 1.3 I. A glycyl radical (top) on a glycine residue in BSS abstracts a hydrogen atom from a cysteine residue (bottom) to form a thiyl radical. II. The thiyl radical then reacts with toluene and abstracts a hydrogen atom from the methyl substituent. III. The resulting benzyl radical reacts with fumarate to form a new C-C bond to form a benzylsuccinyl radical. IV. The hydrogen atom originally abstracted from the toluene molecule transfers from the cysteine residue to the benzylsuccinyl radical to form benzylsuccinate (Fuchs, G. et al. 2011; Beller, H. R. and

Spormann, A. M. 1998; Leutwein, C. and Heider, J. 1999; Krieger, C. J. et al 2001; Leuthner, B. et al. 1998) 10
Chapter 2
Scheme 2.1 Proposed Mechanism for Fumarate Addition to Toluene 39
Figure 2.1 Solubility plotted against the percent biodegradation observed by Prince and Suflita (2007) 42
Figure 2.2 Observed percent biodegradation versus predicted percent biodegradation of the 14 alkylbenzenes in the training data set and the predicted percent biodegradation of six alkylbenzenes in the test data set 44
Figure 2.3 Proposed effects of increased spin density on the energetics of fumarate addition 47
Chapter 3
Figure 3.1 Theoretical reactions: fumarate addition to methane based on the mechanism established for anaerobic biodegradation of larger alkane substrates (Suflita et al. 2004, Gieg and Suflita 2005, Thauer and Shima 2008, Callaghan et al. 2008). Methylthiol is used as the model enzyme active site 59
Figure 3.2 Conformations of fumarate and reaction intermediates defined 64
Figure 3.3 Potential energy surface for the radical addition of methane to fumarate-0,0 66
Figure 3.4 Potential energy surface for the radical addition of methane to three different conformations of fumarate 67
Figure 3.5 Geometries for TS1, TS2-0,0, and TS3-0,0. (Bond lengths are reported in Å.) 68
Appendix A
Figure A.1 Concentrations of sulfate (μM) over time in 40 mL VOA vial microcosms containing general SRB freshwater medium (± 0.25 μL gasoline) 101
Figure A.2 Concentrations of methane (μM) over time in 40 mL VOA vial microcosms containing Bushnell Haas medium and general SRB freshwater medium (± 0.25 μL gasoline) 102
Figure A.3 Amounts of conserved marker (1,1,3-trimethylcyclohexane) in the VOA vial microcosms for days 0, 14 and 24 103
Figure A.4 Relationship between amounts of the conserved marker and methylheptanes in the VOA vial microcosms for days 0, 14 and 24 (created by Roger Prince) 104
Figure A.5 Relationship between amounts of the conserved marker and tetramethylbenzenes in the VOA vial microcosms for days 0, 14 and 24 (created by Roger Prince) 105
Figure A.6 Percent sulfate in Ft. Lupton sediment microcosms (120 mL serum bottles) over time. Bottles were amended with 2 μL of the substrate shown. Values are averages of triplicate systems and are corrected for any sulfate loss in sterile controls 107
Figure A.7 Percent substrate in Ft. Lupton sediment microcosms (120 mL serum bottles) over time. Bottles were amended with 2 μL of the

substrate shown. Values are averages of triplicate systems and are corrected for any sulfate loss in sterile controls 108

Appendix C

Figure C.1 Flow chart of the optimization procedure for locating equilibrium geometries of minima and transition states, adapted from SHODOR resources 116

Abstract

Hydrocarbons are ubiquitous in the environment, originating from both natural and refined sources and are an important class of compounds because of their role in the world's energy requirements, their toxicity, and their direct impact on the chemistry of the troposphere. Anaerobic biodegradation has been shown to be a significant process by which hydrocarbons are attenuated in contaminated environments, geothermal seeps, and oil and gas reservoirs. However, there is a need for more information to answer questions about the microorganisms, the mechanisms, and the conditions involved in these metabolic conversions. The purpose of the work in this dissertation is to contribute to the knowledge gap in two ways: 1) by developing a model that predicts substrate loss rates, and 2) by modeling the energetics of a mechanism with broad applicability in anaerobic hydrocarbon biodegradation.

In the first study (Chapter 2), calculated chemical properties were used as tools in the prediction of rate data. Polarizability and spin density of metabolites were correlated with the extent of anaerobic biodegradation of alkylbenzenes to develop a model that estimates substrate loss rates. A strong correlation was discovered which suggested that the stability of the reaction intermediates affected the rate of biodegradation. The findings help form a basis for predicting relative rates and using theoretical chemistry to describe observed phenomena in real world systems. In the next study (Chapter 3), quantum chemical calculations were performed to model the energetics of a theoretical reaction of anaerobic oxidation of methane. The resulting potential energy surface for the initial reaction was created and the results suggested the reaction is exothermic (-11.2 kcal/mol) and that the addition of methane to fumarate is calculated to be the rate-limiting

step (25.0 kcal/mol). The relative inertness of methane makes it an ideal model substrate in defining the limits of energy barriers and minimal energy requirements for anaerobic metabolism.

The results in these studies provide information that advances our understanding of anaerobic hydrocarbon biodegradation. Ultimately, this information can be used to address questions about mechanism preferences, substrate preferences, biodegradation rates, and energy requirements for conversions in systems worldwide.

CHAPTER 1

Introduction

Background – General Information

Hydrocarbons: Chemistry, Occurrence and Significance. Hydrocarbons are compounds that contain only carbon and hydrogen atoms. Though they only contain two types of atoms, hydrocarbons vary greatly in size and shape. Because carbon atoms can bond to themselves and create strong single, double, or triple bonds, they can form chains thousands of atoms long. Hydrocarbons can be small and linear (e.g., methane), cyclic (e.g., cyclohexane), or create aromatic, conjugated π bond systems (e.g., benzene). Also, carbon atoms can form four bonds; therefore structures may be linear or branched (1). Carbon and hydrogen atoms can combine in so many permutations that there are millions of different hydrocarbon compounds that occur in natural environments and in manmade systems. Though the components are simple, the number of compounds and their variations in size, shape, orientation and mixtures are numerous.

Hydrocarbons exist naturally in gaseous, liquid (oil) and solid forms (2). Major natural sources of hydrocarbons include natural gas reservoirs, petroleum or crude oil reservoirs, tar sand bitumen, shale oil and bituminous coal (2). While the components of these naturally occurring petroleum sources vary and may contain compounds other than hydrocarbons, on average, hydrocarbons make up approximately 70% (by weight) of the material in these reservoirs (3).

Natural gas is composed mostly of methane, with some ethane, propane, and butane (4). In general, methane is the dominant constituent of natural gas, comprising 74-95% by volume (5). Natural gas reservoirs are formed over time as high temperatures

and pressure transform biological material (3) trapped thousands of feet underground and under bodies of water (2, 4). Natural gas may be found in association with oil or as a dry gas (4). Natural gasses are also released from ruminant animals and biological activity in wetlands and landfills (2, 6, 7).

Petroleum or crude oil reservoirs are another source of hydrocarbons. The composition of crude oil also varies, but the constituents that are typically highest in amount by percent weight are linear alkanes, cyclic alkanes and aromatic hydrocarbons such as alkylbenzenes (2). Tar sand bitumen, shale oil and bituminous coal are considered heavier oils, as they are denser, viscous and require more processing than the oils and gases (2). The hydrocarbon content of these heavy oils and solids are approximately 30-40% (2).

The processes by which these reservoirs are formed require a great deal of time. Therefore, hydrocarbons discussed thus far are considered finite resources. Though there are efforts made to find economical means of synthesizing these compounds (2, 8), the quantity and quality of these naturally occurring reservoirs are of great importance to our country and worldwide. Hydrocarbons are of major importance because they comprise the fossil fuels on which we are so dependent for our energy demands. Most are used as energy sources for transportation, electricity and heating (9). Hydrocarbons are also used in manufacturing processes for such material as plastics, cosmetics, and pharmaceuticals (2, 10). Figure 1.1 provides a picture of the US demands for fossil fuels over time and for years to come (9). Figure 1.2 shows the types and uses of fossil fuels and the relationships between the two (based on consumption in the US).

Once hydrocarbons are extracted from these natural sources they are processed, stored, and transported. The US alone has over 2.5 million miles of pipelines designated for the transport of petroleum oil and gas products (11). To get a sense of the amount of product transported in the pipelines every day, in 2010, approximately 22 trillion cubic feet a day of natural gas and 5.5 million barrels a day of crude oil were produced in the US (9).

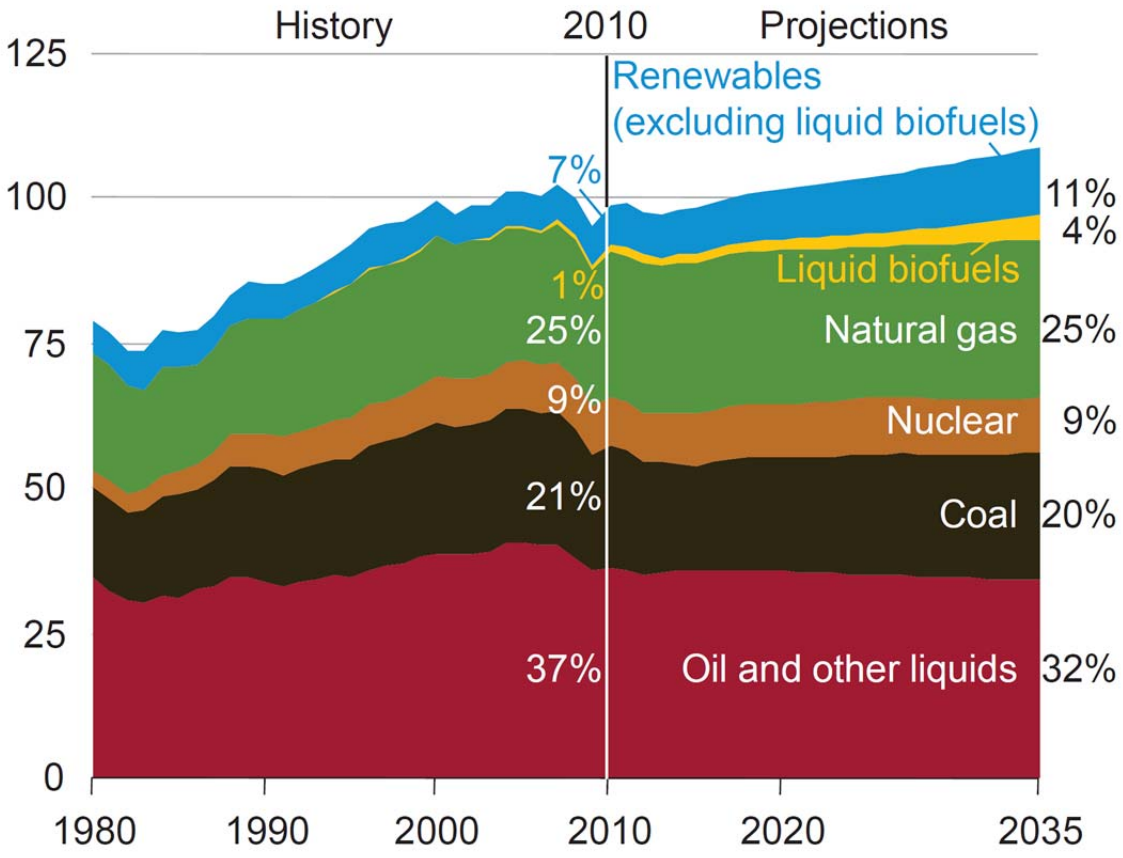

Figure 1.1 U.S. primary energy consumption by fuel 1980-2035 (quadrillion Btu per year) (Source: Annual Energy Outlook 2012 Early Release Overview; U.S. Energy Information Administration, U.S. Department of Energy: Washington, D.C., January 23, 2012; page 7)(9).

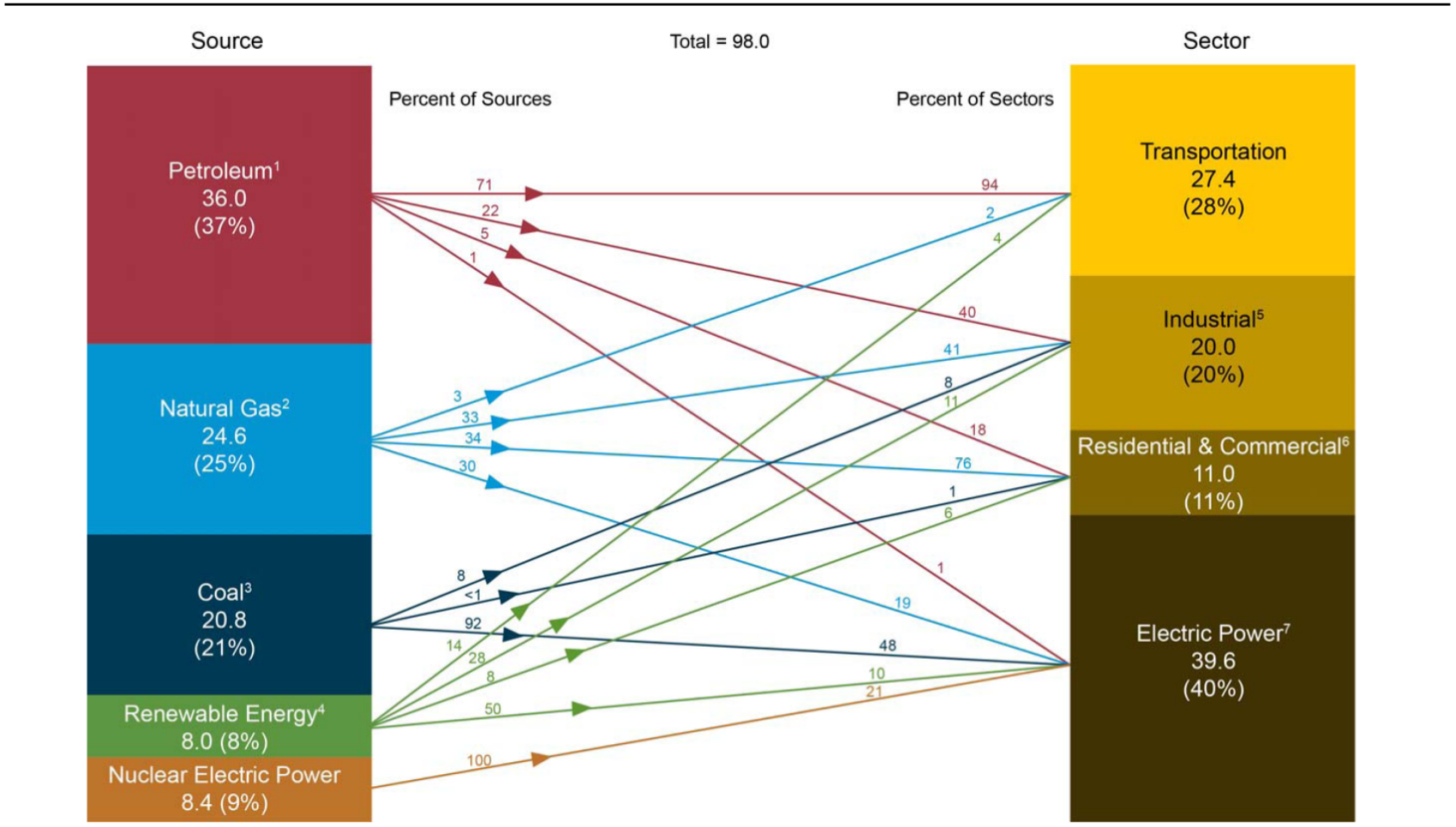

[1] Does not include biofuels that have been blended with petroleum—biofuels are included in "Renewable Energy."
[2] Excludes supplemental gaseous fuels.
[3] Includes less than 0.1 quadrillion Btu of coal coke net exports.
[4] Conventional hydroelectric power, geothermal, solar/PV, wind, and biomass.
[5] Includes industrial combined-heat-and-power (CHP) and industrial electricity-only plants.
[6] Includes commercial combined-heat-and-power (CHP) and commercial electricity-only plants.
[7] Electricity-only and combined-heat-and-power (CHP) plants whose primary business is to sell electricity, or electricity and heat, to the public. Includes 0.1 quadrillion Btu of electricity net imports not shown under "Source."

Notes: Primary energy in the form that it is first accounted for in a statistical energy balance, before any transformation to secondary or tertiary forms of energy (for example, coal is used to generate electricity). • Sum of components may not equal total due to independent rounding.

Sources: U.S. Energy Information Administration, *Annual Energy Review 2010*, Tables 1.3, 2.1b-2.1f , 10.3, and 10.4.

Figure 1.2 Primary Energy Consumption by Source and Sector, 2010. Sources and uses of fossil fuels and the relationships between the two (based on consumption in the US) are displayed. The lines connecting the various sources and demand types display the percentages of each source allocated to different uses on the left. On the right the percentages show the relative amount of each source type that supports that demand sector. This figure is based on data reported in the Annual Energy Review 2010 (US Department of Energy) and was published in that report as Figure 2.0 (page 37 of ref (21)).

Once they are used, either in combustion processes for energy or as material in synthesis processes, hydrocarbons may be re-released into the environment as by-products. Hydrocarbons are released into the environment through human activities such as spills and accidents, and disposal activities. In addition, natural oil seeps also release significant amounts of oil into marine environments (12). BTEX compounds (i.e., benzene, toluene, ethylbenzene, and xylenes) and many PAH compounds are on the EPAs list of priority pollutants (13). Acute responses to exposure to hydrocarbons such as BTEX compounds result in such symptoms as dermal and ocular irritation, nausea, vomiting, headache, dizziness, irritability, confusion, and weakness of extremities (14). Chronic exposure to these compounds leads to human health effects such as: increased risk of cancer, impaired kidney and liver function, and nervous system damage (15). The flammability of these compounds is also a major safety concern with respect to the release of these compounds into the environment (16). Once in the environment, hydrocarbons undergo transport processes such as sorption, evaporation, dispersion, and biodegradation (17). For these reasons, it is important to understand how these chemicals are moving and reacting in the environment.

Anaerobic Hydrocarbon Biodegradation. The topic of fate and transport of hydrocarbons in the environment is an important issue both because of the toxicity of the various compounds and because of the large amount of hydrocarbons in use as discussed in the previous paragraphs. However, it is also an important issue because of the effects that chemical transformations have on the value of hydrocarbons with respect to US and world fuel requirements. Microbial degradation has been shown to be an important process in determining both the fate of hydrocarbons in the environment and the quality

of crude oil and gas reserves. Microorganisms have been shown to use hydrocarbon compounds as sources of energy and to obtain components for cell growth (for an example see ref (18)). Most of the research supporting and studying this process focuses on hydrocarbon biodegradation in aerobic systems. Prior to the 1980s, it was generally considered that anaerobic hydrocarbon biodegradation (i.e., hydrocarbon biodegradation in the absence of molecular oxygen) was not possible. Since the environments in which hydrocarbons are typically found are often anoxic the study of anaerobic hydrocarbon biodegradation is an important piece of the picture in establishing what is happening to hydrocarbons in the environment, and at what rate (19, 20).

Some of the first definitive evidence of anaerobic hydrocarbon biodegradation was published in the 1980s (22, 23) (see ref (24) for a review). Correlations between substrate loss and carbon dioxide production were demonstrated in cultures under methanogenic conditions. These cultures produced $^{14}CO_2$ while maintained on ^{14}C-labeled toluene and benzene (22, 25). In another study, methanogenic cultures enriched from sewage sludge were incubated in ^{18}O-labeled water. In these cultures, the incorporation of ^{18}O in p-cresol and phenol (i.e., metabolites) occurred in incubations in which toluene and benzene were the sole carbon sources, respectively, demonstrating a source of oxygen atoms in metabolites other than molecular oxygen (23). These discoveries provided evidence that anaerobic hydrocarbon biodegradation may be responsible for conversions in natural environments that were not previously considered.

Since that time, anaerobic hydrocarbon biodegradation was established as an important field of research that has applications in many different disciplines. For example, research on oil and natural gas reservoirs demonstrated that microorganisms

degrade the hydrocarbons in the reservoirs and thus decrease their value as fuel sources (26). Characteristics of crude oil and natural gases that are more heavily biodegraded include loss of lighter hydrocarbons such as alkanes, BTEX aromatics (27), and alkylcyclohexanes (26). Other characteristics of heavily degraded oils include an increase in methane concentrations, viscosity and acidity and a decrease in API gravity ((26) and references therein).

Another example of the application of advances in anaerobic hydrocarbon biodegradation is in the field of remediation science. As more is understood about the mechanisms and rates of anaerobic biodegradation, the more useful the information is in the development of remediation technologies, with the goal of protecting human health and natural environments. Bioremediation can be used as a remediation option if it is known that microorganisms are intrinsically abating environmental contaminants, or can be induced to do so effectively. This is a valuable tool in hydrocarbon contamination mitigation (28-30).

Recent work proposed that biodegradation of hydrocarbons in pipelines and storage tanks stimulates metal corrosion. Corrosion of the pipelines and tanks then leads to loss of valuable product, contamination of natural environments, and potential exposure to humans via soils, water and air (31).

Anaerobic oxidation of methane (AOM) is a current topic of research and is thought to be a major process abating the release of methane into the atmosphere (7, 32, 33). Investigations of anaerobic biological biodegradation of methane contribute to our understanding of the biogeochemical cycles of methane (32). They are especially of interest as they relate to human activities and global climate change.

Mechanisms of Anaerobic Hydrocarbon Biodegradation. In the past few decades, a handful of reactions of anaerobic hydrocarbon biodegradation have been proposed based on results from studies using both pure and enrichment cultures (34-38). Evidence is based on using these incubations for the purposes of identifying metabolites, demonstrating substrate loss, measuring electron acceptor depletion, and the production of end products. In addition, isolating organisms capable of anaerobic hydrocarbon degradation, biochemical characterization of the enzymes involved, and genetic characterization of organisms has occurred (for a review see ref (38)).

Thus far, evidence of anaerobic biodegradation of alkylbenzenes, and alkanes (saturated and unsaturated) suggest two mechanisms by which initial activation occurs: fumarate addition and carboxylation (for reviews see references (28, 29, 39-44)). Additional reactions have been observed in investigations with toluene, ethylbenzene and non-substituted aromatic compounds as substrates. In the case of ethylbenzene, dehydrogenation (45-47), fumarate addition (48, 49), and carboxylation (46) have been shown to be potential reaction mechanisms (28). Ethylbenzene and propylbenzene have also demonstrated initial activation via hydroxylation of the ethyl and propyl side chains (34, 45, 47). For substrates without substituents such as benzene and naphthalene, metabolites have been observed that suggest such initial mechanisms as hydroxylation, carboxylation, and methylation followed by fumarate addition ((50) for reviews see references (37, 40, 51)). Once the original substrate has been transformed by one of these initial reactions they seem to be oxidized to a coenzyme A (CoA) derivative for further degradation via known pathways (34).

Because of the evidence discussed here suggesting its ubiquity and ability to

activate a variety of hydrocarbon substrates (see references above), the fumarate addition mechanism is the focus for the remainder of this chapter and the studies presented in Chapters 2 and 3. It should also be noted that the sediments studied in Appendix A are taken from a site on which fumarate addition has been established as a potential mechanism of biodegradation through metabolite analysis during onsite push-pull studies (48, 52), onsite push-pull studies using deuterated substrates (53), and in bench-scale microcosms developed with site sediments (48, 54, 55).

Fumarate Addition Reactions. The free radical addition of fumarate to substrates is an initial mechanism that some anaerobic microorganisms use to convert a variety of hydrocarbons into compounds that can subsequently be used as a source of energy or as building materials of cellular structure. The details of the proposed mechanism are presented in Figure 1.3 and are based on research carried out with microorganisms capable of utilization of toluene (56-59). Isolation of these microorganisms lead to the identification, biochemical, and molecular characterization of the enzyme involved: benzylsuccinate synthase (BSS) (60-62). Characterization of BSS revealed structural similarity to glycyl radical-containing enzymes such as pyruvate formate lyase (59-61). The involvement of these radicals in the fumarate addition mechanism is confirmed by a correlation between the radical appearance in EPR spectroscopy and BSS metabolic activity (59). Evidence of the radical mechanisms is also discussed in Chapter 2.

Hydrocarbon substrates that undergo this proposed transformation are initially converted into a radical by a hydrogen atom abstraction, after which the radical is added to the carbon-carbon double bond of fumarate (for a review see ref (29)). The resulting intermediate is a succinic acid derivative. The presence of these succinic acids is often

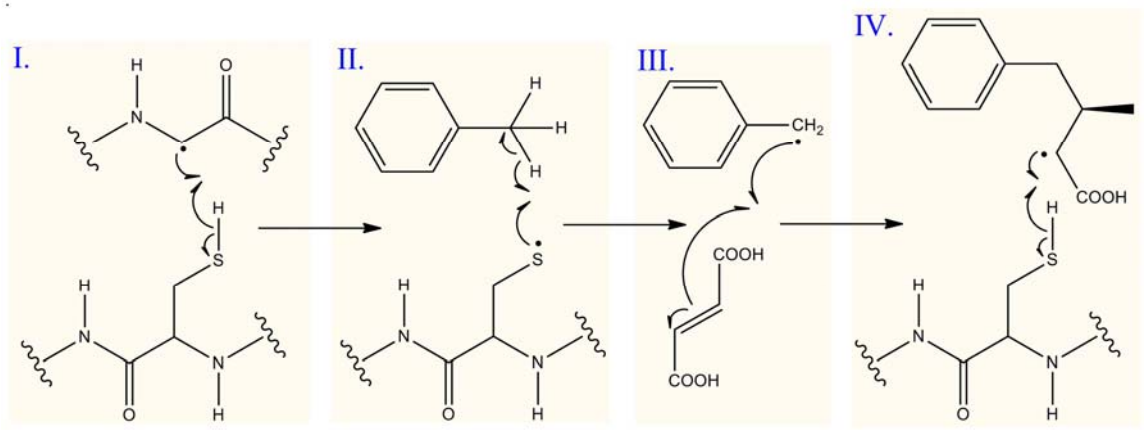

Figure 1.3 I. A glycyl radical (top) on a glycine residue in BSS abstracts a hydrogen atom from a cysteine residue (bottom) to form a thiyl radical. II. The thiyl radical then reacts with toluene and abstracts a hydrogen atom from the methyl substituent. III. The resulting benzyl radical reacts with fumarate to form a new C-C bond to form a benzylsuccinyl radical. IV. The hydrogen atom originally abstracted from the toluene molecule transfers from the cysteine residue to the benzylsuccinyl radical to form benzylsuccinate (34, 57-60).

used as one indicator of biological activity in systems containing hydrocarbons and as evidence that fumarate addition is the mechanism by which biodegradation is occurring (for a review see reference (44), examples include references (31, 53, 55, 63-66)). Fumarate addition to toluene has been studied in the greatest detail, and thus is often used to describe the mechanism (as shown in Figure 1.3).

Hydrocarbon substrates which have been shown to biodegrade by a fumarate addition mechanism include alkanes (saturated and unsaturated) (41, 42, 55, 67, 68), benzene, alkylbenzenes, and PAHs. The remainder of this section describes an overview of the work on alkylbenzene and alkane substrates, as they are the subjects of subsequent chapters.

Fumarate Addition Reactions with Alkylbenzenes. As stated earlier, anaerobic biodegradation of toluene has been studied to the greatest extent of all the alkylbenzene substrates; however, alkylbenzenes other than toluene have been shown to undergo the fumarate addition mechanism through evidence produced from pure culture studies (69-

71) and enrichment cultures (48, 72, 73).

Pure cultures demonstrated the ability of microorganisms to cometabolize substrates such as o-xylene (74); however, loss of m-xylene and o-xylene has been also observed under sulfate-reducing conditions in enrichment cultures independent of the presence of toluene (48, 72, 73). In addition, detection of corresponding succinic acids occurred in enrichment cultures and linked the addition of fumarate to biological loss of toluene, m-xylene, p-xylene, and ethylbenzene (48). Substrates were added to the sediment incubations and loss was correlated with sulfate depletion and methane production (48). Evidence of succinic acid metabolites in xylene biodegradation studies has been demonstrated under sulfate (48, 72, 75, 76), nitrate (77-79), and methanogenic conditions (80). p-Xylene has been shown to biodegrade in enrichment cultures, however more slowly than m- and o-xylene (48, 72, 78, 81-83), and has been degraded cometabolically in toluene-degrading cultures (84-87). It has been proposed that in some instances (e.g., the case of ethylbenzene as a substrate) fumarate addition may be the mechanism by which hydrocarbons are degraded in energy-limited environments by strict anaerobes, whereas a mechanism such as hydroxylation might be utilized by facultative anaerobes (43).

As mentioned previously, a number of studies have investigated toluene as a substrate that can undergo the fumarate addition mechanism (18, 88-90). Cell free extracts derived from the denitrifying bacterium *Thauera aromatic* suggested an initial reaction between toluene and fumarate to form benzylsuccinate as ($^2H_8$)-toluene was converted to ($^2H_7$)-benzylsuccinate (90). The reaction was independent of the presence of ATP and nitrate, but dependent on the presence of fumarate and inhibited by the

introduction of air (90). High-performance liquid chromatography analysis of benzylsuccinate suggests that this initial reaction is highly stereospecific, producing R-(+)-benzylsuccinic acid (57, 58). Evidence of fumarate addition to toluene has been shown in samples under sulfate-reducing conditions (45, 91), iron-reducing conditions (92), methanogenic conditions (93), and under anoxic conditions with phototrophic bacteria (94). Additional studies reporting the detection of benzylsuccinic acids in anaerobic toluene incubations have been summarized in previous reviews (43, 44, 95).

Fumarate Addition Reactions with Alkanes. The two major mechanisms of anaerobic alkane biodegradation identified thus far are fumarate addition and carboxylation (44, 96-98). Anaerobic biodegradation of alkanes via fumarate addition reactions has been demonstrated in a number of studies using pure cultures and consortia (for a review see reference (41)). The substrates in these studies range from C_3 to C_{18} alkanes. In addition, cycloalkanes have been biodegraded under anaerobic conditions. Methane and ethane have been shown to be oxidized under anaerobic conditions; however the mechanisms of biodegradation are not as clearly elucidated. Some proposed mechanisms of methane oxidation are intra-aerobic denitrification (99), acetogenesis, methylogenesis, and reverse methanogenesis (35, 36, 100). The evidence for these mechanisms and the potential of fumarate addition as a reaction are discussed in Chapter 3.

Bacterial strains capable of mineralizing alkanes under sulfate- and nitrate-reducing conditions have been isolated (73, 98, 101-104). With the exception of the sulfate-reducing *Desulfococcus oleovorans* Strain Hxd3 (96, 97), further analysis of these bacterial strains has demonstrated production of fumarate addition metabolites during growth on a variety of n-alkanes (64, 67, 96, 105-108). Incubation with *Desulfoglaeba*

alkanexedens (109) demonstrated degradation of ^{13}C-labeled n-hexane to hexylsuccinic acid by the addition of the fumarate to the subterminal carbon atom (i.e., C2 carbon of hexane) (108). Details of fumarate addition to hexane are discussed further in the following references: Wilkes et al. 2002 (110), Davidova et al. 2005 (108), and Suflita et al. 2004 (review (29)). Work with the denitrifying strain *Azoarcus sp.* HxN1, identified (1-methylpentyl)succinate in n-hexane amended incubations (106). Gas chromatography analysis of (1-methylpentyl)succinate showed the detection of two peaks with identical mass, suggesting the formation of diastereomers (106). In addition, electron paramagnetic resonance results suggested the involvement of a glycyl radical-containing enzyme in a mechanism analogous to toluene (106).

Analysis of alkylsuccinate synthase from *Desulfatibacillum alkenivorans* AK-01 identified two gene clusters that are similar to active genes of benzylsuccinate synthase (107). In addition, growth on hexadecane was correlated with the expression of one of these genes (assA1) (107). Characterization of (1-methylalkyl)succinate synthase protein subunits also suggested similarity to active subunits of benzylsuccinate synthase(111). Characterization of *Azoarcus sp.* HxN1 growth on n-hexane was purported to be activated by (1-methylalkyl)succinate synthase and yielded equal amounts of (2R,1′R)- and (2S,1′R)-(1-methylpentyl)succinate (112).

Mineralization has also been observed in incubations containing enrichment cultures (68, 79). A study performed with enrichment cultures and D_{26}-dodecane as the sole carbon source under sulfate-reducing conditions report the identification of n-dodecylsuccinic acid with all deuterium atoms retained, suggesting the addition of fumarate at the C-D bond (68). Analysis of the samples by gas chromatography resulted

in the detection of two peaks with identical mass suggesting formation of diastereomers in equal amounts (68).

Types of Environments Containing Fumarate Addition Metabolites. Fumarate addition is a mechanism by which a variety of hydrocarbons undergo anaerobic biodegradation and these reactions have been shown to be occurring in natural and manmade systems. Along with other evidence, the presence of succinic acids is widely considered an indicator of biological degradation of hydrocarbons (44). Therefore, their detection in a variety of anaerobic environments suggests that the mechanism is ubiquitous. Examples of environments in which potential metabolites of fumarate addition have been found are presented in Tables 1.1 and 1.2. Both field and laboratory evidence is listed. Additionally, the substrates and microorganisms responsible are listed where known.

Research Challenges and Knowledge Gaps. While there is a great deal of research occurring in the field of anaerobic hydrocarbon biodegradation, there are practical difficulties in studying the processes and, therefore, knowledge gaps exist in the scientific literature and the current understanding. Not all organisms performing the conversion have been isolated, identified and characterized. Likewise, not all evidence of metabolic conversions can be explained by known mechanisms of conversion. Even in cases where there is strong evidence for the mechanisms occurring, extrapolating that knowledge to predict preferences between substrates and mechanisms in more complex environmental systems remains difficult. The identification of metabolites is another challenge (e.g., see ref (65)). Challenges include: isolating and identifying metabolites, synthesizing

Table 1.1 Pure and enrichment culture analyses in which fumarate addition metabolites were detected.

Source Description	Substrate(s)	Electron Acceptors	Strain	Taxonomic Class	Reference
Anoxic lake sediments from the Bad Zwischenahner Meer in Germany	cyclohexane	nitrate	Strain/Consortium	Deltaproteobacteria	Musat et al. 2010 (113)
Ditch sediments from Bremen, Germany	C6 - C8 alkanes	nitrate, nitrite, nitrous oxide	Strain HxN1	Betaproteobacteria	Ehrenreich et al. 2000; Rabus et al. 2001 (103, 106)
Ditch sediments from Bremen, Germany	C8 - C12 alkanes	nitrate, nitrous oxide	Strain OcN1	Betaproteobacteria	Ehrenreich et al. 2000 (103)
Petroleum-contaminated estuarine sediments from New York	C13 - C18 alkanes	sulfate, thiosulfate and sulfite	Strain AK-01	Deltaproteobacteria	So and Young 1999 (114)
Hydrocarbon-polluted Mediterranean marine sediments in France	C13 - C18 alkanes	sulfate, thiosulfate and sulfite	*Desulfobacillum aliphaticivorans CV2803*	Deltaproteobacteria	Cravo-Laureau et al. 2004, Cravo-Laureau et al. 2005 (104, 105)
Oilfield production water, Oklahoma	C6-C10 alkanes	sulfate, thiosulfate	*Dseulfoglaeba alkanexedens* Strain Lake	Deltaproteobacteria	Davidova et al. 2006 (109)

Source Description	Substrate(s)	Electron Acceptors	Strain	Taxonomic Class	Reference
US naval oily wastewater-storage facility, Virginia	C6-C12 alkanes	sulfate, thiosulfate	*Dseulfoglaeba alkanexedens* strain ALDC	Deltaproteobacteria	Davidova et al. 2006 (109)
US naval oily wastewater-storage facility, Virginia	C12	sulfate	consortium		Kropp et al. 2000 (68)
Hydrocarbon seep - Gulf of Mexico	C3-C4 alkanes	sulfate	Strain BuS5	Deltaproteobacteria	Kniemeyer et al. 2007 (64)
Hydrocarbon seep - Guaymas Basin Sediment, California	propane	sulfate	Clone Propane60-GuB	Clostridia	Kniemeyer et al. 2007 (64)
Gas condensate-contaminated aquifer sediments, The Denver Basin in Ft. Lupton, CO	ethylcyclo-pentane	sulfate	consortium	Deltaproteobacteria	Rios-Hernandez et al. 2003 (55)
Gas condensate-contaminated aquifer sediments, The Denver Basin in Ft. Lupton, CO	alicyclic alkanes	sulfate	consortium		Townsend et al. 2004 (54)
Hydrocarbon seep; Zodletone spring in Oklahoma	propane, pentane	sulfate	consortium	Deltaproteobacteria	Savage et al. 2010 (65)
BTEX contaminated aquifer sediments from Bear Lake in Northern Michigan	toluene	nitrate	*Azoarcus tolulyticus*	Betaproteobacteria	Chee-Sanford et al. 1996 (18)

Table 1.2 Field evidence of fumarate addition metabolites.

Source Description	Substrate(s)	Reference
Unconfined aquifer near a bulk fuel terminal (Portland, OR)	toluene, o-xylene	Reusser et al. 2002 (66)
Unconfined aquifer near a former oil refinery (Kansas City, KS)	toluene	Reusser et al. 2002 (66)
Groundwater analysis on former refinery site near the North Platte River in Casper, WY	pentane, C5–C9 unsaturated hydrocarbons	Parisi et al. 2009 (63)
Samples from production wells and processing facilities of an oilfield complex in the North Slope of Alaska	methane	Duncan et al. 2009 (31)

standards, and quantifying these transient chemical species that are often present in small concentrations.

In addition to these knowledge gaps, there are some practical difficulties in obtaining samples and measuring biodegradation both in laboratory and natural environments. For example, obtaining accurate rate data is difficult and expensive. Determining substrate conversion rates is limited by analytical methods for detecting and quantifying substrates, metabolites and products. Another practical difficulty in studying anaerobic hydrocarbon biodegradation is the fact that the environments are often difficult to access. For example, sampling at the bottom of oceans or seas can be costly, dangerous, or impossible. Until recent developments in submersible technology, the communities and chemistry of many anaerobic systems in the ocean were difficult to sample and observe (115). Obtaining samples from oil processing and transportation facilities can be complicated by such challenges as gaining access to facilities (116), safety factors during sampling, and considerations when transporting and storing samples. Also, trying to extract anaerobic microorganisms and replicate anaerobic systems without exposing them to oxygen or contaminating the samples may be difficult (116). Challenges exist in preserving the natural conditions throughout sampling procedures and in the laboratory environment (e.g., anoxic environments may also be under a great deal of pressure and exist at extreme temperatures).

Research Questions and Goals

The purpose of the work in this dissertation is to contribute to the filling of the aforementioned knowledge gap in two ways: 1) by developing a model that estimates substrate loss rates based on chemical properties that can be easily calculated, and 2) by

modeling anaerobic biodegradation of a specific substrate to generate information about the likelihood of the reaction via fumarate addition, the expected reaction sequence, and reaction kinetics. The specifics of this work are presented in greater detail in Chapters 2 and 3, respectively.

Chapter 2 addresses scenarios in which there is an absence of physical data by asking if mechanism-specific properties can predict relative anaerobic hydrocarbon biodegradation rates. This chapter describes the development of a predictive model based on calculated chemical properties of the substrates and the percent of substrate loss. The model was developed using relative extent of biodegradation data for many alkylbenzenes (117). These data were correlated with computed chemical properties that were selected both based on physical phenomena and also based on how these physical phenomena behave in the specific mechanism of interest (i.e., the fumarate addition mechanism). The purpose of this modeling is to provide information about rates and substrate preferences for systems that cannot be measured easily. When compared with environmental chemical analyses, the output is useful in determining which fate and transport processes are occurring in environmental systems. Since hydrocarbon contamination and anaerobic conditions are ubiquitous, the information about the reactivity of these toxic compounds is environmentally relevant and of interest to human health. Another major potential contribution of the model is the establishment of a connection between theory and real-world data, as the calculated values (based on reaction specific chemistry) were correlated to laboratory values collected using contaminated sediments and indigenous microorganisms. The contents of this chapter were published in the article "Polarizability and Spin Density Correlate with the Relative

Anaerobic Biodegradability of Alkylaromatic Hydrocarbons" (118).

Chapter 3 presents a model of a specific and theoretical reaction of anaerobic hydrocarbon biodegradation. The model is used to answer three questions: 1) Could the overall reaction occur as theorized? 2) What would the transition state structures look like? and 3) Based on the potential energy barriers calculated, what is the likely preference for this substrate via fumarate addition? We developed a model based on quantum chemistry that provides information about the likelihood of the reaction, the expected reaction sequence, and the kinetics of the reaction relative to other substrates and mechanisms. Specifically, we used computational chemistry software to develop a potential energy surface for the theoretical initial reaction of methane oxidation via fumarate addition. Ultimately, the model can be used to direct metabolite searches, and give insight into substrate preferences and mechanism preferences for methane and other small alkanes. Also, the process investigated is an important filter for dissolved methane in marine sediments and freshwater environments. Since this process likely prevents the release of large amounts of methane from being released into the atmospheric, it has the potential to impact global temperatures and tropospheric chemistry. The results of the work are original geometries and energy values which represent the potential energy requirements for the conversion of methane via fumarate addition. The molecular stability and low aqueous solubility of methane make it an ideal model substrate in efforts to define the limits of energy barriers and minimal energy requirements for growth in reactions activated by glycyl radical-containing enzymes. The contents of this chapter were submitted for publication in the article "A Potential Energy Surface for Anaerobic Oxidation of Methane via Fumarate Addition" (119).

An additional study (included as Appendix A) addresses the concerns associated with collecting rate data, by exploring if it is possible to improve the ease of collecting substrate loss measurements for many hydrocarbons. We designed an experimental approach to create microcosms for time series analysis that can be measured directly by sacrificial analysis. The design makes use of an established automated method that measures hydrocarbon concentrations in sediment samples from microcosms (the purge and trap system (117)). Automation accommodates more time points and uses less sample. Using less sample is beneficial since the sediment collection can be difficult and expensive, and sample collection activity can disrupt the environment of interest. Another goal is to establish a dataset with many time points to serve as a basis for developing and confirming rate models. Producing rate data for many substrates provides information for decision making, model development, and helping understand general ideas about how these physical systems work. The more quickly in situ concentrations and rate analyses are determined, the sooner it can be established where hydrocarbons are being transported. Therefore, this information has the potential to save time and money, as well as minimize exposure and risks to human health.

Chapters 2, 3 and Appendix A in this dissertation present the background information, the methodology, and the results and discussions for each of the research questions addressed. Chapter 4 presents a discussion about the application of density functional theory calculations to anaerobic hydrocarbon biodegradation research in the context of suggestions for future research. Appendices B and C contain definitions and details of the Computational Chemistry methods referred to in this dissertation, respectively.

Literature Cited

(1) Bruice, P. Y. *Organic Chemistry*. Fifth Edition ed.; Pearson Prentice Hall: Upper Saddle River, NJ 07458, 2007; pp 1319.

(2) Olah, G. A.; Molnár, Á. *Hydrocarbon Chemistry*. 2nd ed.; Wiley-Interscience: 2003; pp 871.

(3) Petrov, A. A. *Petroleum Hydrocarbons*. Springer-Verlag: Berlin, Germany, 1987; pp 255.

(4) *The Future of Natural Gas, An Interdisciplinary MIT Study*; MIT Energy Initiative: Cambridge, MA June 9, 2011; pp 178.

(5) Khilyuk, L. F. *Gas Migration: events preceding earthquakes*. illustrated ed.; Gulf Publishing Company: Houston, Texas, 2000; pp 389.

(6) Ladygina, N.; Dedyukhina, E. G.; Vainshtein, M. B. A review on microbial synthesis of hydrocarbons. *Process Biochemistry* **2006,** *41* (5), 1001-1014.

(7) Conrad, R. The global methane cycle: recent advances in understanding the microbial processes involved. *Environmental Microbiology Reports* **2009,** *1* (5), 285-292.

(8) Hopf, H. *Classics in Hydrocarbon Chemistry: Syntheses, Concepts, Perspectives*. Illustrated ed.; Wiley-VCH: Weinheim, Germany, 2000; pp 547.

(9) *Annual Energy Outlook 2012 Early Release Overview*; U.S. Energy Information Administration, U.S. Department of Energy: Washington, D.C., January 23, 2012; pp 1-13.

(10) Olah, G. A. After oil and gas: methanol economy. *Catalysis Letters* **2004,** *93* (1-2), 1-2.

(11) Pipeline Basics. http://primis.phmsa.dot.gov/comm/PipelineBasics.htm (accessed February 2012).

(12) Kvenvolden, K. A.; Cooper, C. K. Natural seepage of crude oil into the marine environment. *Geo-Marine Letters* **2003,** *23* (3/4), 140-146.

(13) Appendix A to 40 CFR, Part 423--126 Priority Pollutants. http://www.epa.gov/region1/npdes/permits/generic/prioritypollutants.pdf (accessed March 2012).

(14) *Assessing the Effects of the Gulf of Mexico Oil Spill on Human Health: A Summary of the June 2010 Workshop*; 9780309157810; The National Academies Press, Institute of Medicine: 2010; pp 200.

(15) Drinking Water Contaminants. http://water.epa.gov/drink/contaminants/index.cfm#Organic (accessed March 2012).

(16) Butters, T. Congressional Fire and Emergency Services Institute National Advisory Committee. http://www.seafc.org/Assets/dept_1/PM/pdf/DOT%20presentation.pdf (accessed March 2012).

(17) Albaigés, J.; Frei, R. W. *Fate of hydrocarbons in the environment: an analytical approach*. Gordon and Breach Science Publishers: New York, 1986; pp 373.

(18) Chee-Sanford, J. C.; Frost, J. W.; Fries, M. R.; Zhou, J. Z.; Tiedje, J. M. Evidence for acetyl coenzyme a and cinnamoyl coenzyme A in the anaerobic toluene mineralization pathway in Azoarcus tolulyticus Tol-4. *Applied and Environmental Microbiology* **1996,** *62* (3), 964-973.

(19) Aitken, C. M.; Jones, D. M.; Larter, S. R. Anaerobic hydrocarbon biodegradation in deep subsurface oil reservoirs. *Nature* **2004,** *431* (7006), 291-294.

(20) Magot, M.; Ollivier, B.; Patel, B. K. C. Microbiology of petroleum reservoirs. *Antonie Van Leeuwenhoek International Journal of General and Molecular Microbiology* **2000,** *77* (2), 103-116.

(21) *Annual Energy Review 2010*; DOE/EIA-0384(2010); Energy Information Administration Office of Integrated Analysis and Forecasting U.S. Department of Energy: Washington, D.C., October 2011.

(22) Grbic-Galic, D.; Vogel, T. M. Transformation of toluene and benzene by mixed methanogenic cultures. *Applied and Environmental Microbiology* **1987,** *53* (2), 254-260.

(23) Vogel, T. M.; Grbic-Galic, D. Incorporation of Oxygen from Water into Toluene and Benzene during Anaerobic Fermentative Transformation. *Applied and Environmental Microbiology* **1986,** *52* (1), 200-202.

(24) Chakraborty, R.; Coates, J. D. Anaerobic degradation of monoaromatic hydrocarbons. *Applied Microbiology and Biotechnology* **2004,** *64* (4), 437-446.

(25) Rees, J. F.; Wilson, B. H.; Wilson, J. T. Biotransformation of toluene in methanogenic subsurface material. *Abstracts of the Annual Meeting of the American Society for Microbiology* **1985,** *85*, 258.

(26) Head, I. M.; Jones, D. M.; Larter, S. R. Biological activity in the deep subsurface and the origin of heavy oil. *Nature* **2003,** *426* (6964), 344-352.

(27) Rabus, R.; Widdel, F. Utilization of alkylbenzenes during anaerobic growth of pure cultures of denitrifying bacteria on crude oil. *Applied and Environmental Microbiology* **1996,** *62* (4), 1238-1241.

(28) Widdel, F.; Rabus, R. Anaerobic biodegradation of saturated and aromatic hydrocarbons. *Current Opinion in Biotechnology* **2001,** *12* (3), 259-276.

(29) Suflita, J. M.; Davidova, I. A.; Gieg, L. M.; Nanny, M.; Prince, R. C. Anaerobic hydrocarbon biodegradation and the prospects for microbial enhanced energy production. In *Petroleum Biotechnology: Developments and Perspectives*, 2004; Vol. 151, pp 283-305.

(30) Townsend, G. T.; Prince, R. C.; Suflita, J. M. Anaerobic oxidation of crude oil hydrocarbons by the resident microorganisms of a contaminated anoxic aquifer. *Environmental Science & Technology* **2003,** *37* (22), 5213-5218.

(31) Duncan, K. E.; Gieg, L. M.; Parisi, V. A.; Tanner, R. S.; Green Tringe, S.; Bristow, J.; Suflita, J. M. Biocorrosive Thermophilic Microbial Communities in Alaskan North Slope Oil Facilities. *Environmental Science & Technology* **2009,** *43* (20), 7977-7984.

(32) Reeburgh, W. S. Oceanic Methane Biogeochemistry. *Chemical Reviews* **2007,** *107* (2), 486-513.

(33) Knittel, K.; Boetius, A. Anaerobic Methane Oxidizers. In *Handbook of Hydrocarbon and Lipid Microbiology*, Timmis, K. N., Ed. Springer-Verlag: Berlin Heidelberg, 2010; pp 2023-2032.

(34) Fuchs, G.; Boll, M.; Heider, J. Microbial degradation of aromatic compounds - from one strategy to four. *Nature Reviews Microbiology* **2011,** *9* (11), 803-816.

(35) Thauer, R. K.; Shima, S. Methane as fuel for anaerobic microorganisms. *Annals of the New York Academy of Sciences* **2008,** *1125*, 158-170.

(36) Wu, M. L.; Ettwig, K. F.; Jetten, M. S. M.; Strous, M.; Keltjens, J. T.; van Niftrik, L. A new intra-aerobic metabolism in the nitrite-dependent anaerobic methane-oxidizing bacterium *Candidatus* 'Methylomirabilis oxyfera'. *Biochemical Society Transactions* **2011,** *39*, 243-248.

(37) Meckenstock, R. U.; Mouttaki, H. Anaerobic degradation of non-substituted aromatic hydrocarbons. *Current Opinion in Biotechnology* **2011,** *22* (3), 406-414.

(38) Widdel, F.; Knittel, K.; Galushko, A. Anaerobic Hydrocarbon-Degrading Microorganisms: An Overview. In *Handbook of Hydrocarbon and Lipid Microbiology*, Timmis, K. N., Ed. Springer-Verlag: Berlin Heidelberg, 2010; pp 1997-2021.

(39) Tierney, M.; Young, L. Y. Anaerobic Degradation of Aromatic Hydrocarbons. In *Handbook of Hydrocarbon and Lipid Microbiology*, Timmis, K. N., Ed. Springer-Verlag: Berlin Heidelberg, 2010; pp 925-934.

(40) Boll, M.; Heider, J. Anaerobic Degradation of Hydrocarbons: Mechanisms of C–H-Bond Activation in the Absence of Oxygen. In *Handbook of Hydrocarbon and Lipid Microbiology*, Timmis, K. N., Ed. Springer-Verlag: Berlin Heidelberg, 2010; pp 1011-1024.

(41) Mbadinga, S. M.; Wang, L.; Zhou, L.; Liu, J. F.; Gu, J. D.; Mu, B. Z. Microbial communities involved in anaerobic degradation of alkanes. *International Biodeterioration & Biodegradation* **2011,** *65* (1), 1-13.

(42) Grossi, V.; Cravo-Laureau, C.; Guyoneaud, R.; Ranchou-Peyruse, A.; Hirschler-Rea, A. Metabolism of n-alkanes and n-alkenes by anaerobic bacteria: A summary. *Organic Geochemistry* **2008,** *39* (8), 1197-1203.

(43) Heider, J. Adding handles to unhandy substrates: anaerobic hydrocarbon activation mechanisms. *Current Opinion in Chemical Biology* **2007,** *11* (2), 188-194.

(44) Gieg, L. M.; Suflita, J. M. Metabolic indicators of anaerobic hydrocarbon biodegradation in petroleum-laden environments. In *Petroleum Microbiology*, 2005; pp 337-356.

(45) Rabus, R.; Heider, J. Initial reactions of anaerobic metabolism of alkylbenzenes in denitrifying and sulfate reducing bacteria. *Archives of Microbiology* **1998,** *170* (5), 377-384.

(46) Rabus, R.; Widdel, F. Anaerobic degradation of ethylbenzene and other aromatic-hydrocarbons by new denitrifying bacteria. *Archives of Microbiology* **1995,** *163* (2), 96-103.

(47) Ball, H. A.; Johnson, H. A.; Reinhard, M.; Spormann, A. M. Initial reactions in anaerobic ethylbenzene oxidation by a denitrifying bacterium, strain EB1. *Journal of Bacteriology* **1996,** *178* (19), 5755-5761.

(48) Elshahed, M. S.; Gieg, L. M.; McInerney, M. J.; Suflita, J. M. Signature metabolites attesting to the in situ attenuation of alkylbenzenes in anaerobic environments. *Environmental Science & Technology* **2001,** *35* (4), 682-689.

(49) Kniemeyer, O.; Fischer, T.; Wilkes, H.; Glockner, F. O.; Widdel, F. Anaerobic degradation of ethylbenzene by a new type of marine sulfate-reducing bacterium. *Applied and Environmental Microbiology* **2003,** *69* (2), 760-768.

(50) Mancini, S. A.; Devine, C. E.; Elsner, M.; Nandi, M. E.; Ulrich, A. C.; Edwards, E. A.; Lollar, B. S. Isotopic Evidence Suggests Different Initial Reaction Mechanisms for Anaerobic Benzene Biodegradation. *Environmental Science & Technology* **2008,** *42* (22), 8290-8296.

(51) Coates, J. D.; Chakraborty, R.; McInerney, M. J. Anaerobic benzene biodegradation - a new era. *Research in Microbiology* **2002,** *153* (10), 621-628.

(52) Gieg, L. M.; Kolhatkar, R. V.; McInerney, M. J.; Tanner, R. S.; Harris, S. H.; Sublette, K. L.; Suflita, J. M. Intrinsic bioremediation of petroleum hydrocarbons in a gas condensate-contaminate aquifer. *Environmental Science & Technology* **1999,** *33* (15), 2550-2560.

(53) Gieg, L. M.; Alumbaugh, R. E.; Field, J. A.; Jones, J.; Istok, J. D.; Suflita, J. M. Assessing *in situ* rates of anaerobic hydrocarbon bioremediation. *Microbial Biotechnology* **2009,** 2, 222-233.

(54) Townsend, G. T.; Prince, R. C.; Suflita, J. M. Anaerobic biodegradation of alicyclic constituents of gasoline and natural gas condensate by bacteria from an anoxic aquifer. *Fems Microbiology Ecology* **2004,** *49* (1), 129-135.

(55) Rios-Hernandez, L. A.; Gieg, L. M.; Suflita, J. M. Biodegradation of an alicyclic hydrocarbon by a sulfate-reducing enrichment from a gas condensate-contaminated aquifer. *Applied and Environmental Microbiology* **2003,** *69* (1), 434-443.

(56) Leuthner, B.; Heider, J. A two-component system involved in regulation of anaerobic toluene metabolism in *Thauera aromatica*. *Fems Microbiology Letters* **1998,** *166* (1), 35-41.

(57) Beller, H. R.; Spormann, A. M. Analysis of the novel benzylsuccinate synthase reaction for anaerobic toluene activation based on structural studies of the product. *Journal of Bacteriology* **1998,** *180* (20), 5454-5457.

(58) Leutwein, C.; Heider, J. Anaerobic toluene-catabolic pathway in denitrifying *Thauera aromatica*: activation and beta-oxidation of the first intermediate, (R)-(+)-benzylsuccinate. *Microbiology-Uk* **1999,** *145*, 3265-3271.

(59) Krieger, C. J.; Roseboom, W.; Albracht, S. P. J.; Spormann, A. M. A stable organic free radical in anaerobic benzylsuccinate synthase of *Azoarcus* sp strain T. *Journal of Biological Chemistry* **2001,** *276* (16), 12924-12927.

(60) Leuthner, B.; Leutwein, C.; Schulz, H.; Horth, P.; Haehnel, W.; Schiltz, E.; Schagger, H.; Heider, J. Biochemical and genetic characterization of benzylsuccinate synthase from *Thauera aromatica*: a new glycyl radical enzyme catalysing the first step in anaerobic toluene metabolism. *Molecular Microbiology* **1998,** *28* (3), 615-628.

(61) Coschigano, P. W.; Wehrman, T. S.; Young, L. Y. Identification and analysis of genes involved in anaerobic toluene metabolism by strain T1: Putative role of a glycine free radical. *Applied and Environmental Microbiology* **1998,** *64* (5), 1650-1656.

(62) Kühner, S.; Wöhlbrand, L.; Fritz, I.; Wruck, W.; Hultschig, C.; Hufnagel, P.; Kube, M.; Reinhardt, R.; Rabus, R. Substrate-dependent regulation of anaerobic degradation pathways for toluene and ethylbenzene in a denitrifying bacterium, strain EbN1. *Journal of Bacteriology* **2005,** *187* (4), 1493-1503.

(63) Parisi, V. A.; Brubaker, G. R.; Zenker, M. J.; Prince, R. C.; Gieg, L. M.; da Silva, M. L. B.; Alvarez, P. J. J.; Suflita, J. M. Field metabolomics and laboratory assessments of anaerobic intrinsic bioremediation of hydrocarbons at a petroleum-contaminated site. *Microbial Biotechnology* **2009,** 2, 202-212.

(64) Kniemeyer, O.; Musat, F.; Sievert, S. M.; Knittel, K.; Wilkes, H.; Blumenberg, M.; Michaelis, W.; Classen, A.; Bolm, C.; Joye, S. B.; Widdel, F. Anaerobic oxidation of short-chain hydrocarbons by marine sulphate-reducing bacteria. *Nature* **2007,** *449*, 898-902.

(65) Savage, K. N.; Krumholz, L. R.; Gieg, L. M.; Parisi, V. A.; Suflita, J. M.; Allen, J.; Philp, R. P.; Elshahed, M. S. Biodegradation of low-molecular-weight alkanes under mesophilic, sulfate-reducing conditions: metabolic intermediates and community patterns. *Fems Microbiology Ecology* **2010,** *72* (3), 485-495.

(66) Reusser, D. E.; Istok, J. D.; Beller, H. R.; Field, J. A. In situ transformation of deuterated toluene and xylene to benzylsuccinic acid analogues in BTEX-contaminated aquifers. *Environmental Science & Technology* **2002,** *36* (19), 4127-4134.

(67) Wilkes, H.; Kuhner, S.; Bolm, C.; Fischer, T.; Classen, A.; Widdel, F.; Rabus, R. Formation of n-alkane- and cycloalkane-derived organic acids during anaerobic growth of a denitrifying bacterium with crude oil. *Organic Geochemistry* **2003,** *34* (9), 1313-1323.

(68) Kropp, K. G.; Davidova, I. A.; Suflita, J. M. Anaerobic oxidation of n-dodecane by an addition reaction in a sulfate-reducing bacterial enrichment culture. *Applied and Environmental Microbiology* **2000,** *66* (12), 5393-5398.

(69) Krieger, C. J.; Beller, H. R.; Reinhard, M.; Spormann, A. M. Initial reactions in anaerobic oxidation of m-xylene by the denitrifying bacterium *Azoarcus* sp strain T. *Journal of Bacteriology* **1999,** *181* (20), 6403-6410.

(70) Achong, G. R.; Rodriguez, A. M.; Spormann, A. M. Benzylsuccinate synthase of *Azoarcus* sp strain T: Cloning, sequencing, transcriptional organization, and its role in anaerobic toluene and m-xylene mineralization. *Journal of Bacteriology* **2001,** *183* (23), 6763-6770.

(71) Morasch, B.; Richnow, H. H.; Vieth, A.; Schink, B.; Meckenstock, R. U. Stable isotope fractionation caused by glycyl radical enzymes during bacterial degradation of aromatic compounds. *Applied and Environmental Microbiology* **2004,** *70* (5), 2935-2940.

(72) Edwards, E. A.; Wills, L. E.; Reinhard, M.; Grbic-Galic, D. Anaerobic degradation of toluene and xylene by aquifer microoganisms under sulfate-reducing conditions. *Applied and Environmental Microbiology* **1992,** *58* (3), 794-800.

(73) Rueter, P.; Rabus, R.; Wilkes, H.; Aeckersberg, F.; Rainey, F. A.; Jannasch, H. W.; Widdel, F. Anaerobic oxidation of hydrocarbons in crude-oil by new types of sulfate-reducing bacteria. *Nature* **1994,** *372* (6505), 455-458.

(74) Beller, H. R.; Spormann, A. M. Anaerobic activation of toluene and o-xylene by addition to fumarate in denitrifying strain T. *Journal of Bacteriology* **1997,** *179* (3), 670-676.

(75) Morasch, B.; Schink, B.; Tebbe, C. C.; Meckenstock, R. U. Degradation of o-xylene and m-xylene by a novel sulfate-reducer belonging to the genus *Desulfotomaculum*. *Archives of Microbiology* **2004,** *181* (6), 407-417.

(76) Harms, G.; Zengler, K.; Rabus, R.; Aeckersberg, F.; Minz, D.; Rossello-Mora, R.; Widdel, F. Anaerobic oxidation of o-xylene, m-xylene, and homologous alkylbenzenes by new types of sulfate-reducing bacteria. *Applied and Environmental Microbiology* **1999,** *65* (3), 999-1004.

(77) Evans, P. J.; Mang, D. T.; Young, L. Y. Degradation of toluene and m-xylene and transformation of o-xylene by denitrifying enrichment cultures. *Applied and Environmental Microbiology* **1991,** *57* (2), 450-454.

(78) Häner, A.; Hohener, P.; Zeyer, J. Degradation of p-xylene by a denitrifying enrichment culture. *Applied and Environmental Microbiology* **1995,** *61* (8), 3185-3188.

(79) Rabus, R.; Wilkes, H.; Schramm, A.; Harms, G.; Behrends, A.; Amann, R.; Widdel, F. Anaerobic utilization of alkylbenzenes and n-alkanes from crude oil in

an enrichment culture of denitrifying bacteria affiliating with the beta-subclass of *Proteobacteria*. *Environmental Microbiology* **1999,** *1* (2), 145-157.

(80) Edwards, E. A.; Grbic-Galic, D. Anaerobic Degradation of Toluene and o-Xylene by a Methanogenic Consortium. *Applied and Environmental Microbiology* **1994,** *60* (1), 313-322.

(81) Morasch, B.; Meckenstock, R. U. Anaerobic degradation of p-xylene by a sulfate-reducing enrichment culture. *Current Microbiology* **2005,** *51* (2), 127-130.

(82) Spormann, A. M.; Widdel, F. Metabolism of alkylbenzenes, alkanes, and other hydrocarbons in anaerobic bacteria. *Biodegradation* **2000,** *11* (2-3), 85-105.

(83) Rotaru, A.-E.; Probian, C.; Wilkes, H.; Harder, J. Highly enriched *Betaproteobacteria* growing anaerobically with p-xylene and nitrate. *Fems Microbiology Ecology* **2010,** *71* (3), 460-468.

(84) Biegert, T.; Fuchs, G. Anaerobic oxidation of toluene (analogues) to benzoate (analogues) by whole cells and by cell extracts of a denitrifying *Thauera* sp. *Archives of Microbiology* **1995,** *163* (6), 407-417.

(85) Anders, H. J.; Kaetzke, A.; Kampfer, P.; Ludwig, W.; Fuchs, G. Taxonomic Position of Aromatic-Degrading Denitrifying Pseudomonad Strains K 172 and KB 740 and Their Description as New Members of the Genera *Thauera*, as *Thauera aromatica* sp. nov., and *Azoarcus*, as *Azoarcus evansii* sp. nov., Respectively, Members of the Beta Subclass of the *Proteobacteria*. *International Journal of Systematic Bacteriology* **1995,** *45* (2), 327-333.

(86) Rabus, R.; Widdel, F. Conversion studies with substrate analogues of toluene in a sulfate-reducing bacterium, strain Tol2. *Archives of Microbiology* **1995,** *164* (6), 448-451.

(87) Rabus, R.; Nordhaus, R.; Ludwig, W.; Widdel, F. Complete Oxidation of Toluene under Strictly Anoxic Conditions by a New Sulfate-Reducing Bacterium. *Applied and Environmental Microbiology* **1993,** *59* (5), 1444-1451.

(88) Evans, P. J.; Ling, W.; Goldschmidt, B.; Ritter, E. R.; Young, L. Y. Metabolites Formed during Anaerobic Transformation of Toluene and o-Xylene and Their Proposed Relationship to the Initial Steps of Toluene Mineralization. *Applied and Environmental Microbiology* **1992,** *58* (2), 496-501.

(89) Beller, H. R.; Reinhard, M.; Grbic-Galic, D. Metabolic By-Products of Anaerobic Toluene Degradation by Sulfate-Reducing Enrichment Cultures. *Applied and Environmental Microbiology* **1992,** *58* (9), 3192-3195.

(90) Biegert, T.; Fuchs, G.; Heider, F. Evidence that anaerobic oxidation of toluene in the denitrifying bacterium *Thauera aromatica* is initiated by formation of benzylsuccinate from toluene and fumarate. *European Journal of Biochemistry* **1996,** *238* (3), 661-668.

(91) Beller, H. R.; Spormann, A. M.; Sharma, P. K.; Cole, J. R.; Reinhard, M. Isolation and characterization of a novel toluene-degrading, sulfate-reducing bacterium. *Applied and Environmental Microbiology* **1996,** *62* (4), 1188-1196.

(92) Kane, S. R.; Beller, H. R.; Legler, T. C.; Anderson, R. T. Biochemical and genetic evidence of benzylsuccinate synthase in toluene-degrading, ferric iron-reducing *Geobacter metallireducens*. *Biodegradation* **2002,** *13* (2), 149-154.

(93) Beller, H. R.; Edwards, E. A. Anaerobic toluene activation by benzylsuccinate synthase in a highly enriched methanogenic culture. *Applied and Environmental Microbiology* **2000,** *66* (12), 5503-5505.

(94) Zengler, K.; Richnow, H. H.; Rossello-Mora, R.; Michaelis, W.; Widdel, F. Methane formation from long-chain alkanes by anaerobic microorganisms. *Nature* **1999,** *401* (6750), 266-269.

(95) Boll, M.; Fuchs, G.; Heider, J. Anaerobic oxidation of aromatic compounds and hydrocarbons. *Current Opinion in Chemical Biology* **2002,** *6* (5), 604-611.

(96) Callaghan, A. V.; Gieg, L. M.; Kropp, K. G.; Suflita, J. M.; Young, L. Y. Comparison of mechanisms of alkane metabolism under sulfate-reducing conditions among two bacterial isolates and a bacterial consortium. *Applied and Environmental Microbiology* **2006,** *72* (6), 4274-4282.

(97) So, C. M.; Phelps, C. D.; Young, L. Y. Anaerobic transformation of alkanes to fatty acids by a sulfate-reducing bacterium, strain Hxd3. *Applied and Environmental Microbiology* **2003,** *69* (7), 3892-3900.

(98) Aeckersberg, F.; Bak, F.; Widdel, F., Anaerobic oxidation of saturated hydrocarbons to CO_2 by a new type of sulfate-reducing bacterium. *Archives of Microbiology* **1991,** *156* (1), 5-14.

(99) Ettwig, K. F.; Butler, M. K.; Le Paslier, D.; Pelletier, E.; Mangenot, S.; Kuypers, M. M. M.; Schreiber, F.; Dutilh, B. E.; Zedelius, J.; de Beer, D.; Gloerich, J.; Wessels, H. J. C. T.; van Alen, T.; Luesken, F.; Wu, M. L.; van de Pas-Schoonen, K. T.; den Camp, H. J. M. O.; Janssen-Megens, E. M.; Francoijs, K.-J.; Stunnenberg, H.; Weissenbach, J.; Jetten, M. S. M.; Strous, M. Nitrite-driven anaerobic methane oxidation by oxygenic bacteria. *Nature* **2010,** *464* (7288), 543-550.

(100) Caldwell, S. L.; Laidler, J. R.; Brewer, E. A.; Eberly, J. O.; Sandborgh, S. C.; Colwell, F. S. Anaerobic oxidation of methane: Mechanisms, bioenergetics, and the ecology of associated microorganisms. *Environmental Science & Technology* **2008,** *42* (18), 6791-6799.

(101) Aeckersberg, F.; Rainey, F. A.; Widdel, F. Growth, natural relationships, cellular fatty acids and metabolic adaptation of sulfate-reducing bacteria that utilize long-chain alkanes under anoxic conditions. *Archives of Microbiology* **1998,** *170* (5), 361-369.

(102) So, C. M.; Young, L. Y. Isolation and characterization of a sulfate-reducing bacterium that anaerobically degrades alkanes. *Applied and Environmental Microbiology* **1999,** *65* (7), 2969-2976.

(103) Ehrenreich, P.; Behrends, A.; Harder, J.; Widdel, F. Anaerobic oxidation of alkanes by newly isolated denitrifying bacteria. *Archives of Microbiology* **2000,** *173* (1), 58-64.

(104) Cravo-Laureau, C.; Matheron, R.; Cayol, J. L.; Joulian, C.; Hirschler-Réa, A. *Desulfatibacillum aliphaticivorans* gen. nov., sp nov., an n-alkane- and n-alkene-degrading, sulfate-reducing bacterium. *International Journal of Systematic and Evolutionary Microbiology* **2004,** *54*, 77-83.

(105) Cravo-Laureau, C.; Grossi, V.; Raphel, D.; Matheron, R.; Hirschler-Rea, A. Anaerobic n-alkane metabolism by a sulfate-reducing bacterium, *Desulfatibacillum aliphaticivorans* strain CV2803. *Applied and Environmental Microbiology* **2005,** *71* (7), 3458-3467.

(106) Rabus, R.; Wilkes, H.; Behrends, A.; Armstroff, A.; Fischer, T.; Pierik, A. J.; Widdel, F. Anaerobic initial reaction of n-alkanes in a denitrifying bacterium: Evidence for (1-methylpentyl)succinate as initial product and for involvement of an organic radical in n-hexane metabolism. *Journal of Bacteriology* **2001,** *183* (5), 1707-1715.

(107) Callaghan, A. V.; Wawrik, B.; Chadhain, S. M. N.; Young, L. Y.; Zylstra, G. J. Anaerobic alkane-degrading strain AK-01 contains two alkylsuccinate synthase genes. *Biochemical and Biophysical Research Communications* **2008,** *366* (1), 142-148.

(108) Davidova, I. A.; Gieg, L. M.; Nanny, M.; Kropp, K. G.; Suflita, J. M. Stable isotopic studies of n-alkane metabolism by a sulfate-reducing bacterial enrichment culture. *Applied and Environmental Microbiology* **2005,** *71* (12), 8174-8182.

(109) Davidova, I. A.; Duncan, K. E.; Choi, O. K.; Suflita, J. M. *Desulfoglaeba alkanexedens* gen. nov., sp nov., an n-alkane-degrading, sulfate-reducing

bacterium. *International Journal of Systematic and Evolutionary Microbiology* **2006,** *56*, 2737-2742.

(110) Wilkes, H.; Rabus, R.; Fischer, T.; Armstroff, A.; Behrends, A.; Widdel, F. Anaerobic degradation of n-hexane in a denitrifying bacterium: Further degradation of the initial intermediate (1-methylpentyl)succinate via C-skeleton rearrangement. *Archives of Microbiology* **2002,** *177* (3), 235-243.

(111) Grundmann, O.; Behrends, A.; Rabus, R.; Amann, J.; Halder, T.; Heider, J.; Widdel, F. Genes encoding the candidate enzyme for anaerobic activation of n-alkanes in the denitrifying bacterium, strain HxN1. *Environmental Microbiology* **2008,** *10* (2), 376-385.

(112) Jarling, R.; Sadeghi, M.; Drozdowska, M.; Lahme, S.; Buckel, W.; Rabus, R.; Widdel, F.; Golding, B. T.; Wilkes, H. Stereochemical Investigations Reveal the Mechanism of the Bacterial Activation of n-Alkanes without Oxygen. *Angewandte Chemie-International Edition* **2012,** *51* (6), 1334-1338.

(113) Musat, F.; Wilkes, H.; Behrends, A.; Woebken, D.; Widdel, F. Microbial nitrate-dependent cyclohexane degradation coupled with anaerobic ammonium oxidation. *Isme Journal* **2010,** *4*, (10), 1290-1301.

(114) So, C. M.; Young, L. Y. Initial reactions in anaerobic alkane degradation by a sulfate reducer, strain AK-01. *Applied and Environmental Microbiology* **1999,** *65* (12), 5532-5540.

(115) Ocean Explorer: Submersibles. oceanexplorer.noaa.gov/technology/subs/subs.html (accessed February 2012).

(116) Magot, M. Indigenous microbial communities in oil fields. *Petroleum Microbiology* **2005**, 21-33.

(117) Prince, R. C.; Suflita, J. M. Anaerobic biodegradation of natural gas condensate can be stimulated by the addition of gasoline. *Biodegradation* **2007,** *18* (4), 515-523.

(118) Beasley, K. K.; Gieg, L. M.; Suflita, J. M.; Nanny, M. A. Polarizability and Spin Density Correlate with the Relative Anaerobic Biodegradability of Alkylaromatic Hydrocarbons. *Environmental Science & Technology* **2009,** *43* (13), 4995-5000.

(119) Beasley, K. K.; Nanny, M. A Potential Energy Surface for Anaerobic Oxidation of Methane via Fumarate Addition. *Submitted* **2012**.

CHAPTER 2

Polarizability and Spin Density Correlate with the Relative Anaerobic Biodegradability of Alkylaromatic Hydrocarbons

With the exception of some minor editorial differences, this chapter is reproduced with permission from Beasley, K. K.; Gieg, L. M.; Suflita, J. M.; Nanny, M. A. Polarizability and Spin Density Correlate with the Relative Anaerobic Biodegradability of Alkylaromatic Hydrocarbons. Environmental Science & Technology 2009, 43 (13), 4995-5000.

Abstract

Polarizability ($\langle\alpha\rangle$) and spin density (SD) of benzyl radical intermediates calculated using Gaussian 03 were correlated with the extent of anaerobic biodegradation for 17 C_1 to C_4 parent alkylbenzenes. The percent anaerobic biodegradation of the hydrocarbon series was determined in a previous study using an inoculum from a gas condensate-contaminated aquifer incubated under sulfate-reducing conditions. Many of the parent compounds are known to be biodegraded in the absence of oxygen by fumarate addition reactions. Percent biodegradation over a 100 day incubation (predicted) = -1.044 <R> + 908.271SD - 586.197 (R^2 = 0.839; all p-values ≤ 0.058). This correlation suggests that compounds forming more stable alkylbenzyl radical intermediates biodegrade by fumarate addition more slowly than their counterparts forming less stable radicals. More highly substituted molecules including isopropylbenzene, 1-ethyl-2,6-dimethylbenzene and 1-ethyl-3,4-dimethylbenzene did not fit the model. The assumption of biodegradation

by fumarate addition reaction was independently verified with several substrates. These findings help form a basis for predicting the relative rate of alkylbenzene metabolism in anaerobic environments.

Introduction

Hydrocarbons are ubiquitous in the environment. They are naturally present in oil and gas reservoirs that comprise a major source of the world's energy supply. In addition, hydrocarbons are unintentionally introduced to the environmental compartments through numerous routes associated with the processing, storage, use, transfer, and disposal of refined petroleum products. Therefore, the attenuation of hydrocarbons is a major economic and environmental concern in modern society. Anaerobic biodegradation has emerged as a major fate process affecting the composition of petroleum hydrocarbons in reservoirs and in contaminated environments (e.g., refs 1-9, and references therein). Existing studies provide a basis to help predict the fate and rate of hydrocarbon decay in the absence of molecular oxygen.

Laboratory studies indicate that fumarate addition is an important mechanism by which a variety of hydrocarbons are degraded under anaerobic conditions (5, 7). Fumarate addition is a strategy used by nitrate-reducing, sulfate-reducing, methanogenic, and anoxygenic phototrophic bacteria to activate hydrocarbons in the absence of molecular oxygen (3, 4, 9). This mechanism has been found to be prevalent for a variety of hydrocarbon substrates including cyclic and linear alkanes (10, 11) and methylnaphthalenes (12, 13). Alkylbenzenes have also been shown to degrade by fumarate addition (3, 4, 6) wherein evidence from numerous studies show that toluene, ethylbenzene, all three xylene conformers, and some trimethylbenzene isomers are

subject to this metabolic fate process (14-20). In addition to the laboratory analyses, evaluation of field samples indicates the presence of fumarate addition metabolites in hydrocarbon-contaminated sites (10, 11, 21-24). In fact, in situ biotransformation rates have been obtained for toluene, *o*- and *m*-xylene, and ethylbenzene in conjunction with the formation of the corresponding isotopically labeled fumarate addition metabolites (19, 25).

Since fumarate addition to toluene has been studied most extensively, the known details of this reaction are presented here. The proposed pathway (Scheme 2.1) (26) is hypothesized to be initiated by a hydrogen atom abstraction from the benzylic carbon to form a benzyl radical intermediate (structure II). The hydrogen atom abstraction is followed by the addition of fumarate to form a benzylsuccinyl radical intermediate (structure III). Subsequently, the original hydrogen atom abstracted from toluene recombines with the benzylsuccinyl radical intermediate to form benzylsuccinate (structure IV). The benzylsuccinate product of this bioconversion may react further to form a coenzyme A derivative, which is further degraded to benzoyl-CoA (26-28), an easily degradable metabolic intermediate common to many anaerobic biodegradation pathways.

Numerous studies support an initial hydrogen radical abstraction proposed in the fumarate addition mechanism. Electron paramagnetic resonance spectroscopy results show evidence of a stable organic free radical on a residue of benzylsuccinate synthase (BSS) (29, 30), the enzyme responsible for the anaerobic catalysis of toluene. In addition,

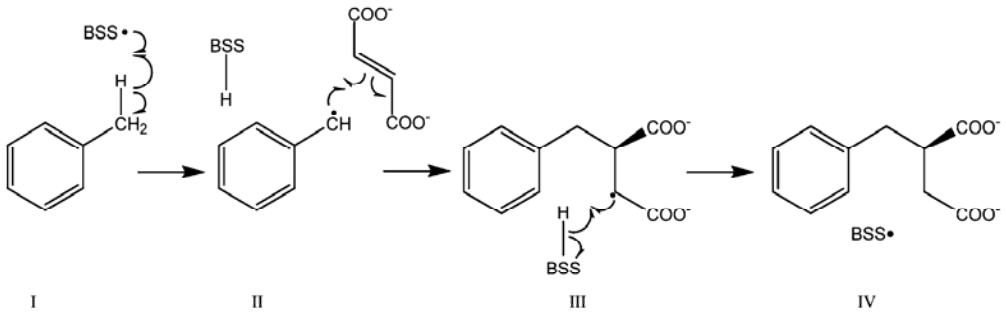

Scheme 2.1 Proposed Mechanism for Fumarate Addition to Toluene (BSS = Benzylsuccinate Synthase; H Represents the Exact Same Atom in Structures II and III; Adapted from Beller 1998 (26)).

predicted amino acid sequences of BSS residues show a strong similarity to residues important in other glycyl radical enzymes (26, 31-33). The radical addition mechanism is further supported by the observation that fumarate addition to hydrocarbons occurs at the site with the lowest homolytic C–H bond dissociation energy (7). Observed primary kinetic isotope effects and isotope fractionation studies also support the hypothesis that the homolytic C–H bond cleavage is the rate-limiting step in fumarate addition to alkylbenzenes (34, 35).

In an effort to discover the range of substrates that are subject to biodegradation in hydrocarbon contaminated anaerobic sediments, Prince and Suflita (36) measured substrate concentrations of over 60 hydrocarbon compounds in laboratory incubations under methanogenic and sulfate-reducing conditions. An analysis of the results suggested that the relative order of anaerobic biodegradation of alkyl monoaromatic compounds depended on the number, type, and position of the alkyl substituent(s) on the aromatic ring. Further, biodegradation patterns ranged widely with different substrates and did not correlate with substrate aqueous solubility (Figure 2.1). Since solubility, often used as a surrogate measurement of bioavailability, was not correlated to the relative rates of biodegradation calculated in this study, we considered other factors that could impact relative rates that are specific to the fumarate addition mechanism of alkyl monoaromatic hydrocarbon biodegradation. Our objective was to determine if there are computable properties that quantify the localization of free spin in benzyl radical intermediates that predict the order of biodegradation of alkylbenzenes in anaerobic sediment. We hypothesize that the stability of the benzyl radical intermediate plays an important role in determining substrate preference, and thus the order of alkylbenzene biodegradation

susceptibility. Specifically, spin density, a measure of free spin concentrated on the benzylic carbon after hydrogen atom abstraction, and polarizability, a measure of the degree to which electron movement throughout the molecule can be induced in the radical, were calculated. These two properties were used to develop a model based upon resonance stabilization of the benzyl radical intermediate that can be used as a tool for predicting relative rates of fumarate addition. Ultimately, this information could be applied as a remediation tool to predict degradation in hydrocarbon-contaminated plumes or to model patterns of hydrocarbon biodegradation in naturally occurring reservoirs.

Materials and Methods

Electronic Parameters. The computer program Gaussian 03 (37) was used to determine the average polarizability $\langle\alpha\rangle$ and spin density of 17 benzyl radical intermediates. Average polarizability was calculated with respect to a static electric field and expressed as an average of three diagonal components, $\langle\alpha\rangle = (\alpha_{xx} + \alpha_{yy} + \alpha_{zz})/3$. Spin density distribution was calculated by the Mulliken population analysis procedure. The radical intermediates analyzed were selected by assuming that the hydrogen atom transfer (HAT) occurred at the site with the highest potential for radical stabilization by alkyl groups by hyperconjugation (e.g., ref 38). For example, for a substrate such as 1-ethyl-2-methylbenzene, the radical was assumed to be formed by removing one of the benzyl hydrogen atoms on the ethyl side chain rather than one on the methyl side chain. And in the case of ethylbenzene, the radical was assumed to be formed by removing one of the benzyl hydrogen atoms on the substituent rather than one of the methyl hydrogen atoms as confirmed by experimental metabolite analysis (15).

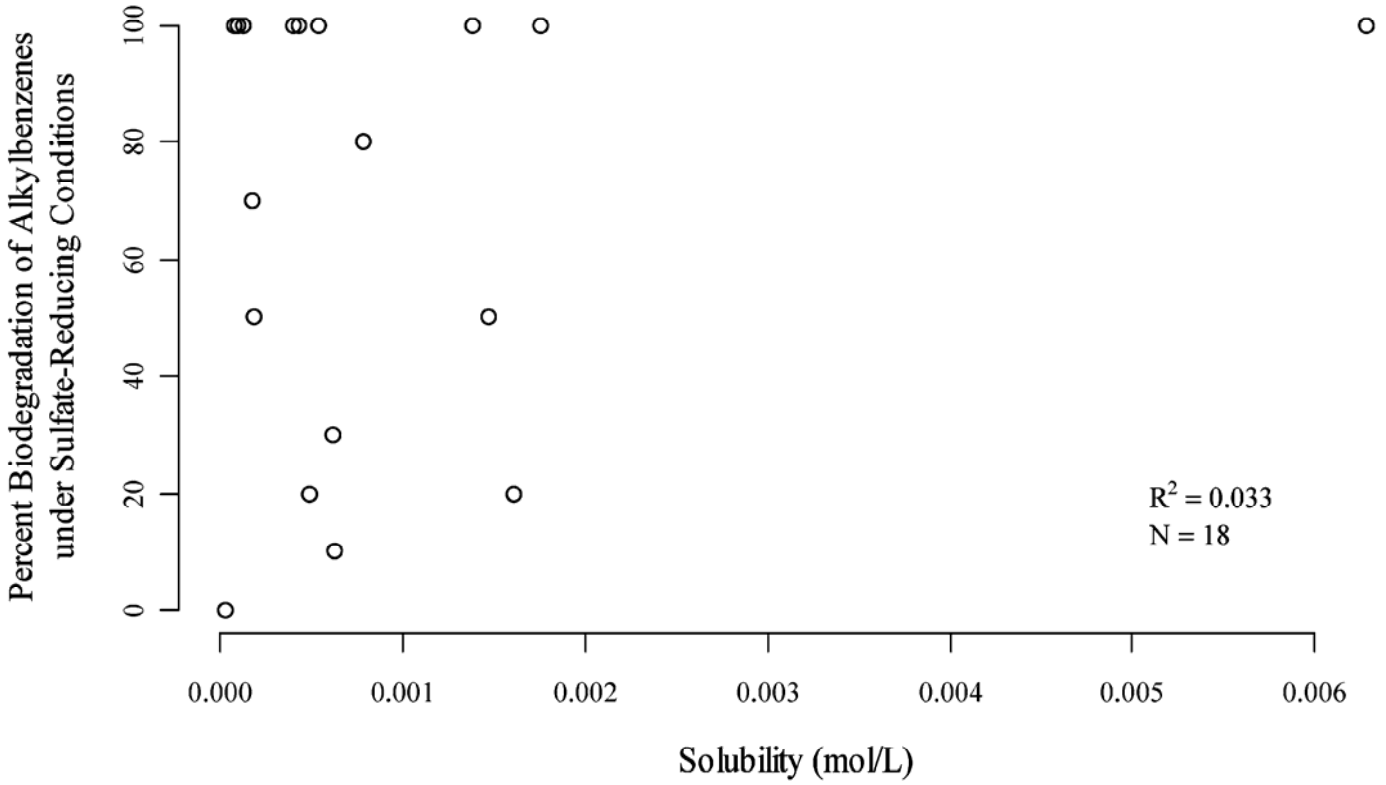

Figure 2.1 Solubility (mol/L, Lide 2000 and Yalkowsky 2003) plotted against the percent biodegradation observed by Prince and Suflita (2007) (36, 46, 47).

Geometry optimizations and frequency calculations were performed using the density functional theory B3LYP (39-41) procedure with the 6-31+G(d,p) basis set. Solvation effects were not taken into account.

Relative Biodegradation Rates in the Training Data Set. The training data set used for analysis was that reported by Prince and Suflita (36) who collected anaerobic biodegradation rate data over 100 days for 30 alkylbenzenes. Substrate concentrations were measured in incubations containing sediment and groundwater from a gas condensate-contaminated aquifer. Specifically, the data set used was from those incubations amended with 1 μL of standard gasoline and 20 mM sodium sulfate to maintain sulfate-reducing conditions. Seventeen alkylbenzenes were assessed in the training analysis.

Relative Biodegradation Rates in the Test Data Set. The test data set of biodegradation rates used in this analysis were measured in incubations prepared from the same hydrocarbon contaminated site as described by Prince and Suflita (36). These incubations were prepared by combining 25 g of contaminated sediment with 40 mL of groundwater collected from an upgradient, uncontaminated well as described by Gieg et al. (21). The incubations were amended with 2 μL (~15 to 18 μmol, or~28 μg/L) of one of the following six deuterium-labeled hydrocarbons: toluene-d_8, *o*-xylene-d_{10}, *m*-xylene-d_{10}, ethylbenzene-d_{10}, 1,3,5-trimethylbenzene-d_{12}, or 1,2,4-trimethylbenzene-d_{12} rather than gasoline. Triplicates and autoclaved controls were prepared for each substrate and substrate-unamended controls. Sulfate concentrations were monitored using ion chromatography analysis and hydrocarbon concentrations were monitored through GC analysis (42). Deuterated metabolites were identified by GC-MS analysis following

organic extraction and derivatization (19, 22). Fumarate addition metabolites were identified by comparison to authentic standards when available.

Results

Training Data Set. The seventeen alkylbenzenes considered for modeling included methyl-, ethyl-, and propylbenzenes with as many as four substituents on the aromatic ring. The data for all alkylbenzyl radical intermediates are presented in Table 2.1. The best model resulting from multiple regression analysis of these data includes average polarizability and spin density as independent variables (eq 1). Considering only main effects (43), polarizability has a negative relationship while spin density exhibits a positive relationship with percent biodegradation.

$$\%\text{biodegradation}_{,\text{Predicted}} = -1.923 < \alpha > +639.148\ \text{SD} - 267.964 \qquad (1)$$

$N = 17$; $R^2 = 0.581$; all p-values ≤ 0.015.

In an attempt to improve these results, dimethyl-ethylbenzenes (two isomers) and isopropylbenzene were omitted from the data set for a second regression analysis because they had larger and/or numerous substituents. The Pearson coefficient for the model excluding the radicals from these compounds was significantly improved as shown in eq 2.

$$\%\text{biodegradation,Predicted} = -1.044 < \alpha > +908.271\ \text{SD} - 586.197 \qquad (2)$$

$N = 14$; $R^2 = 0.839$; all p-values ≤ 0.058.

Table 2.1 Calculated Electronic Properties of the Seventeen Alkylbenzene Radical Intermediates and Their Corresponding Percent Biodegradation[a]

benzyl radical intermediate	percent biodegradation observed (*36*)	average polarizability ⟨α⟩	spin density (SD)
Methylbenzenes			
toluene	100	84.58	0.850
o-xylene	20	96.77	0.791
m-xylene	100	97.99	0.847
p-xylene	50	99.44	0.840
1,3,5-trimethylbenzene	100	111.51	0.844
1,2,3-trimethylbenzene (C2)	10	109.29	0.791
1,2,4-trimethylbenzene (C2)	20	110.40	0.787
1,2,4,5-tetramethylbenzene	0	124.43	0.801
1,2,3,5-tetramethylbenzene (C2)	0	124.33	0.784
Ethylbenzenes			
ethylbenzene	100	97.77	0.863
1-ethyl-2-methylbenzene (C1)	30	109.65	0.819
1-ethyl-3-methylbenzene (C1)	100	111.18	0.863
1-ethyl-4-methylbenzene (C1)	80	112.73	0.860
1-ethyl-2,6-dimethylbenzene (C1)	0	122.05	0.833
1-ethyl-3,4-dimethylbenzene (C1)	0	125.30	0.862
Propylbenzenes			
n-propylbenzene	100	111.02	0.913
isopropylbenzene	100	110.41	0.796

[a] The notation in parentheses indicates the position on the aromatic ring of the substituent from which the hydrogen atom was abstracted in the model.

Common measures of bioavailability and other energetic variables calculated using Gaussian 03 (as described in the Materials and Methods) were also included in the regression analysis for this data set. When included, solubility, K_{ow}, energies of the frontier molecular orbitals, and free energies of the radical intermediates resulted in much weaker models (data are not shown). Models were evaluated using backward elimination (43).

Test Data Set. A comparison of the test data set to the model (eq 2) is shown in Figure 2. The training data set (14 compounds) was measured after 100 days and the data used from the test data set (six compounds) was measured after 98 days. Negative values in the test data set were treated as 0 values since no biodegradation occurred (1,2,4-trimethylbenzene was the only case). Figure 2 shows the degree to which the model (eq 2) predicted the biodegradation values in the test data set ($R^2 = 0.078$).

The inclusion of ethylbenzene in the test data set had a strong effect on how well the test data fit the model. The Pearson coefficient for the data set including ethylbenzene is 0.078 and is 0.760 without ethylbenzene (Figure 2.2). Speculations as to why this is the case are presented in the discussion.

Metabolite Analysis. The results of the metabolite analysis of the test data set showed that succinyl derivatives were formed from toluene, *o*-xylene, *m*-xylene, and 1,3,5-trimethylbenzene under sulfate-reducing conditions (19). In addition, further breakdown products (i.e., toluates) were present in these systems. For 1,2,4-trimethylbenzene, succinyl products were not detected, but dimethylbenzoate was detected, which is likely a further breakdown product following the presumed fumarate addition reaction (19, 22,42).

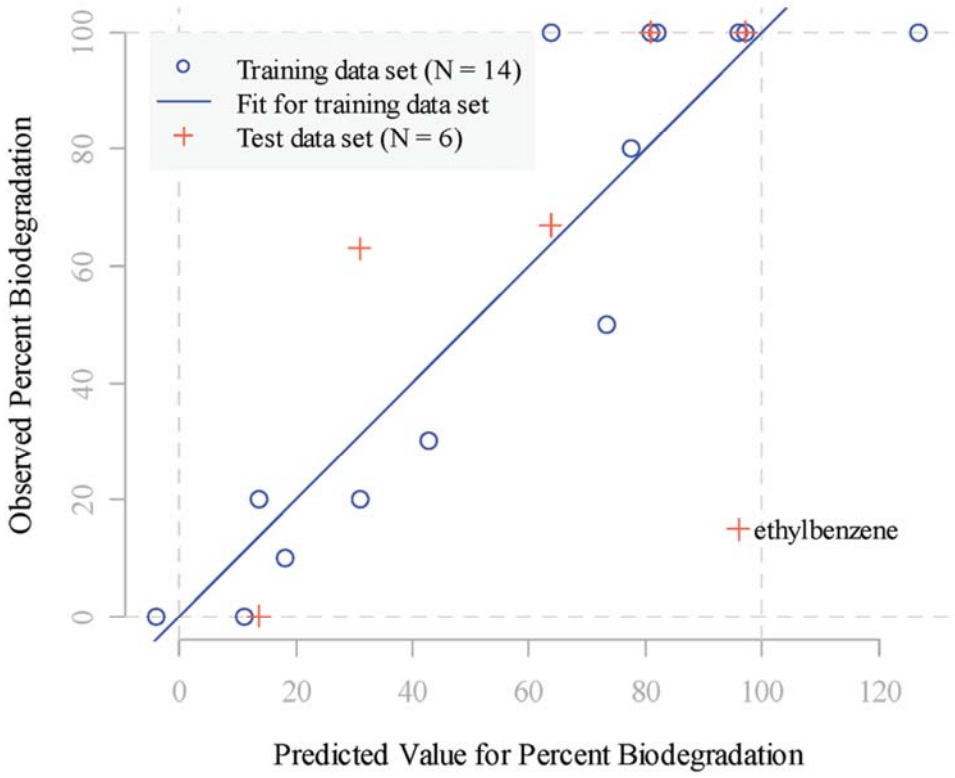

Figure 2.2 Observed percent biodegradation versus predicted percent biodegradation of the 14 alkylbenzenes in the training data set (O) and the predicted percent biodegradation of six alkylbenzenes in the test data set (+). For the training data set (O), the percent biodegradation, predicted = -1.044 < α> + 908.271 SD - 586.197 (N = 14; R^2 = 0.839; all p-values ≤0.058) (eq 2). For the test data set (+), analyses were conducted both including (R^2 = 0.078) and excluding ethylbenzene (R^2 = 0.760).

Discussion

Our initial analysis shows that average polarizability and spin density of alkyl benzyl radical intermediates are good predictors of relative rates of biodegradation based on observations with laboratory incubations (36). These electronic properties were calculated with the density functional theory based procedure, B3LYP, in combination with basis set 6-31+G(d,p). This procedure and basis set combination has been shown to provide good prediction of these electronic properties (44).

Fourteen alkylbenzene isomers were used to create the biodegradation predictive model presented in eq 2. Our results suggest that eq 2 becomes a weaker predictor of relative biodegradation rates as the number of carbons in each alkyl side chain increases and the number of alkyl substituents increases. For example, the model fits well when benzene is substituted with one or two linear alkyl groups (comprised of up to three carbons); or, even substituted with four methyl groups. The model weakens, however, when there are three substituents if at least one is an ethyl group, or when the side chains are branched (i.e., isopropylbenzene). Polarizability and spin density do not account for steric effects and it is possible that steric interactions are the cause of the weaker correlation with data for alkylbenzenes with larger substituents. Equation 2 predictions for percent biodegradation of 1-ethyl-2,6-dimethylbenzene and 1-ethyl-3,4-dimethylbenzene (43% and 66%, respectively) are each greater than the observed percent biodegradation (0% biodegradation for both). This finding is consistent with the idea that steric influence negatively affects the enzymatic process, either at the active site or by hindering substrate transport across the bacterial cellular membrane. However, the predicted value (from eq 2) for percent biodegradation of isopropylbenzene (22%) is less than the observed percent biodegradation (100%). Clearly, there is an unaccounted factor(s) that needs to be included in model development in order to expand predictive capabilities to alkylbenzenes with larger and more branched substituents.

For both eqs 1 and 2, spin density has a positive coefficient. A possible explanation for the positive relationship between spin density and percent biodegradation for a majority of the substrates tested is illustrated in a reaction coordinate diagram in Figure 2.3 (adapted from Himo 2002) (45). Increased spin density on the benzylic carbon of the

radical intermediate corresponds to decreased delocalization of the spin in the conjugated π-bonds. If the π system does not delocalize the free spin well, then the energy required to abstract the hydrogen atom homolytically ($E_{a,1}$) is greater. In other words, as the spin density increases, the energy of the first transition state increases. An increased spin density may also affect the energy of the second transition state ($E_{a,2}$). If more of the free spin is localized on the benzylic carbon of the radical intermediate, it
may be more available to create a new C–C bond with the π electrons in the double bond of fumarate (thus lowering Ea,2). Therefore, for the intermediate, the forward reaction becomes more favorable and reforming the parent substrate becomes less favorable.
An increase in polarizability would result in a lower $E_{a,1}$ and thus the benzyl radical intermediate is more easily reached. However, $E_{a,1r}$ is also lowered, so it is also easier to return to the reactants. For both eqs 1 and 2, polarizability is associated with a negative coefficient. Our explanation for the positive relationship between spin density and percent biodegradation is that a more polarizable molecule has the potential to better delocalize electrons in the conjugated π-bonds. If the electrons are delocalized, it may be more difficult to create a new C–C bond with the π electrons in the double bond of fumarate (thus increasing $E_{a,2}$). For the intermediate, the forward reaction becomes less favorable and reforming the parent substrate becomes more favorable.

When validating eq 2 with a test data set, the model failed when ethylbenzene was included (R^2 = 0.078). However, the data supported the model very well when excluding ethylbenzene (R^2 = 0.760). The training data set microcosms were amended with trace amounts of gasoline (1 μL), but the test microcosms were not. At this site, the dependence of ethylbenzene biodegradation on the presence of the gasoline had been

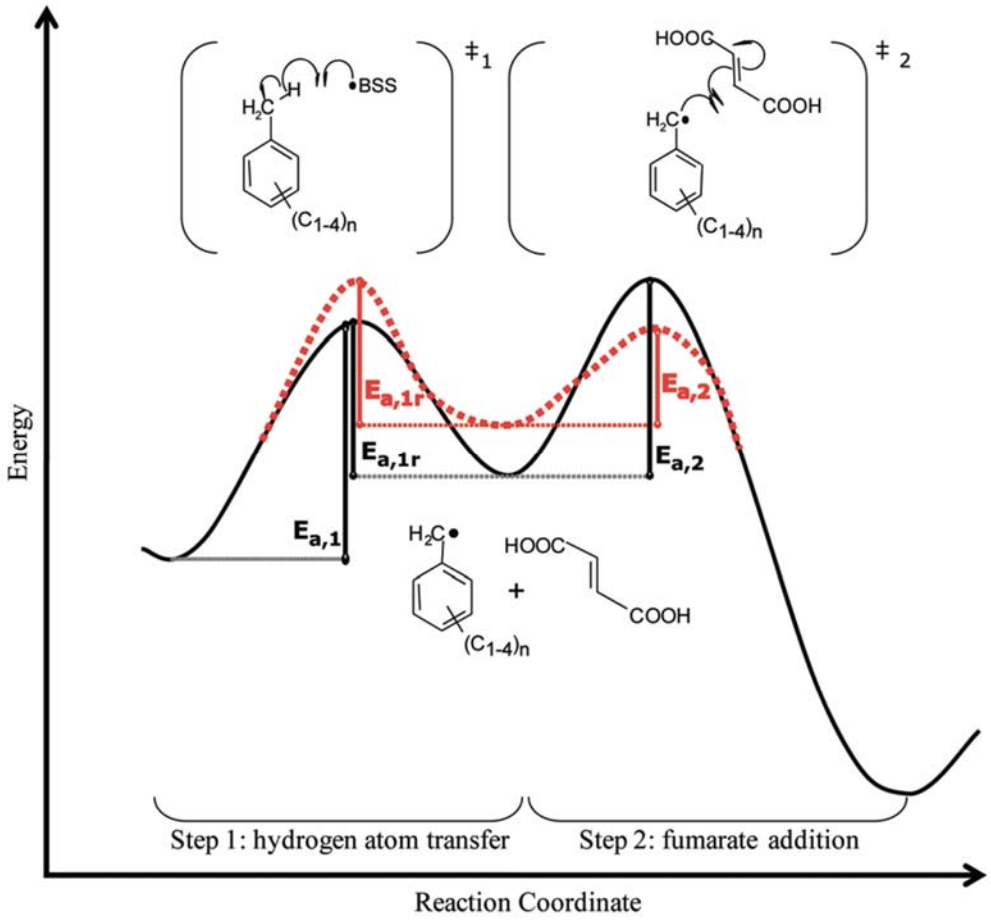

Figure 2.3 Proposed effects of increased spin density on the energetics of fumarate addition (adapted from (45)). The dotted line demonstrates the proposed changes to the reaction energetics caused by an increase in spin density localized on the benzylic carbon of the radical intermediate.

observed and was attributed to the promotion of biodegradation by components of the gasoline (36). In fact, of all other alkylbenzenes used for the model in this paper, it was the substrate whose biodegradation was most affected by the gasoline amendment. In 100 days, only 10% of ethylbenzene had biodegraded in the absence of gasoline, whereas 100% of ethylbenzene biodegradation was observed in the gasoline amended microcosms (36). So, omitting the ethylbenzene data from the test data set in order to make a fair comparison between the two data sets is reasonable.

Spin density and polarizability were selected based on the potential influence they have on the energetics of the fumarate addition mechanism. The observed relationship highlights important differences in substrate preferences independent of site conditions. Therefore, the relationship presented in this paper may exist in a variety of electron-accepting conditions where microbes utilize the same enzymatic systems. The significance of this finding is that substrate specific electronic parameters could be used to predict in situ substrate preferences independent of electron-accepting conditions. Therefore, we hypothesize that this model is applicable under any conditions that sustain BSS activity. However, in this study, only sulfate-reducing conditions were examined, therefore support for this hypothesis requires further testing.

We conclude that polarizability and spin density reflect the construct of radical character; therefore, the strong relationships shown in eq 2 and Figure 2 support the purported radical mechanism for fumarate addition. Under ideal conditions, anaerobic biodegradation of these alkylbenzenes may be predicted using these calculated properties of the radical intermediates, especially when fumarate addition metabolites have been identified onsite. The fumarate addition mechanism could represent a trend in anaerobic hydrocarbon activation and metabolism. If the relative rates of substrate degradation can be predicted based on thermodynamics of the metabolic reaction (as well as site conditions), there is a potential for using computational chemistry tools to determine fate and transport of hydrocarbons in sulfate-reducing systems; when characterizing natural reservoirs or developing remediation strategies, energetics of the mechanism would be key in determining biodegradation patterns.

Acknowledgements

We thank Dr. James Kubicki, Dr. Ralph Wheeler, Dr. Charles Rice, and Will Beasley for their advice and assistance. Some of the computing for this project was performed at the OU Supercomputing Center for Education and Research (OSCER) at the University of Oklahoma. OSCER Director Henry Neeman and Manager of Operations Brandon George provided valuable technical expertise. This work was supported by the National Science Foundation. Financial support was provided in part by a Department of Education Graduate Assistance in Areas of National Need Fellowship (Award No. P200A030155). Any findings, opinions, or conclusions are those of the author and not necessarily those of the funding agencies.

Literature Cited

(1) Head, I. M.; Jones, D. M.; Larter, S. R. Biological activity in the deep subsurface and the origin of heavy oil. *Nature* **2003**, 426 (6964), 344–352.

(2) Röling, W. F. M.; Head, I. M.; Larter, S. R. The microbiology of hydrocarbon degradation in subsurface petroleum reservoirs: perspectives and prospects. *Res. Microbiol.* **2003**, 154 (5), 321– 328.

(3) Foght, J. Anaerobic biodegradation of aromatic hydrocarbons: Pathways and prospects. *J. Mol. Microbiol. Biotechnol.* **2008**, 15 (2-3), 93–120.

(4) Heider, J. Adding handles to unhandy substrates: anaerobic hydrocarbon activation mechanisms. *Curr. Opin. Chem. Biol.* **2007**, 11 (2), 188–194.

(5) Rabus, R. F., Biodegradation of hydrocarbons under anoxic conditions. In *Petroleum Microbiology*; Ollivier, B., Magot, M., Eds.; ASM Press: Washington, DC, 2005; pp 277-299.

(6) Chakraborty, R.; Coates, J. D. Anaerobic degradation of monoaromatic hydrocarbons. *Appl. Microbiol. Biotechnol.* **2004**, 64 (4), 437–446.

(7) Suflita, J. M.; Davidova, I. A.; Gieg, L. M.; Nanny, M.; Prince, R. C., Anaerobic hydrocarbon biodegradation and the prospects for microbial enhanced energy production. In *Pet. Biotechnol.: Dev. Perspect.*, 2004; Vol. 151, pp 283-305.

(8) Widdel, F.; Rabus, R. Anaerobic biodegradation of saturated and aromatic hydrocarbons. *Curr. Opin. Biotechnol.* **2001**, 12 (3), 259–276.

(9) Heider, J.; Spormann, A. M.; Beller, H. R.; Widdel, F. Anaerobic bacterial metabolism of hydrocarbons. *FEMS Microbiol. Rev.* **1998**, 22 (5), 459–473.

(10) Rios-Hernandez, L. A.; Gieg, L. M.; Suflita, J. M. Biodegradation of an alicyclic hydrocarbon by a sulfate-reducing enrichment from a gas condensate-contaminated aquifer. *Appl. Environ. Microbiol.* **2003**, 69 (1), 434–443.

(11) Davidova, I. A.; Gieg, L. M.; Nanny, M.; Kropp, K. G.; Suflita, J. M. Stable isotopic studies of n-alkane metabolism by a sulfate-reducing bacterial enrichment culture. *Appl. Environ. Microbiol.* **2005**, 71 (12), 8174–8182.

(12) Annweiler, E.; Materna, A.; Safinowski, M.; Kappler, A.; Richnow, H. H.; Michaelis, W.; Meckenstock, R. U. Anaerobic degradation of 2-methylnaphthalene by a sulfate-reducing enrichment culture. *Appl. Environ. Microbiol.* **2000**, 66 (12), 5329–5333.

(13) Florin, M.; Alexander, G.; Jacob, J.; Friedrich, W.; Michael, K.; Richard, R.; Heinz, W.; Bernhard, S.; Ralf, R. Anaerobic degradation of naphthaleneand2-methylnaphthalene by strains of marine sulfate-reducing bacteria. *Environ. Microbiol.* **2009**, 11 (1), 209–219.

(14) Harms, G.; Zengler, K.; Rabus, R.; Aeckersberg, F.; Minz, D.; Rossello-Mora, R.; Widdel, F. Anaerobic oxidation of *o*-xylene, *m*-xylene, and homologous alkylbenzenes by new types of sulfate-reducing bacteria. *Appl. Environ. Microbiol.* **1999**, 65 (3), 999–1004.

(15) Kniemeyer, O.; Fischer, T.; Wilkes, H.; Glockner, F. O.; Widdel, F. Anaerobic degradation of ethylbenzene by a new type of marine sulfate-reducing bacterium. *Appl. Environ. Microbiol.* **2003**, 69 (2), 760–768.

(16) Morasch, B.; Richnow, H. H.; Vieth, A.; Schink, B.; Meckenstock, R. U. Stable isotope fractionation caused by glycyl radical enzymes during bacterial degradation of aromatic compounds. *Appl. Environ. Microbiol.* **2004**, 70 (5), 2935–2940.

(17) Morasch, B.; Schink, B.; Tebbe, C. C.; Meckenstock, R. U. Degradation of *o*-xylene and *m*-xylene by a novel sulfate-reducer belonging to the genus *Desulfotomaculum*. *Arch. Microbiol.* **2004**, 181 (6), 407–417.

(18) Rabus, R.; Heider, J. Initial reactions of anaerobic metabolism of alkylbenzenes in denitrifying and sulfate reducing bacteria. *Arch. Microbiol.* **1998**, 170 (5), 377–384.

(19) Gieg, L. M.; Alumbaugh, R. E.; Field, J. A.; Jones, J.; Istok, J. D.; Suflita, J. M. Assessing in situ rates of anaerobic hydrocarbon bioremediation. *Microbial*

Biotechnol. **2009**, 2, 222–233.

(20) Parisi, V. A.; Brubaker, G. R.; Zenker, M. J.; Prince, R. C.; Gieg, L. M.; da Silva, M. L. B.; Alvarez, P. J. J.; Suflita, J. M. Field metabolomics and laboratory assessments of anaerobic intrinsic bioremediation of hydrocarbons at a petroleum-contaminated site. *Microbial Biotechnol.* **2009**, 2, 202–212.

(21) Gieg, L. M.; Kolhatkar, R. V.; McInerney, M. J.; Tanner, R. S.; Harris, S. H.; Sublette, K. L.; Suflita, J.M.Intrinsic bioremediation of petroleum hydrocarbons in a gas condensate-contaminate aquifer. *Environ. Sci. Technol.* **1999**, 33 (15), 2550–2560.

(22) Gieg, L. M.; Suflita, J. M. Detection of anaerobic metabolites of saturated and aromatic hydrocarbons in petroleum-contaminated aquifers. *Environ. Sci. Technol.* **2002**, 36 (17), 3755–3762.

(23) Beller, H. R.; Kane, S. R.; Legler, T. C.; McKelvie, J. R.; Lollar, B. S.; Pearson, F.; Balser, L.; MacKay, D. M. Comparative assessments of benzene, toluene, and xylene natural attenuation by quantitative polymerase chain reaction analysis of a catabolic gene, signature metabolites, and compound-specific isotope analysis. *Environ. Sci. Technol.* **2008**, 42 (16), 6065–6072.

(24) Gieg, L. M.; Suflita, J. M., Metabolic indicators of anaerobic hydrocarbon biodegradation in petroleum-laden environments. In *Petroleum Microbiology*; Ollivier, B., Magot, M., Eds.; ASM Press: Washington, DC, 2005; pp 337-356.

(25) Reusser, D. E.; Istok, J. D.; Beller, H. R.; Field, J. A. In situ transformation of deuterated toluene and xylene to benzylsuccinic acid analogues in BTEX-contaminated aquifers. *Environ. Sci. Technol.* **2002**, 36 (19), 4127–4134.

(26) Beller, H. R.; Spormann, A. M. Analysis of the novel benzylsuccinate synthase reaction for anaerobic toluene activation based on structural studies of the product. *J. Bacteriol.* **1998**, 180 (20), 5454–5457.

(27) Biegert, T.; Fuchs, G.; Heider, F. Evidence that anaerobic oxidation of toluene in the denitrifying bacterium *Thauera aromatica* is initiated by formation of benzylsuccinate from toluene and fumarate. *Eur. J. Biochem.* **1996**, 238 (3), 661–668.

(28) Beller, H. R.; Spormann, A. M. Anaerobic activation of toluene and *o*-xylene by addition to fumarate in denitrifying strain T. *J. Bacteriol.* **1997**, 179 (3), 670–676.

(29) Krieger, C. J.; Roseboom, W.; Albracht, S. P. J.; Spormann, A. M. A stable organic free radical in anaerobic benzylsuccinate synthase of *Azoarcus* sp strain T. *J. Biol. Chem.* **2001**, 276 (16), 12924–12927.

(30) Duboc-Toia, C.; Hassan, A. K.; Mulliez, E.; Ollagnier-de Choudens, S.; Fontecave, M.; Leutwein, C.; Heider, J. Very high-field EPR study of glycyl radical enzymes. *J. Am. Chem. Soc.* **2003**, 125 (1), 38–39.

(31) Coschigano, P. W.; Wehrman, T. S.; Young, L. Y. Identification and analysis of genes involved in anaerobic toluene metabolism by strain T1: Putative role of a glycine free radical. *Appl. Environ. Microbiol.* **1998**, 64 (5), 1650–1656.

(32) Leuthner, B.; Leutwein, C.; Schulz, H.; Horth, P.; Haehnel, W.; Schiltz, E.; Schagger, H.; Heider, J. Biochemical and genetic characterization of benzylsuccinate synthase from *Thauera aromatica*: a new glycyl radical enzyme catalysing the first step in anaerobic toluene metabolism. *Mol. Microbiol.* **1998**, 28 (3), 615–628.

(33) Verfurth, K.; Pierik, A. J.; Leutwein, C.; Zorn, S.; Heider, J. Substrate specificities and electron paramagnetic resonance properties of benzylsuccinate synthases in anaerobic toluene and *m*-xylene metabolism. *Arch. Microbiol.* **2004**, 181 (2), 155–162.

(34) Krieger, C. J.; Beller, H. R.; Reinhard, M.; Spormann, A. M. Initial reactions in anaerobic oxidation of *m*-xylene by the denitrifying bacterium *Azoarcus* sp strain T. *J. Bacteriol.* **1999**, 181 (20), 6403– 6410.

(35) Steinbach, A.; Seifert, R.; Annweiler, E.; Michaelis, W. Hydrogen and carbon isotope fractionation during anaerobic biodegradation of aromatic hydrocarbons–A field study. *Environ. Sci. Technol.* **2004**, 38 (2), 609–616.

(36) Prince, R. C.; Suflita, J. M. Anaerobic biodegradation of natural gas condensate can be stimulated by the addition of gasoline. *Biodegradation* **2007**, 18 (4), 515–523.

(37) Frisch, M. J. T., G. W.; Schlegel, H. B.; Scuseria, G. E.; Robb, M. A.; Cheeseman, J. R.; Montgomery, Jr., J. A.; Vreven, T.; Kudin, K. N.; Burant, J. C.; Millam, J. M.; Iyengar, S. S.; Tomasi, J.; Barone, V.; Mennucci, B.; Cossi, M.; Scalmani, G.; Rega, N.; Petersson, G. A.; Nakatsuji, H.; Hada, M.; Ehara, M.; Toyota, K.; Fukuda, R.; Hasegawa, J.; Ishida, M.; Nakajima, T.; Honda, Y.; Kitao, O.; Nakai, H.; Klene, M.; Li, X.; Knox, J. E.; Hratchian, H. P.; Cross, J. B.; Bakken, V.; Adamo, C.; Jaramillo, J.; Gomperts, R.; Stratmann, R. E.; Yazyev, O.; Austin, A. J.; Cammi, R.; Pomelli, C.; Ochterski, J. W.; Ayala, P. Y.; Morokuma, K.; Voth, G. A.; Salvador, P.; Dannenberg, J. J.; Zakrzewski, V. G.; Dapprich, S.; Daniels, A. D.; Strain, M. C.; Farkas, O.; Malick, D. K.; Rabuck, A. D.; Raghavachari, K.; Foresman, J. B.; Ortiz, J. V.; Cui, Q.; Baboul, A. G.; Clifford, S.; Cioslowski, J.; Stefanov, B. B.; Liu, G.; Liashenko, A.; Piskorz, P.; Komaromi, I.; Martin, R. L.; Fox, D. J.; Keith, T.; Al-Laham, M. A.; Peng, C. Y.; Nanayakkara, A.; Challacombe, M.; Gill, P. M. W.; Johnson, B.; Chen, W.; Wong, M. W.; Gonzalez, C.; and Pople, J. A.; Gaussian 03, Revision C.02, Gaussian, Inc.: Wallingford CT,

2004.

(38) Bruice, P. Y. *Organic Chemistry*. 5th ed.; Pearson Prentice Hall: Upper Saddle River, NJ, 2007; pp 1319.

(39) Becke, A. D. Density-functional exchange-energy approximation with correct asymptotic-behavior. *Phys. Rev. A* **1988**, 38 (6), 3098–3100.

(40) Becke, A. D., III. The role of exact exchange. *J. Chem. Phys.* **1993**, 98 (7), 5648–5652.

(41) Becke, A. D. A new mixing of Hartree-Fock and local density-functional theories. *J. Chem. Phys.* **1993**, 98 (2), 1372–1377.

(42) Elshahed, M. S.; Gieg, L. M.; McInerney, M. J.; Suflita, J. M. Signature metabolites attesting to the in situ attenuation of alkylbenzenes in anaerobic environments. *Environ. Sci. Technol.* **2001**, 35 (4), 682–689.

(43) Hays, W. L. *Statistics*, 5th ed.; Wadsworth: Belmont, CA, 1994; p 1112.

(44) Librando, V.; Alparone, A. Electronic polarizability as a predictor of biodegradation rates of dimethylnaphthalenes. An ab initio and density functional theory study. *Environ. Sci. Technol.* **2007**, 41 (5), 1646–1652.

(45) Himo, F. Catalytic mechanism of benzylsuccinate synthase, a theoretical study. *J. Phys. Chem. B* **2002**, 106 (31), 7688–7692.

(46) Lide, D. R. *Handbook of Chemistry and Physics*, 81st ed.; CRC Press: Boca Raton, FL, 2000.

(47) Yalkowsky, S. H.; He, Y. *Handbook of Aqueous Solubility Data*; CRC Press: Boca Raton, FL, 2003; pp 1512.

CHAPTER 3

A Potential Energy Surface for Anaerobic Oxidation of Methane via Fumarate Addition

Submitted by Beasley, K. K. and Nanny, M. A .

Abstract

Microbially mediated anaerobic oxidation of methane (AOM) is an important sink in the global methane cycle, however the mechanism and microorganisms responsible for this oxidation are not fully known. Using quantum chemical calculations, fumarate addition to methane was examined to determine if it could be an energetically feasible mechanism for AOM. A potential energy surface (PES) for the initial reaction was created and the results suggest the reaction is exothermic, with a calculated overall energy change between - 9.8 and -11.2 kcal/mol. The addition of methane to fumarate is calculated to be the rate-limiting step with an energy barrier of 25.0 to 25.3 kcal/mol. Of the three possible molecular configurations of fumarate considered, the one that presents the least steric obstacles to the addition reaction with methane yields the greatest energy gain. While 11.2 kcal/mol may support growth under energy limited conditions it is unknown if enzymes can mediate an energetic barrier of 25 kcal/mol. These calculated energies provide values for what could be one of the least reactive substrates to undergo fumarate addition; making methane a model substrate in defining the limits of energy barriers and minimal energy requirements for growth in reactions activated by glycyl radical-containing enzymes.

Introduction

Microbially mediated anaerobic oxidation of methane (AOM) is considered an important sink for dissolved methane in marine sediments and anoxic surface water. Evidence of AOM has been reported in a variety of environments. Samples from fresh water sediments in agricultural areas, flood plains, marine environments, hydrocarbon seeps, freshwater lakes (oligotrophic and eutrophic), rice paddies, freshwater peat lands, landfills, salt lakes, and contaminated ground water are included (1-13). A global methane budget analysis estimates microbial oxidation of methane to be the largest sink in the oceanic methane budget before emission to the atmosphere (1, 14) and calculates AOM to be responsible for the consumption of approximately 382.4 Tg of methane per year in oceanic sediments and seeps (1, 15).

As more information about methanotrophic communities became available, it was suggested that the mechanism responsible for AOM varies depending on the redox conditions (16). Recent research has focused on at least two mechanisms by which AOM occurs: reverse methanogenesis and intra-aerobic denitrification (17). Reverse methanogenesis is a mechanism by which methanotrophy occurs in the reverse process of methanogenesis (1, 16, 18). The process is catalyzed by anaerobic methanotrophic archaea (ANME) in marine, sulfate-reducing environments (1, 16, 19-21). Evidence suggests that reverse methanogenesis could involve an enzyme responsible for catalyzing methanogenesis: methyl-coenzyme M reductase (MCR) (3, 18, 22, 23). MCR-1 isolated from a methanogen (not identified as a methanotroph, *Methanothermobacter marburgensis*) was shown to catalyze the incorporation of $^{13}CH_4$ into methyl-coenzyme M (18). Additionally, all but one of the enzymes responsible for methanogenesis has

been identified in ANME cultures and all but one of those identified have been shown to catalyze reversible reactions (21). AOM facilitated by ANME seems to be dependent on the presence of deltaproteobacteria, however the details of this association is not well understood (for reviews, see refs (2, 21, 24)).

Recently, another mechanism of AOM was discovered using samples collected from freshwater sediments in the Netherlands. The studies revealed that not all consortia that show evidence of AOM contain the ANME thought to be responsible for reverse methanogenesis (6, 25). The freshwater sediments were rich in nitrates due to runoff from agricultural activity in the watershed and demonstrated AOM under nitrite-reducing conditions. Sediment samples from the same freshwater locations were later used in the discovery of intra-aerobic denitrification by Candidatus *Methylomirabilis oxyfera* (4, 17, 25), a process in which diatomic oxygen is produced from nitrite (17, 26). This may not be considered a strictly anaerobic mechanism, as the oxygen produced is subsequently available for aerobic oxidation of methane, in a reaction catalyzed by methane monooxygenase (for a review see ref (26)).

Evidence of these two mechanisms has been produced using samples under sulfate- and nitrate- reducing conditions. Acetogenesis and methylogenesis have also been proposed as mechanisms of AOM under sulfate-reducing conditions (for a review see ref (27)). AOM also occurs under iron- and manganese-reducing conditions in marine samples; however the organisms and mechanisms responsible for the conversion are not yet identified (28). Considering the magnitude of the global AOM activity and the diversity of conditions and environments in which it occurs, it is likely that other mechanisms of conversion exist and have yet to be identified.

Fumarate addition was proposed as a potentially favorable mechanism for AOM under nitrate-reducing conditions in 2008 (16). Evidence supporting this hypothesis was that the glycyl radical-containing enzymes responsible for fumarate addition are capable of an initial activation of relatively inert substrates such as small n-alkanes (29). Fumarate addition has been found to be a prevalent mechanism of hydrocarbon biodegradation for a diverse range of substrates under sulfate- and nitrate-reducing conditions (for reviews see refs (30-32)), including saturated alkane substrates ranging from C_3 to C_{19} (for review see ref (33)).

In recent work, evidence of low molecular weight alkane metabolism by the fumarate addition mechanism was discovered in two distinct environments, a low-salinity artesian spring and marine basins. Enrichment cultures from an artesian spring hydrocarbon seep in Oklahoma metabolized n-propane and n-pentane under sulfate-reducing conditions. Fumarate addition is proposed to be the mechanism of biodegradation in these samples based on the identification of n-propylsuccinnic acid (a fumarate addition intermediate) by GC-MS analysis (34). In samples from marine environments (specifically, the Gulf of Mexico and the Guayamas Basin), propane and butane metabolism was linked to sulfate depletion. Propane was shown to biodegrade by sulfate-reducing consortia and butane by a sulfate-reducing bacterium by addition of succinic acid at the at the terminal and subterminal carbon atoms (35). Iso- and n–propylsuccinic acids were extracted from the sediment samples grown with propane and identified by GC-MS analysis. In addition, (1-methylpropyl)succinate was identified in the extracts from the samples utilizing butane as a substrate, suggesting fumarate addition as the mechanism of biodegradation in both marine environments. Ethane biodegradation

was also clearly coupled with sulfide production in these samples, however at slower rates and metabolites in those samples were not isolated.

The metabolism of propane and butane via fumarate addition in hydrocarbon rich environments leads to speculations as to whether or not the mechanism could also convert smaller alkanes such as ethane and methane. As stated in Thauer and Shima (2008) (16):

> The dissociation energy of the C-H bonds of C2 of propane and of other alkanes is near +410 kJ/mol [98 kcal/mol] and thus 60 kJ/mol [14 kcal/mol] higher than that of the C-H bond in the glycine residue of the alkylsuccinate synthase [...]. The difference of 60 kJ/mol evidently can be overcome in the transition state of the enzyme; otherwise, the reaction would not be catalyzed. The question is: could such a mechanism also work for AOM? (16)

Novel field evidence suggests that the answer to that question may be: yes. Fumarate addition could be an initial mechanism for AOM as potential metabolites of the mechanism have been identified in systems exposed to low molecular weight hydrocarbons. The detection of C_1-C_4 fumarate addition metabolites (alkylsuccinates) by GC-MS analysis in oil production water samples from the Alaska North Slope (ANS) ranged in concentration from 0.8 to 2.2 μM (36). Specifically, 2-methylsuccinate (the intermediate produced in the third and final reaction presented in Figure 3.1) was detected at a mean concentration of 2.08 ± 1.10 μM in samples from product wells, and the central processing facility. In addition, butanoic acid, was detected in these samples, this compound would be a metabolite of further 2-methylsuccincate degradation assuming it undergoes an analogous C-skeleton rearrangement that n-hexane experiences in the fumarate addition mechanism (36, 37). These metabolites were detected in samples from wells that are regularly exposed to methane; the interesting source of the

substrates in the ANS samples was the purposeful reinjection of low molecular weight gases to maintain pressure in the reservoirs. Fumarate addition metabolites were not identified in samples from the sea water wells that did not contain low molecular weight hydrocarbons. If AOM is occurring in these systems, it is unlikely to be occurring by the reverse methanogenesis mechanism since there is a disparity in the 16S sequences for archaea and deltaproteobacteria performed on these samples as compared to those of communities thought to be responsible for reverse methanogenesis (36). And, intra-aerobic denitrification is unlikely to be occurring in these sulfate-rich environments.

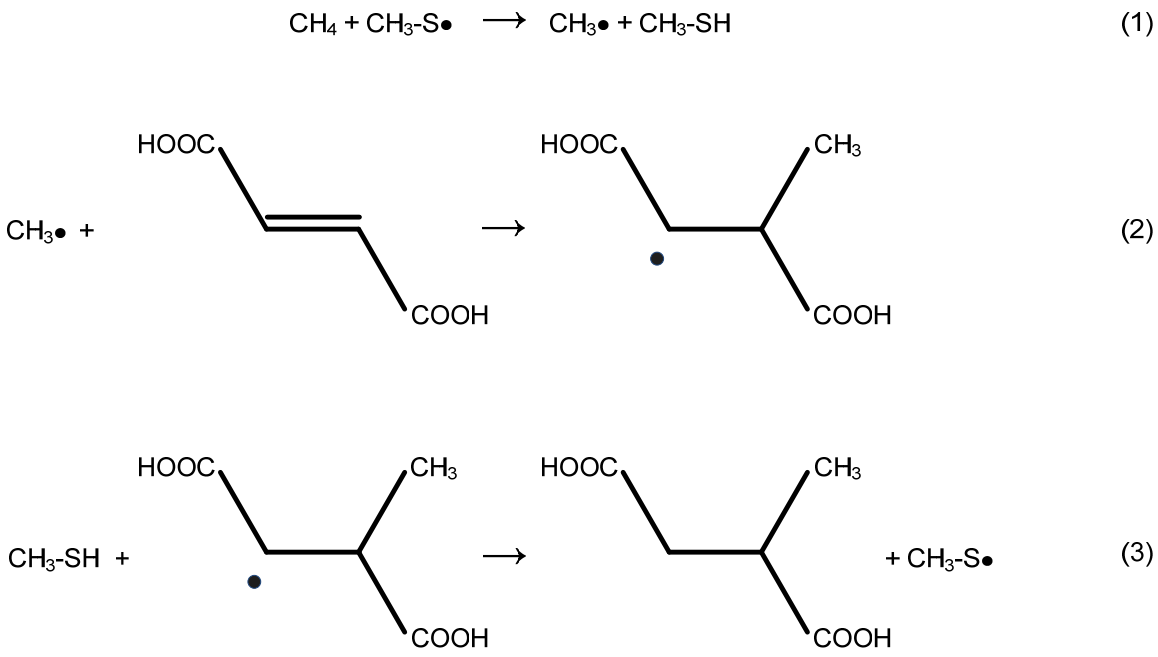

Figure 3.1 Theoretical reactions: fumarate addition to methane based on the mechanism established for anaerobic biodegradation of larger alkane substrates (Suflita et al. 2004 (31), Gieg and Suflita 2005 (32), Thauer and Shima 2008 (16), Callaghan et al. 2008 (38)). Methylthiol is used as the model enzyme active site.

Therefore, it is probable that fumarate addition is a mechanism responsible for initiating AOM under some conditions, especially in hydrocarbon reservoirs and environments contaminated by low molecular weight hydrocarbons.

The model in this study focuses on methane as a substrate because of the evidence suggesting its potential for reacting by a fumarate addition mechanism, and its importance in atmospheric chemistry and global temperature regulation. In addition, some chemical properties of methane make it a good model compound for a number of other reasons. The small size of the methane molecule translates into faster computation times; this factor makes it a good starting point for geometry optimization calculations. The molecular stability and low aqueous solubility of methane make it an ideal model substrate in efforts to define the limits of energy barriers and minimal energy requirements for growth in reactions activated by glycyl radical-containing enzymes. If AOM via fumarate addition is shown to occur cometabolically during fumarate addition to larger alkanes, then methane is similar enough to the alkanes acting as the primary substrates to be activated by the glycyl radical-containing enzymes. In that case the potential energy surface (PES) provides insight into substrate properties that prevent or support complete mineralization; making methane a good model substrate for anaerobic biodegradation of alkanes via fumarate addition.

This work attempts to determine potential energy barriers to give more insight into the likelihood of this reaction and to learn more about substrate preferences and the energetic boundaries of microbially mediated anaerobic oxidation. For the purposes of this analysis, the initial reaction mechanism of AOM via fumarate addition is hypothesized to be analogous to the degradation mechanism proposed for larger n-

alkanes (31, 32) by alkylsuccinate synthase (38). Alkylsuccinate synthase is a glycyl radical containing enzyme that can facilitate fumarate addition to C_6-C_8 (39) and C_{13}-C_{18} hydrocarbons (40) under nitrate- and sulfate-reducing conditions, respectively. The alkylsuccinate sythanase gene product has been shown to be involved in anaerobic biodegradation of n-hexadecane (38). The assA1 gene has also shown potential as a biomarker for fumarate addition of alkanes and has been found in environments in which alkylsuccinate intermediates have been isolated (41). The analogous AOM reaction with the glycyl radical-containing enzyme is the radical addition of fumarate to methane to form 2-methylsuccinate (16). The theoretical reaction is shown in Figure 3.1.

The purpose of this investigation was to perform quantum chemical calculations to investigate the energetics of the fumarate addition reactions of methane as mediated by alkylsuccinate synthase (as shown in Figure 3.1). The output was used to create a PES containing the stationary points relevant to this mechanism. Equilibrium geometry determinations and intrinsic reaction coordinate (IRC) analyses revealed the barriers and confirmed the transition state structures for those stationary points. The PES was analyzed to determine if the overall reaction would occur as theorized, what the transition state structures look like and to discuss the likelihood of the processes based on the potential energy barriers calculated.

Methods

Computational Approach. Geometry optimization and frequency calculations were computed using both Gaussian 03 (42) and 09 (43). A PES for the proposed fumarate addition reaction for methane was generated using the unrestricted B3LYP exchange-correlation functional (44-46) with the 6-31+G(d,p) basis set. Once stationary points

were located, the resulting zero-point energies were scaled by 0.9786 (47) before being added to the summed electronic energies. Frequency calculations were performed to verify that the resulting minima and transition states had no imaginary frequencies and one imaginary frequency, respectively. Transition state structure analyses were conducted using a number of different techniques. Initial guesses for structures were obtained using molecular mechanics, quadratic synchronous transit methods, potential surface scans and relaxed scans. Saddle points were then located using the Berny algorithm. Visualization of the molecular displacement corresponding to the transition vector (using GaussView 3.09 (48)) as well as IRC analyses were used to confirm transition state structures. All calculations were performed using an ultrafine (99,590) integration grid of the density. Calculations were run assuming a gas-phase reaction model and solvation effects were not taken into account.

Enzyme model. In the absence of further knowledge of the enzyme responsible for AOM by fumarate addition, we assumed that the theoretical reaction proceeded in a manner analogous to that of alkylsuccinate synthase activation of larger alkanes (38). Based on evidence that glycine and cysteine residue components in the alkylsuccinate synthase gene assA are conserved and their locations consistent with other glycyl radical-containing enzymes such as benzylsuccinate synthase (BSS) (38), we assume that the active site is the thiyl radical component of the cysteine residue as it is for BSS activation of alkylaromatic hydrocarbons. Therefore, methylthiol was used as the model of the cysteine residue that reacts with methane. This model is consistent with previous studies modeling fumarate addition reactions activated by BSS (49) and pyruvate formate-lyase

(50). And, similar S-H bond strengths (50-52) and spin densities (53) were calculated for methylthiol and larger, more accurate, models of the cysteine residue.

Substrate Conformations. Three different conformations of fumarate were included in this analysis as reactants. The nomenclature used to refer to these conformations is defined in Figure 3.2 along with their corresponding intermediate compounds. The fumarate conformations differ only in the dihedral angle made by atoms 1, 2, 3, and 4 (∠1-2-3-4) or 3, 4, 5, and 6 (∠3-4-5-6). The four possible intermediate compounds that result differ in these angles as well as which carbon atom of fumarate the methane adds to in the model (atom #3 or atom #4).

Results

The numerical results of the calculations are depicted in Figures 3.3 and 3.4. Figure 3.3 shows the PES and optimized equilibrium geometry for fumarate-0,0, the most energetically favorable reaction calculated, and Figure 3.4 shows the relative energy output for all fumarate conformations. In this section, the results from Figure 3.3 are discussed step by step.

The first step modeled is the homolytic cleavage of the nonpolar C-H bond in methane by the methylthiyl radical (Figure 3.1, reaction 1). The results show that this step has a barrier of 22.2 kcal/mol and is highly endothermic (20.6 kcal/mol). As predicted based on the calculated energies, the geometry of the optimized transition state (Figure 3.5, TS1) more closely resembles that of the products as the bond length from the transferred H atom to the C atom of the methyl group is 1.68 Å (1.09 Å in methane) and 1.43 Å to the sulfur atom of the thiyl group (1.35 Å in methyl thiol). TS1 has one imaginary frequency of 417 cm^{-1}.

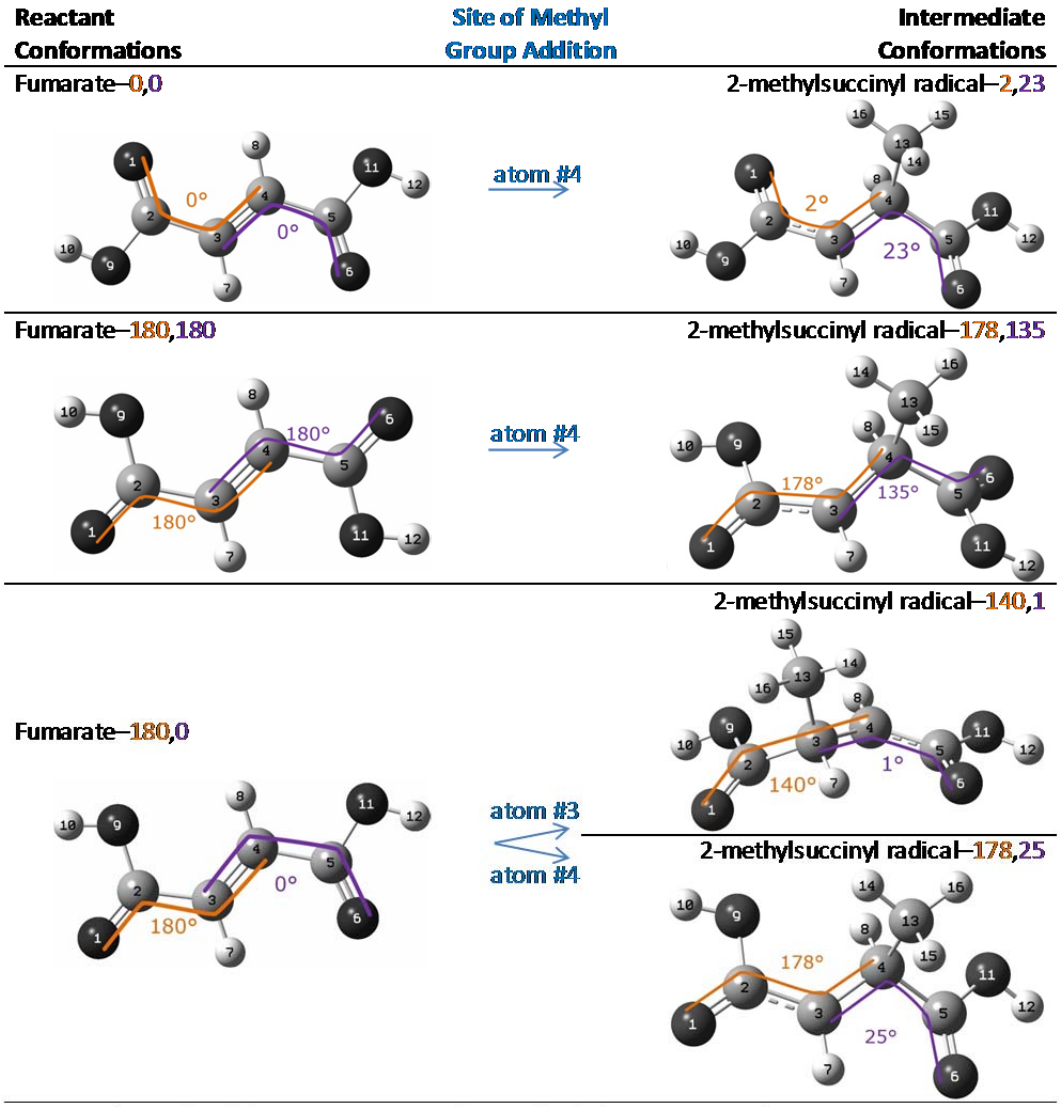

Figure 3.2. Conformations of fumarate and reaction intermediates defined.

The second step modeled is the creation of the C-C bond between the methyl radical and one of the carbon atoms from the C-C double bond of fumarate to form the 2-methylsuccinyl radical (Figure 3.1, reaction 2). Since the relative potential energy values for the three conformations of fumarate are similar for reactions 2 and 3, the values for fumarate-0,0 only are discussed here (the optimized equilibrium geometric arrangements for the different conformations do vary, however, and are discussed further in the next section). The energy barrier calculated for this step is 4.4 kcal/mol and the step is exothermic by 23.9 kcal/mol. Considering this step in conjunction with the previous step, the overall calculated barrier is 25.0 kcal/mol, therefore the formation of this bond is the rate limiting step with a final overall energy of -3.3 kcal/mol. The transition state structure for step 2 (Figure 3.5, TS2-0,0) has one imaginary frequency of 281 cm^{-1}. The distance from fumarate to the methyl radical is 2.46 Å and the fumarate portion is still fairly planar. The new C-C bond in the product, 2-methylsuccinyl radical-2,23, has a bond length of 1.56 Å and the fumarate portion is more distorted rather than planar.

The final step in the proposed reaction is the H atom transfer from methyl thiol to the 2-methylsuccinyl radical to form 2-methylsuccinic acid (Figure 3.1, reaction 3). This step has a calculated barrier of 5.1 kcal/mol and is exothermic by 7.9 kcal/mol. The transition state structure for this step (Figure 3.5, TS3-0,0) has one imaginary frequency of 1099 cm^{-1}. As predicted by the relative energy output, the TS structure more closely resembles the 2-methylsuccinyl radical intermediate and methylthiol rather than 2-methylsuccinic acid. The transferred H atom is 1.49 Å from the sulfur atom and 1.51 Å from the carbon (1.35 Å in methylthiol and 1.09 Å in 2-methylsuccinic acid). The final relative energy of all three steps is -11.2 kcal/mol.

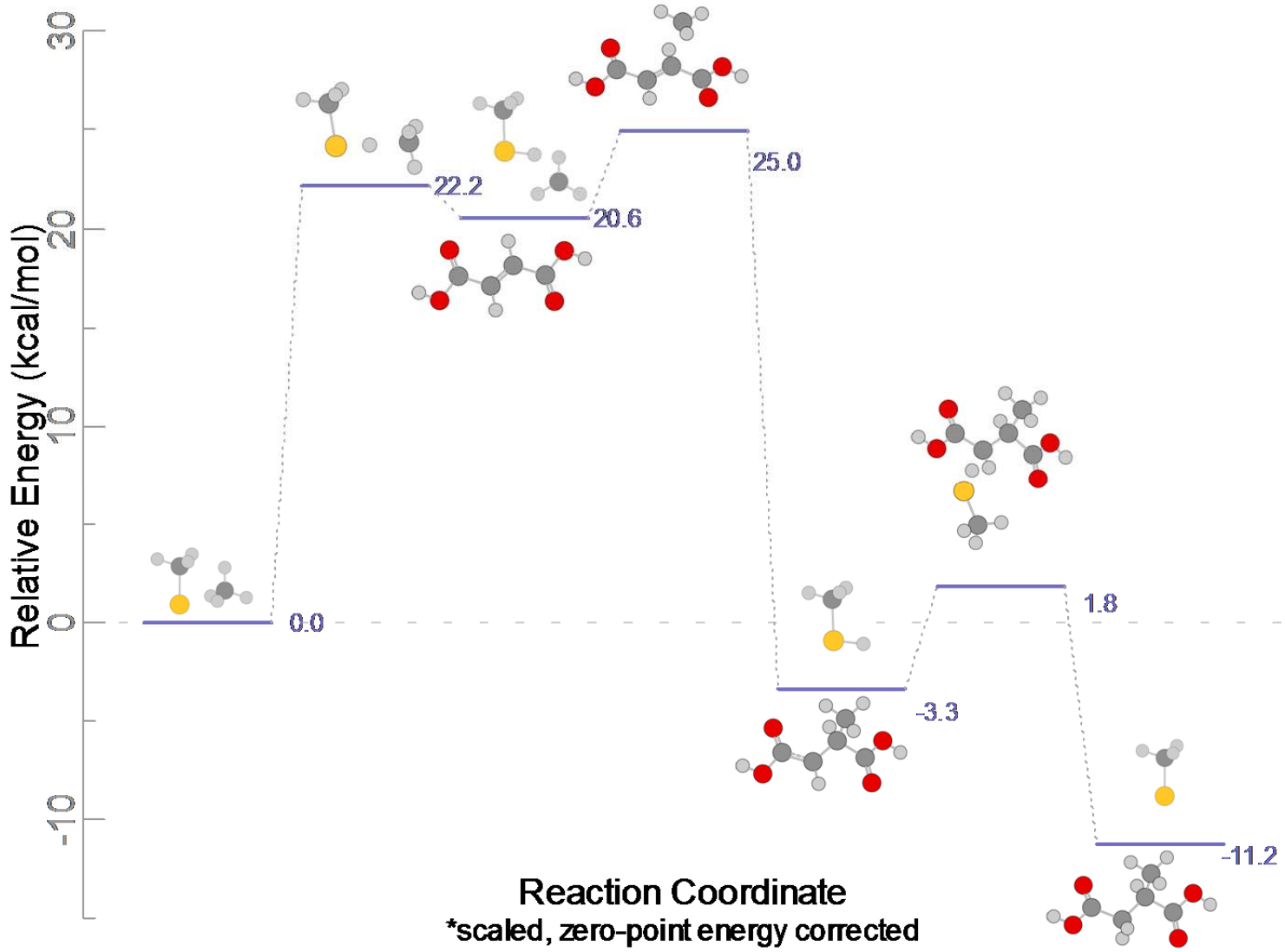

Figure 3.3 Potential energy surface for the radical addition of methane to fumarate-0,0.

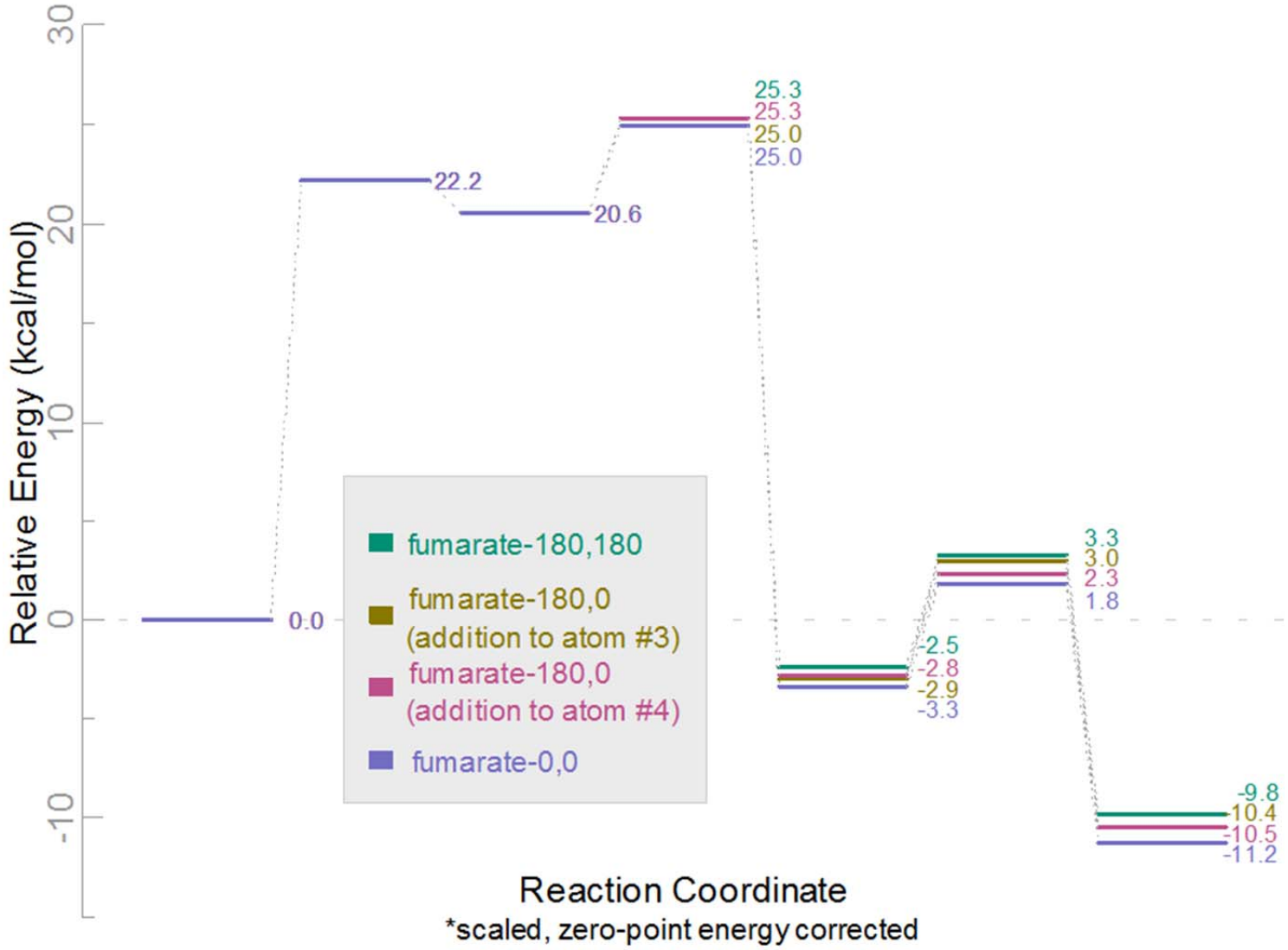

Figure 3.4 Potential energy surface for the radical addition of methane to three different conformations of fumarate.

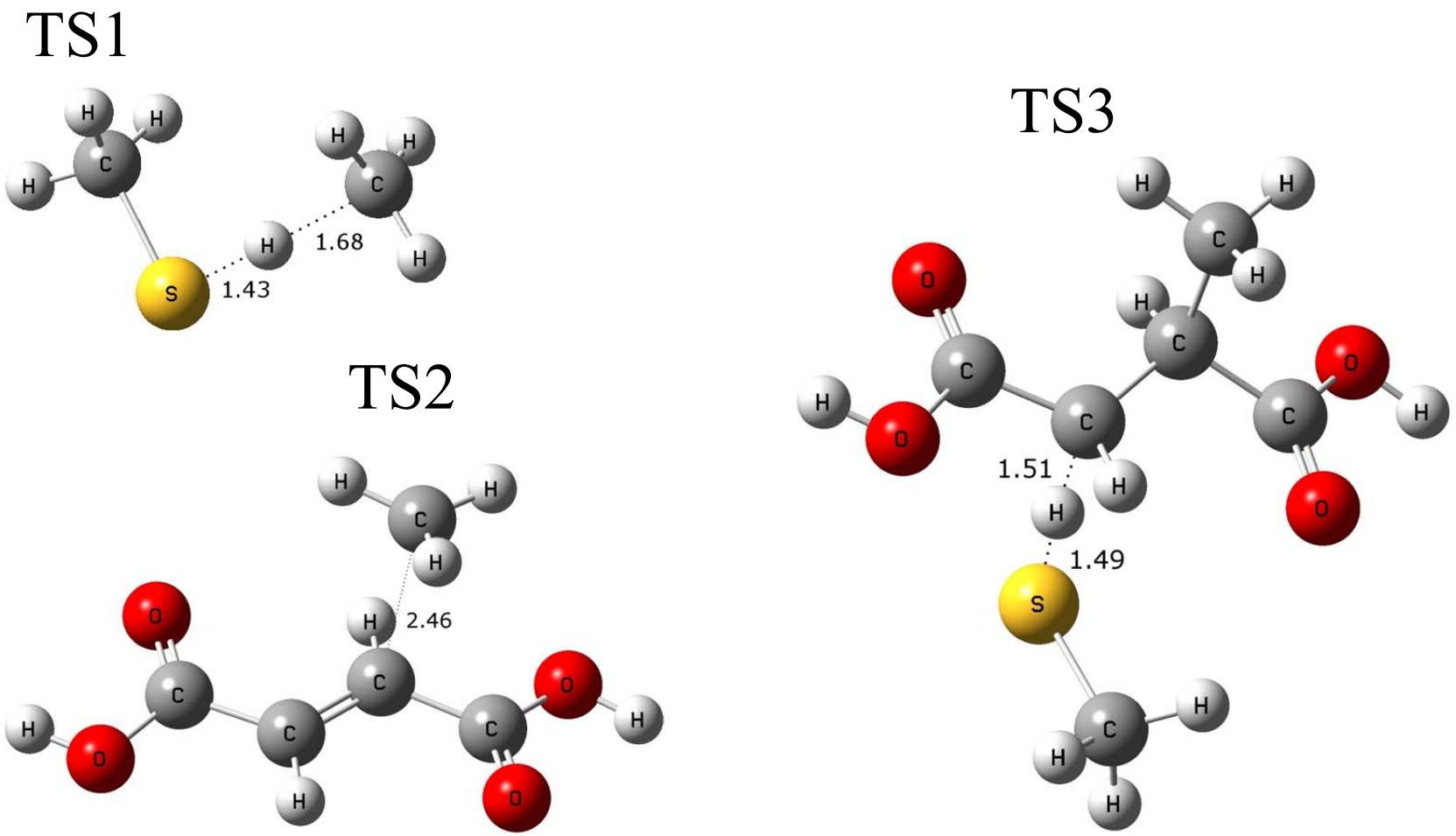

Figure 3.5 Geometries for TS1, TS2-0,0, and TS3-0,0. (Bond lengths are reported in Å.)

Discussion

Small n-alkanes are considered relatively unreactive under anaerobic conditions, yet AOM is an important process by which large amounts of methane generated in marine sediments are prevented from entering the water column. Many details of how the microorganisms in these specialized environments perform these conversions are unknown. This study used quantum chemical computations to quantify the electronic barriers of a plausible theoretical mechanism, AOM via fumarate addition (presented in Figures 3.3 and 3.4). The PES displayed in Figure 3.4 shows that step 1 (Figure 3.1) is an unfavorable reaction, all other steps in the proposed reaction scheme are determined to be favorable and the overall energy change is calculated to be exothermic by 9.8 to 11.2 kcal/mol. The overall rate-limiting step is the addition of the methyl radical to fumarate to form a new C-C bond (54) with a barrier between 25.0 and 25.3 kcal/mol depending on the conformation of fumarate. In addition, IRC analyses confirmed the stationary points of interest on the PES presented in Figures 3.3 and 3.4. This suggests that each step in the reaction could proceed as presented in Figure 3.1 without forming any intermediates not shown.

The energetic barrier to this reaction is high and is consistent with the fact that the thiyl radical is much more stable than the methyl radical and the bond dissociation energy of the methane C-H bond is greater than that for the S-H bond in methyl thiol (52, 55). Therefore, it would be interesting to determine if and how an enzymatic system could be responsible for lowering the barrier to the C-C bond formation. The recent discovery of [4Fe-4S] clusters in BSS is consistent with two hypotheses of how this glycyl radical-containing enzyme facilitates the addition of fumarate to alkylbenzenes (56). One

potential role is based on mechanistic information about pyruvate formate lyase which suggests the involvement of FeS clusters in the stabilization of free electrons during the reduction of S-adenosylmethionine , an oxidizing substrate utilized in the generation of the glycyl radical (for a review see refs (57, 58)). Additionally, an investigation of FeS clusters in aconitase (another glycyl radical-containing enzyme) demonstrated their ability to bind substrate carboxyl groups (59), suggesting that FeS clusters could bind to the carboxyl groups of fumarate (56).

Whether or not 25.0 kcal/mol is a reasonable energy barrier for methanotrophs to overcome is unknown. For comparison, the C-C bond has also been shown to be the rate-limiting step in DFT calculations performed on BSS mediated degradation of toluene. However, the calculated barrier was much lower, 15 kcal/mol, and was calculated using the B3LYP method with a larger basis set than that used in this study (6-311+G(2d,2p)) (49, 53). While the mechanism is analogous to the fumarate addition mechanism presented here; the initial substrate is more prone to radical formation than methane due to the resonance stabilization from the benzyl group. So, it is possible that a comparison of the two substrates provides a range of the barriers to reactions from potentially the least to one of the most reactive substrates that undergo fumarate addition. Another useful comparison would be calculated barriers of methane versus other small n-alkanes, for example ethane or propane metabolism catalyzed by alkyl succinate synthase. The output from these calculations would contribute to the understanding of the probable substrate range and energetic range of glycyl radical-containing enzymes that catalyze radical addition across C-C double bonds.

The overall potential energy gain of 11.2 kcal/mol is likely sufficient for bacterial growth in the anaerobic freshwater and saltwater environments where AOM occurs. As the conversion is theoretical and microorganisms responsible for the reaction are not identified or characterized, a standard reference that serves as an appropriate starting point would be an energy gain of approximately 4.8 kcal/mol (20 kJ/mol electron donor), the minimum energy requirement for microbial growth of syntrophic bacteria in energy limited environments (60). This value was determined using enrichment cultures, and it is expected that microorganisms are more efficient under natural conditions (61, 62). Values based on a reaction transport model (using geochemical data from the Skagerrak Strait, Denmark) determined a minimum bioenergic requirement (ΔG_{BR}) for AOM of approximately 2.6 kcal/mol (11 kJ/mol of methane) (63). Of course these free energy values are dependent on environmental conditions. It is also possible that even for constant minimal energy requirements for microbial growth, ATP produced per electron transferred increases with depth in the marine environment, as energy released by the net AOM reaction changes (62). And, it is likely that the energy required to produce ATP varies with temperature, pressure, solution composition and substrate concentrations (64).

An analysis of transition state structures revealed that the optimized geometry for TS1 more closely resembles that of the products, whereas TS2 and TS3 geometries are more reactant-like (Figure 3.5). These results are consistent with the Hammond postulate and recent correlations developed between reaction enthalpy and transition state structures for carbon-centered radical additions to alkenes (65). The correlations were built using DFT calculations which showed a direct relationship between the

exothermicity of the radical addition reaction and a greater distance between the radical and alkene in the transition state structure (65).

In addition, the scans and IRC calculations performed in the pursuit of transition state structures showed that the PES is very flat (i.e., low imaginary frequency) around these stationary points. The dihedral angles of fumarate were altered a great deal in the process of accommodating the radical groups, but the resulting energies were not that much lower. As a result, analyses for transition state structures often required "verytight" convergence criteria for the geometry, small step sizes, and the use of an "ultrafine" integration grid for the density. For TS2 analysis, the transition state for one conformation was used as a starting point in finding the transition states for other conformations (i.e., a scan of the dihedral angles performed starting at one saddle point led to the saddle point for the other conformation). Finding TS3 structures using this method was not successful. Rather, scans from the products (of reaction 3) that incrementally lengthened the bond of interest were used and sometimes compared to scans that started with the reactants (of reaction 3). The point of overlap of the two scans was then used as a starting structure in the Berny algorithm.

The formation of succinic acid diastereomers has been demonstrated in investigations of alkane biodegradation (66, 67); whereas biodegradation of toluene demonstrated high stereoselectivity (68, 69). It is possible that a transition state structure in which fumarate is more planar and the PES is relatively flat (such as at the TS2 saddle point) provides more opportunity to form two enantiomers. These factors could account for the diastereomers found in equal amounts in systems demonstrating biodegradation of n-hexane (66) and n-dodecane (67).

Comparing the three different conformations of fumarate in the analysis leads to some insights with respect to the spatial requirements for the addition of the methyl radical to fumarate. Overall, the energy differences between the different conformations are not large (see Figure 3.4). Fumarate-0,0 is the conformation with the most favorable overall energy gain and fumarate-180,180 is least favorable overall. This could be due to steric factors, as the formation of 2-methylsuccinyl radical from fumarate-0,0 requires a distortion of approximately 22 degrees in the original dihedral angles (see Figure 3.2); whereas for fumarate-180,180, the distortion is 45 degrees. For both conformations, the length of the new C-C bond is calculated to be 1.56 Å. Though the overall difference in energy is small (1.4 kcal/mol), the electronic structure of fumarate-180,180 requires more space for the addition of the methyl group. This is further supported by an analysis of the methyl addition to fumarate-180,0. If the methyl group is added to atom #4, the distortion is 24 degrees (to form 2-methylsuccinyl radical-178,25), however the distortion is approximately 41 degrees when it is added to atom #3 (to form 2-methylsuccinyl radical-140,1). Perhaps the enzymatic mode of action is holding fumarate in a favorable geometry or providing radical stabilization. However, this analysis is limited as all calculations performed were gas-phase calculations and thus do not account for any constraints that the system has on how freely the molecules involved can move in the enzyme. Nor does the PES account for any kinetic energy in the system; therefore it is unknown how closely the in situ physical systems resemble the minimized reaction path.

Previous work suggests a connection between the spin density and polarizability of the benzyl radical intermediates and relative rates of substrate biodegradation via the fumarate addition reaction mechanism (70). Beasley et al. (2009) states, "[The]

correlation [found] suggests that compounds forming more stable alkylbenzyl radical intermediates biodegrade by fumarate addition more slowly than their counterparts forming less stable radicals." (70). Applying these conclusions to AOM via fumarate addition implies that the formation of methylsuccinnate would occur quickly since the methylene radical is very unstable. The unstable methylene radical intermediate would also be energetically expensive to form. As predicted based on bond dissociation energies, after reaction 1, the formation of the parent substrate has a lower activation energy (1.6 kcal/mol) than the formation of the 2-methylsuccinyl radical (4.7 and 4.4 kcal/mol). The ratio of these two values may prove to be an indicator of biodegradability of hydrocarbons via fumarate addition (70). Or perhaps (when comparing substrates that undergo fumarate addition) the difference between the energy of the initial radical formation and overall energy gain may give insight into the likelihood that the conversion takes place via this mechanism.

This work shows how the potential energy of this system changes as the atoms in fumarate and methane change in the theoretical reaction of AOM via fumarate addition. The results support the possibility of AOM via fumarate addition by the mechanism presented. However, the barrier to the reaction as modeled is high and would require that the microorganisms responsible for the transformation work by decreasing the energy to create the new C-C sigma bond. Or, perhaps the environment in which the reaction occurs is specialized so that it effectively reduces the minimal energy requirements for catabolism. The differences in the relative energies of all fumarate conformers is small, however, the molecular conformation offering the most space for the methyl group addition has the lowest energy barriers and greatest overall energy gain.

Acknowledgments

We thank Dr. Joseph Suflita (University of Oklahoma, Department of Botany and Microbiology; University of Oklahoma, Institute for Energy and the Environment), Dr. Ralph Wheeler (Duquesne University, Department of Chemistry and Biochemistry), Dr. Paul Cook (University of Oklahoma, Department of Chemistry and Biochemistry), Dr. Scott Boesch (University of Oklahoma, Department of Chemistry and Biochemistry), and Dr. William Beasley (Howard Live Oak, LLC) for their advice and input in the academic areas of Microbiology, Computational Chemistry, Biochemistry, Statistics, and the graphical representation of data. Some of the computing for this project was performed at the OU Supercomputing Center for Education and Research (OSCER) at the University of Oklahoma. Dr. Charles Rice (University of Oklahoma, Department of Chemistry and Biochemistry), Henry Neeman (OSCER Director), Brandon George (Manager of Operations), and David Akin (Senior Systems Administrator) provided valuable technical expertise and resources. Financial support was provided in part by a Department of Education Graduate Assistance in Areas of National Need Fellowship (Award No. P200A030155). Any findings, opinions, or conclusions are those of the author and not necessarily those of the funding agencies.

Literature Cited

(1) Reeburgh, W. S. Oceanic Methane Biogeochemistry. *Chemical Reviews* **2007,** *107* (2), 486-513.

(2) Beal, E. J.; Claire, M. W.; House, C. H. High rates of anaerobic methanotrophy at low sulfate concentrations with implications for past and present methane levels. *Geobiology* **2011,** *9* (2), 131-139.

(3) Håvelsrud, O. E.; Haverkamp, T. H. A.; Kristensen, T.; Jakobsen, K. S.; Rike, A. G. A metagenomic study of methanotrophic microorganisms in Coal Oil Point seep sediments. *BMC Microbiology* **2011,** *11*.

(4) Ettwig, K. F.; van Alen, T.; van de Pas-Schoonen, K. T.; Jetten, M. S. M.; Strous, M. Enrichment and Molecular Detection of Denitrifying Methanotrophic Bacteria of the NC10 Phylum. *Applied and Environmental Microbiology* **2009,** *75* (11), 3656-3662.

(5) Deutzmann, J. S.; Schink, B. Anaerobic Oxidation of Methane in Sediments of Lake Constance, an Oligotrophic Freshwater Lake. *Applied and Environmental Microbiology* **2011,** *77* (13), 4429-4436.

(6) Raghoebarsing, A. A.; Pol, A.; van de Pas-Schoonen, K. T.; Smolders, A. J. P.; Ettwig, K. F.; Rijpstra, W. I. C.; Schouten, S.; Damste, J. S. S.; Op den Camp, H. J. M.; Jetten, M. S. M.; Strous, M. A microbial consortium couples anaerobic methane oxidation to denitrification. *Nature* **2006,** *440* (7086), 918-921.

(7) Smith, R. L.; Howes, B. L.; Garabedian, S. P. In situ measurement of methane oxidation in groundwater by using natural-gradient tracer tests. *Applied and Environmental Microbiology* **1991,** *57* (7), 1997-2004.

(8) Eller, G.; Kanel, L. K.; Kruger, M. Cooccurrence of aerobic and anaerobic methane oxidation in the water column of lake plusssee. *Applied and Environmental Microbiology* **2005,** *71* (12), 8925-8928.

(9) Murase, J.; Kimura, M. Methane production and its fate in paddy fields. 6. Anaerobic oxidation of methane in plow layer soil. *Soil Science and Plant Nutrition* **1994,** *40* (3), 505-514.

(10) Murase, J.; Kimura, M. Methane production and its fate in paddy fields. 7. Electron accepters responsible for anaerobic methane oxidation. *Soil Science and Plant Nutrition* **1994,** *40* (4), 647-654.

(11) Smemo, K. A.; Yavitt, J. B. Evidence for anaerobic CH_4 oxidation in freshwater peatlands. *Geomicrobiology Journal* **2007,** *24* (7-8), 583-597.

(12) Grossman, E. L.; Cifuentes, L. A.; Cozzarelli, I. M. Anaerobic methane oxidation in a landfill-leachate plume. *Environmental Science & Technology* **2002,** *36* (11), 2436-2442.

(13) Islas-Lima, S.; Thalasso, F.; Gomez-Hernandez, J. Evidence of anoxic methane oxidation coupled to denitrification. *Water Research* **2004,** *38* (1), 13-16.

(14) Conrad, R. The global methane cycle: recent advances in understanding the microbial processes involved. *Environmental Microbiology Reports* **2009,** *1* (5), 285-292.

(15) Hinrichs, K. U.; Boetius, A. The Anaerobic Oxidation of Methane: New Insights in Microbial Ecology and Biogeochemistry. In *Ocean Margin Systems*, Wefer, G.;

Billett, D.; Hebbeln, D.; Jørgensen, B.; Schlüter, M.; Van Weering, T., Eds. Springer-Verlag Berlin Heidelberg: 2002; pp 457-477.

(16) Thauer, R. K.; Shima, S. Methane as fuel for anaerobic microorganisms. *Annals of the New York Academy of Sciences* **2008,** *1125*, 158-170.

(17) Ettwig, K. F.; Butler, M. K.; Le Paslier, D.; Pelletier, E.; Mangenot, S.; Kuypers, M. M. M.; Schreiber, F.; Dutilh, B. E.; Zedelius, J.; de Beer, D.; Gloerich, J.; Wessels, H. J. C. T.; van Alen, T.; Luesken, F.; Wu, M. L.; van de Pas-Schoonen, K. T.; den Camp, H. J. M. O.; Janssen-Megens, E. M.; Francoijs, K.-J.; Stunnenberg, H.; Weissenbach, J.; Jetten, M. S. M.; Strous, M. Nitrite-driven anaerobic methane oxidation by oxygenic bacteria. *Nature* **2010,** *464* (7288), 543-550.

(18) Scheller, S.; Goenrich, M.; Boecher, R.; Thauer, R. K.; Jaun, B. The key nickel enzyme of methanogenesis catalyses the anaerobic oxidation of methane. *Nature* **2010,** *465* (7298), 606-609.

(19) Hinrichs, K. U.; Hayes, J. M.; Sylva, S. P.; Brewer, P. G.; DeLong, E. F. Methane-consuming archaebacteria in marine sediments. *Nature* **1999,** *398* (6730), 802-805.

(20) Boetius, A.; Ravenschlag, K.; Schubert, C. J.; Rickert, D.; Widdel, F.; Gieseke, A.; Amann, R.; Jørgensen, B. B.; Witte, U.; Pfannkuche, O. A marine microbial consortium apparently mediating anaerobic oxidation of methane. *Nature* **2000,** *407* (6804), 623-626.

(21) Thauer, R. K. Anaerobic oxidation of methane with sulfate: on the reversibility of the reactions that are catalyzed by enzymes also involved in methanogenesis from CO_2. *Current Opinion in Microbiology* **2011,** *14* (3), 292-299.

(22) Hallam, S. J.; Girguis, P. R.; Preston, C. M.; Richardson, P. M.; DeLong, E. F. Identification of methyl coenzyme M reductase A (mcrA) genes associated with methane-oxidizing archaea. *Applied and Environmental Microbiology* **2003,** *69* (9), 5483-5491.

(23) Hallam, S. J.; Putnam, N.; Preston, C. M.; Detter, J. C.; Rokhsar, D.; Richardson, P. M.; DeLong, E. F. Reverse methanogenesis: Testing the hypothesis with environmental genomics. *Science* **2004,** *305* (5689), 1457-1462.

(24) Knittel, K.; Boetius, A. Anaerobic Methane Oxidizers. In *Handbook of Hydrocarbon and Lipid Microbiology*, Timmis, K. N., Ed. Springer-Verlag: Berlin Heidelberg, 2010; pp 2023-2032.

(25) Ettwig, K. F.; Shima, S.; van de Pas-Schoonen, K. T.; Kahnt, J.; Medema, M. H.; op den Camp, H. J. M.; Jetten, M. S. M.; Strous, M. Denitrifying bacteria

anaerobically oxidize methane in the absence of *Archaea*. *Environmental Microbiology* **2008,** *10* (11), 3164-3173.

(26) Wu, M. L.; Ettwig, K. F.; Jetten, M. S. M.; Strous, M.; Keltjens, J. T.; van Niftrik, L. A new intra-aerobic metabolism in the nitrite-dependent anaerobic methane-oxidizing bacterium *Candidatus* 'Methylomirabilis oxyfera'. *Biochemical Society Transactions* **2011,** *39*, 243-248.

(27) Caldwell, S. L.; Laidler, J. R.; Brewer, E. A.; Eberly, J. O.; Sandborgh, S. C.; Colwell, F. S. Anaerobic oxidation of methane: Mechanisms, bioenergetics, and the ecology of associated microorganisms. *Environmental Science & Technology* **2008,** *42* (18), 6791-6799.

(28) Beal, E. J.; House, C. H.; Orphan, V. J. Manganese- and Iron-Dependent Marine Methane Oxidation. *Science* **2009,** *325* (5937), 184-187.

(29) Heider, J. Adding handles to unhandy substrates: anaerobic hydrocarbon activation mechanisms. *Current Opinion in Chemical Biology* **2007,** *11* (2), 188-194.

(30) Boll, M.; Heider, J. Anaerobic Degradation of Hydrocarbons: Mechanisms of C–H-Bond Activation in the Absence of Oxygen. In *Handbook of Hydrocarbon and Lipid Microbiology*, Timmis, K. N., Ed. Springer-Verlag: Berlin Heidelberg, 2010; pp 1011-1024.

(31) Suflita, J. M.; Davidova, I. A.; Gieg, L. M.; Nanny, M.; Prince, R. C. Anaerobic hydrocarbon biodegradation and the prospects for microbial enhanced energy production. In *Studies in Surface Science and Catalysis* **2004,** *151*, 283-305.

(32) Gieg, L. M.; Suflita, J. M. Metabolic indicators of anaerobic hydrocarbon biodegradation in petroleum-laden environments. In *Petroleum Microbiology* **2005**, 337-356.

(33) Mbadinga, S.M.; Wang, L.; Zhou, L.; Liu, J.F.; Gu, J.D.; Mu, B.Z. Microbial communities involved in anaerobic degradation of alkanes. *International Biodeterioration & Biodegradation* **2011,** *65* (1), 1-13.

(34) Savage, K. N.; Krumholz, L. R.; Gieg, L. M.; Parisi, V. A.; Suflita, J. M.; Allen, J.; Philp, R. P.; Elshahed, M. S. Biodegradation of low-molecular-weight alkanes under mesophilic, sulfate-reducing conditions: metabolic intermediates and community patterns. *Fems Microbiology Ecology* **2010,** *72* (3), 485-495.

(35) Kniemeyer, O.; Musat, F.; Sievert, S. M.; Knittel, K.; Wilkes, H.; Blumenberg, M.; Michaelis, W.; Classen, A.; Bolm, C.; Joye, S. B.; Widdel, F. Anaerobic oxidation of short-chain hydrocarbons by marine sulphate-reducing bacteria. *Nature* **2007,** *449*, 898-902.

(36) Duncan, K. E.; Gieg, L. M.; Parisi, V. A.; Tanner, R. S.; Green Tringe, S.; Bristow, J.; Suflita, J. M. Biocorrosive Thermophilic Microbial Communities in Alaskan North Slope Oil Facilities. *Environmental Science & Technology* **2009,** *43* (20), 7977-7984.

(37) Wilkes, H.; Rabus, R.; Fischer, T.; Armstroff, A.; Behrends, A.; Widdel, F. Anaerobic degradation of n-hexane in a denitrifying bacterium: Further degradation of the initial intermediate (1-methylpentyl)succinate via C-skeleton rearrangement. *Archives of Microbiology* **2002,** *177* (3), 235-243.

(38) Callaghan, A. V.; Wawrik, B.; Chadhain, S. M. N.; Young, L. Y.; Zylstra, G. J. Anaerobic alkane-degrading strain AK-01 contains two alkylsuccinate synthase genes. *Biochemical and Biophysical Research Communications* **2008,** *366* (1), 142-148.

(39) Grundmann, O.; Behrends, A.; Rabus, R.; Amann, J.; Halder, T.; Heider, J.; Widdel, F. Genes encoding the candidate enzyme for anaerobic activation of n-alkanes in the denitrifying bacterium, strain HxN1. *Environmental Microbiology* **2008,** *10* (2), 376-385.

(40) Callaghan, A. V.; Gieg, L. M.; Kropp, K. G.; Suflita, J. M.; Young, L. Y. Comparison of mechanisms of alkane metabolism under sulfate-reducing conditions among two bacterial isolates and a bacterial consortium. *Applied and Environmental Microbiology* **2006,** *72* (6), 4274-4282.

(41) Callaghan, A. V.; Davidova, I. A.; Savage-Ashlock, K.; Parisi, V. A.; Gieg, L. M.; Suflita, J. M.; Kukor, J. J.; Wawrik, B. Diversity of Benzyl- and Alkylsuccinate Synthase Genes in Hydrocarbon-Impacted Environments and Enrichment Cultures. *Environmental Science & Technology* **2010,** *44* (19), 7287-7294.

(42) Frisch, M. J. T., G. W.; Schlegel, H. B.; Scuseria, G. E.; Robb, M. A.; Cheeseman, J. R.; Montgomery, Jr., J. A.; Vreven, T.; Kudin, K. N.; Burant, J. C.; Millam, J. M.; Iyengar, S. S.; Tomasi, J.; Barone, V.; Mennucci, B.; Cossi, M.; Scalmani, G.; Rega, N.; Petersson, G. A.; Nakatsuji, H.; Hada, M.; Ehara, M.; Toyota, K.; Fukuda, R.; Hasegawa, J.; Ishida, M.; Nakajima, T.; Honda, Y.; Kitao, O.; Nakai, H.; Klene, M.; Li, X.; Knox, J. E.; Hratchian, H. P.; Cross, J. B.; Bakken, V.; Adamo, C.; Jaramillo, J.; Gomperts, R.; Stratmann, R. E.; Yazyev, O.; Austin, A. J.; Cammi, R.; Pomelli, C.; Ochterski, J. W.; Ayala, P. Y.; Morokuma, K.; Voth, G. A.; Salvador, P.; Dannenberg, J. J.; Zakrzewski, V. G.; Dapprich, S.; Daniels, A. D.; Strain, M. C.; Farkas, O.; Malick, D. K.; Rabuck, A. D.; Raghavachari, K.; Foresman, J. B.; Ortiz, J. V.; Cui, Q.; Baboul, A. G.; Clifford, S.; Cioslowski, J.; Stefanov, B. B.; Liu, G.; Liashenko, A.; Piskorz, P.; Komaromi, I.; Martin, R. L.; Fox, D. J.; Keith, T.; Al-Laham, M. A.; Peng, C. Y.; Nanayakkara, A.; Challacombe, M.; Gill, P. M. W.; Johnson, B.; Chen, W.;

Wong, M. W.; Gonzalez, C.; and Pople, J. A. *Gaussian 03, Revision C.02*, Gaussian, Inc.: Wallingford, CT, 2004.

(43) Frisch, M. J. T., G. W.; Schlegel, H. B.; Scuseria, G. E.; Robb, M. A.; Cheeseman, J. R.; Scalmani, G.; Barone, V.; Mennucci, B.; Petersson, G. A.; Nakatsuji, H.; Caricato, M.; Li, X.; Hratchian, H. P.; Izmaylov, A. F.; Bloino, J.; Zheng, G.; Sonnenberg, J. L.; Hada, M.; Ehara, M.; Toyota, K.; Fukuda, R.; Hasegawa, J.; Ishida, M.; Nakajima, T.; Honda, Y.; Kitao, O.; Nakai, H.; Vreven, T.; Montgomery, Jr., J. A.; Peralta, J. E.; Ogliaro, F.; Bearpark, M.; Heyd, J. J.; Brothers, E.; Kudin, K. N.; Staroverov, V. N.; Kobayashi, R.; Normand, J.; Raghavachari, K.; Rendell, A.; Burant, J. C.; Iyengar, S. S.; Tomasi, J.; Cossi, M.; Rega, N.; Millam, N. J.; Klene, M.; Knox, J. E.; Cross, J. B.; Bakken, V.; Adamo, C.; Jaramillo, J.; Gomperts, R.; Stratmann, R. E.; Yazyev, O.; Austin, A. J.; Cammi, R.; Pomelli, C.; Ochterski, J. W.; Martin, R. L.; Morokuma, K.; Zakrzewski, V. G.; Voth, G. A.; Salvador, P.; Dannenberg, J. J.; Dapprich, S.; Daniels, A. D.; Farkas, Ö.; Foresman, J. B.; Ortiz, J. V.; Cioslowski, J.; Fox, D. J. *Gaussian 09, Revision A.1*, Gaussian, Inc.: Wallingford, CT, 2009.

(44) Becke, A. D. Density-functional thermochemistry. III. The role of exact exchange. *Journal of Chemical Physics* **1993,** *98* (7), 5648-5652.

(45) Becke, A. D. A new mixing of Hartree-Fock and local density-functional theories. *Journal of Chemical Physics* **1993,** *98* (2), 1372-1377.

(46) Becke, A. D. Density-functional exchange-energy approximation with correct asymptotic-behavior. *Physical Review A* **1988,** *38* (6), 3098-3100.

(47) Irikura, K. K.; Johnson III, R. D.; Kacker, R. N.; Kessel, R. Uncertainties in scaling factors for ab initio vibrational zero-point energies. *Journal of Chemical Physics* **2009,** *130* (11), 114102-1-11.

(48) Dennington II, R., Keith, T., Millam, J., Eppinnett, K., Hovell, W.L., Ray Gilliland, R. *GaussView, Version 3.09*, Semichem, Inc.: Shawnee Mission, KS, 2003.

(49) Himo, F. Catalytic mechanism of benzylsuccinate synthase, a theoretical study. *Journal of Physical Chemistry B* **2002,** *106* (31), 7688-7692.

(50) Himo, F.; Eriksson, L. A. Catalytic mechanism of pyruvate formate-lyase (PFL). A theoretical study. *Journal of the American Chemical Society* **1998,** *120* (44), 11449-11455.

(51) Guo, J. D.; Luo, Y.; Himo, F. DNA repair by spore photoproduct lyase: A density functional theory study. *Journal of Physical Chemistry B* **2003,** *107* (40), 11188-11192.

(52) Rauk, A.; Yu, D.; Armstrong, D. A. Oxidative damage to and by cysteine in proteins: An ab initio study of the radical structures, C-H, S-H, and C-C bond dissociation energies, and transition structures for H abstraction by thiyl radicals. *Journal of the American Chemical Society* **1998,** *120* (34), 8848-8855.

(53) Himo, F. C-C bond formation and cleavage in radical enzymes, a theoretical perspective. *Biochimica Et Biophysica Acta-Bioenergetics* **2005,** *1707* (1), 24-33.

(54) Murdoch, J. R. What is the rate-limiting step of a multistep reaction? *Journal of Chemical Education* **1981,** *58* (1), 32-36.

(55) Haynes, W. M. *CRC handbook of chemistry and physics*. 92nd ed.; CRC Press: Boca Raton, FL, 2011.

(56) Hilberg, M.; Pierik, A. J.; Bill, E.; Friedrich, T.; Lippert, M.-L.; Heider, J. Identification of FeS clusters in the glycyl-radical enzyme benzylsuccinate synthase via EPR and Mossbauer spectroscopy. *Journal of Biological Inorganic Chemistry* **2012,** *17* (1), 49-56.

(57) Frey, P. A.; Hegeman, A. D.; Ruzicka, F. J. The radical SAM superfamily. *Critical Reviews in Biochemistry and Molecular Biology* **2008,** *43* (1), 63-88.

(58) Vey, J. L.; Drennan, C. L. Structural Insights into Radical Generation by the Radical SAM Superfamily. *Chemical Reviews* **2011,** *111* (4), 2487-2506.

(59) Kennedy, M. C.; Werst, M.; Telser, J.; Emptage, M. H.; Beinert, H.; Hoffman, B. M. Mode of substrate carboxyl binding to the $[4Fe\text{-}4S]^{+}$ cluster of reduced aconitase as studied by ^{17}O and ^{13}C electron-nuclear double resonance spectroscopy. *Proceedings of the National Academy of Sciences of the United States of America* **1987,** *84* (24), 8854-8858.

(60) Schink, B. Energetics of syntrophic cooperation in methanogenic degradation. *Microbiology and Molecular Biology Reviews* **1997,** *61* (2), 262-280.

(61) Hoehler, T. M. Biological energy requirements as quantitative boundary conditions for life in the subsurface. *Geobiology* **2004,** *2* (4), 205-215.

(62) Regnier, P.; Dale, A. W.; Arndt, S.; LaRowe, D. E.; Mogollon, J.; Van Cappellen, P. Quantitative analysis of anaerobic oxidation of methane (AOM) in marine sediments: A modeling perspective. *Earth-Science Reviews* **2011,** *106* (1-2), 105-130.

(63) Dale, A. W.; Regnier, P.; Knab, N. J.; Jorgensen, B. B.; Van Cappellen, P. Anaerobic oxidation of methane (AOM) in marine sediments from the Skagerrak (Denmark): II. Reaction-transport modeling. *Geochimica Et Cosmochimica Acta* **2008,** *72* (12), 2880-2894.

(64) Larowe, D. E.; Helgeson, H. C. Quantifying the energetics of metabolic reactions in diverse biogeochemical systems: electron flow and ATP synthesis. *Geobiology* **2007,** *5* (2), 153-168.

(65) Lalevee, J.; Allonas, X.; Fouassier, J. P. Addition of carbon-centered radicals to double bonds: Influence of the alkene structure. *Journal of Organic Chemistry* **2005,** *70* (3), 814-819.

(66) Rabus, R.; Wilkes, H.; Behrends, A.; Armstroff, A.; Fischer, T.; Pierik, A. J.; Widdel, F. Anaerobic initial reaction of n-alkanes in a denitrifying bacterium: Evidence for (1-methylpentyl)succinate as initial product and for involvement of an organic radical in n-hexane metabolism. *Journal of Bacteriology* **2001,** *183* (5), 1707-1715.

(67) Kropp, K. G.; Davidova, I. A.; Suflita, J. M. Anaerobic oxidation of n-dodecane by an addition reaction in a sulfate-reducing bacterial enrichment culture. *Applied and Environmental Microbiology* **2000,** *66* (12), 5393-5398.

(68) Beller, H. R.; Spormann, A. M. Analysis of the novel benzylsuccinate synthase reaction for anaerobic toluene activation based on structural studies of the product. *Journal of Bacteriology* **1998,** *180* (20), 5454-5457.

(69) Leutwein, C.; Heider, J. Anaerobic toluene-catabolic pathway in denitrifying Thauera aromatica: activation and beta-oxidation of the first intermediate, (R)-(+)-benzylsuccinate. *Microbiology-Uk* **1999,** *145*, 3265-3271.

(70) Beasley, K. K.; Gieg, L. M.; Suflita, J. M.; Nanny, M. A. Polarizability and Spin Density Correlate with the Relative Anaerobic Biodegradability of Alkylaromatic Hydrocarbons. *Environmental Science & Technology* **2009,** *43* (13), 4995-5000.

Chapter 4

The Application of Density Functional Theory (DFT) Calculations to Anaerobic Hydrocarbon Biodegradation Research: Suggestions for Future Research

Abstract

In Chapter 3, the fumarate addition mechanism was examined in order to determine if it is an energetically feasible mechanism for microbially mediated anaerobic oxidation of methane (AOM). The future work proposed in this chapter (Chapter 4) is to expand that work to include ethane, propane, and butane as model substrates. The objective of this study would be to create four potential energy surfaces (PESs) for the initial radical addition reaction using quantum chemical calculations. The results would be used to determine the relative likelihood of each reaction in comparison to one another and to toluene, a more readily degraded substrate. PESs for the proposed fumarate addition reactions using methane, ethane, propane and butane as substrates would be generated using the unrestricted B3LYP/6-311+G(2d,2p) exchange-correlation functional and basis set. This basis set is larger than the one used in Chapter 3. One molecular conformation of fumarate (fumarate-0,0 in Figure 3.2) would be used to complete the calculations as it was determined to be most favorable in the results presented in Chapter 3.

Introduction

The studies presented in Chapters 2 and 3 demonstrate applications of density functional theory (DFT) calculations to anaerobic hydrocarbon biodegradation research. To describe the potential for use of chemical calculations in applications to anaerobic

hydrocarbon biodegradation this chapter briefly highlights the types of applications presented in Chapters 2 and 3. In addition, this chapter discusses a proposal for a future project that would be worthwhile to pursue in light of the results of the research presented in Chapters 2 and 3. Since the future research recommendations include computational calculations similar to those used previously, the methods section of this chapter discusses how the computational methods used in Chapter 3 would be applied to the proposed work and how they might be revised and why. The method section is followed by a discussion about the significance of the proposed study.

The computations performed in the studies previously presented in this dissertation were used to elucidate three types of information about chemical reactions: 1) the likelihood that a theoretical reaction will occur (Chapter 3), 2) the sequence by which the reaction occurs (Chapter 3), and 3) specific chemical properties to use as predictors of extent of the reaction (Chapter 2). Though there is a need for refined, mechanism specific quantitative structure activity relationships (QSARs) (1), using calculated chemical properties as predictors of biodegradation rates is not a goal of the proposed future research. Rather, the focus of the recommendations for future research in this chapter is the creation of more potential energy surfaces (PESs) for reactions of other substrates via fumarate addition.

In Chapter 3, the likelihood of a reaction occurring and the characterization of the reaction sequence were assessed by creating a PES. As discussed in Cramer (2004) (2) computational theory can play an effective role in the qualitative determination of the likelihood of a specific reaction based on the calculated barriers. A calculated PES elucidates likely steps in the reaction sequence and the number of transition states (2).

PES results can also provide information about reaction kinetics as reactions with higher reactions barriers occur more slowly (2).

Proposed Research

In furthering the application of computational chemistry to anaerobic hydrocarbon biodegradation, a logical next step from the work presented in Chapter 3 would be to expand the calculations completed to include more substrates. Specifically, to create PESs for microbially mediated fumarate addition to ethane, propane, and butane. Metabolite analyses provided evidence that propane and butane undergo anaerobic biodegradation by fumarate addition (3), whereas ethane (3) and methane (4) are suspected substrates for this mechanism (as discussed in Chapter 3). Evidence of ethane metabolism was demonstrated in enrichment culture incubations, though the observed rates were slower than those for propane and butane metabolism and the detection of fumarate addition metabolites was not reported (3). Of course, the different rates and lack of accumulation of metabolites are not solely dependent on formation kinetics. For example, in a system in which 2-methylsuccinic acid derivatives are not isolated, fumarate addition reaction intermediates of methane and ethane may react more rapidly than those of propane and butane, or aqueous concentrations of the substrates of interest and other compounds may affect the concentrations of methyl- and ethylsuccinic acid derivatives. However, since it is possible that ethane and methane are metabolized more slowly or cometabolically, they serve as good comparisons to the other two substrates.

Intrinsic reaction coordinate (IRC) calculations (as used in Chapter 3) would be required for the generation of the PESs, however, the determination of these paths for multiple substrates using a larger basis set also provides opportunity for another

application of DFT calculations to hydrocarbon biodegradation research. Reaction rates can be determined from IRC calculations using complex models (5) that provide an accuracy much greater than those based on activation energies. These theoretical rates can be compared to one another to determine relative biodegradability rates, and they also serve as comparisons to rates established in laboratory work. Enrichment cultures that can grow on ethane, propane and butane have been reported in previous studies (3, 6). Such cultures can be used to establish biodegradation rates and to isolate metabolites. Predicted rates can then be compared to rates calculated from IRC output. The comparison of substrate loss, metabolite formation and IRC rates provide evidence of the mechanism of biodegradation and substrate preference. If the calculated values correspond to laboratory derived data for ethane, propane and butane, methane oxidation rates may also be predicted.

Proposed Methods

With a few exceptions, the methods for this proposed work would be the same as those used in Chapter 3 (see the Methods section of Chapter 3). Definitions and details of these methods can be found in Appendices A and B, respectively. The DFT calculations performed for the study presented in Chapter 3 utilized the B3LYP method to calculate equilibrium geometries for energy minimums and transition states. This method has been used to characterize the energetics of enzymatic systems (for a review see ref (7)), determine mechanisms of biodegradation (8) and calculate predictors in QSARs (9). The B3LYP density functional theory method is widely used, scalable, and is considered to have an optimal balance between accuracy and computation time (or resources required)

(2, 5, 10, 11). The application of B3LYP to enzymatic reactions has been shown to be almost as accurate as resource-intensive ab intio methods (12).

Since a comparison of the energetics of the four proposed reactions could involve small differences in energy (of a few kcal/mol) these analyses would probably require a larger basis set for increased accuracy. While the 6-31+G(d,p) basis set (used in the work in Chapters 2 and 3) has accurately calculated enthalpies of formation for organic molecules (13), increasing the basis set increases the accuracy of the computations and should be done if the available computational resources allow. A benefit to increasing the size of the basis set after the completion of the study presented in Chapter 3 is that all of the geometries calculated in Chapter 3 could serve as an excellent starting point for initial guesses for all four proposed reactions. A good example of a basis set to use would be 6-311+G(2d,2p). Previously, this basis set was utilized in characterization studies for benzylsuccinate synthase (14) and pyruvate formate lyase (15) activated reactions, which allows the values to be compared to activation energies overcome by those enzymes. Additionally, calculations performed at this level of theory have a history of accurate predictions of thermodynamic and kinetic parameters for a variety of organic reactions (8, 16-18). The expected errors for both basis sets are within 3-5 kcal/mol (12). Both basis sets are available as built in basis sets in the Gaussian 09 software package (19).

The types of calculations that would be computed are the same as those calculated in Chapter 3. Equilibrium geometries would need to be located for the products, intermediates and products of each of the four reactions. The energies computed would then be corrected for zero-point energy contributions. For the zero-point energy (ZPE)

calculations reported in Chapter 3, a scale-factor of 0.9786 was used; the recommended correction for ZPE calculations using the B3LYP/6-31+g(d,p) basis set (20). Each ZPE was multiplied by this number before it was added to the sum of electronic energies. The same would be done using the larger basis set, though the corresponding scale-factor would change. The resulting values would be used to create the stationary points of the PESs.

The transition state analyses determine the structure and energy of the barriers to reaction. These would be completed as they were in Chapter 3 for methane, using relaxed scans, rigid scans and QST3 methods (quadratic synchronous transit; see the Discussion section of Chapter 3). One difference between this work and the previous work is that the transition states located in the PES presented in Chapter 3 may serve as good starting points for the searches at the higher level of theory. Transition state analyses involve locating a stationary point that is a first-order saddle point, meaning that the point represents a minimum in all directions of the PES with the exception of one. The transition state structure represents the maximum in the direction of the reaction coordinate of interest (5) (an example of a reaction coordinate of interest is presented in Chapter 3, Figure 3.3). Therefore, the second order derivatives of the potential energy, the Hessians, would be positive except for the one corresponding to the frequency of the movement of interest (5) (e.g., the lengthening of the C-H bond that is being homolytically abstracted).

Transition state structures would be confirmed using IRC calculations. These calculations determine if the saddle point located is – in fact – the energy maximum along the reaction path of interest (2). The IRCs calculated in Chapter 3 and proposed for

this study follow the path of steepest descent in two directions, beginning at the transition state structure and ending with the stationary points corresponding to its associated reactants and products (2). As discussed earlier, the calculations can also be used in the determination of reaction rates. However, IRC calculations would have to be performed at a high level of theory for this application.

One other point to consider for this proposed work that would differ from the work presented in Chapter 3 is using one molecular conformation of fumarate (fumarate-0,0 in Figure 3.2) to complete the calculations. The use of one conformation would significantly reduce the number of computations required for this analysis. As the fumarate-0,0 conformation was determined to be most favorable in the results presented in Chapter 3, that would be an appropriate starting point. On the other hand, linear and branched isomers of propane and butane should be considered to assess the impact that branching has on the energy and structure of the transition states (i.e., energy barriers).

Significance

The work proposed in this chapter is novel and important in several ways. First, the generated PESs would provide information about the geometries and energetics of four small n-alkanes as substrates in enzymatic reactions. Methane, ethane, propane and butane are the main constituents of natural gas (21), therefore the processes by which they biodegrade in anaerobic environments is of environmental significance. Processes controlling the concentrations of these compounds affect their potential to be fuel sources, hazards, and disturbances to natural environmental systems. For example, as discussed in Chapter 3, methane is an important substrate to investigate because of its importance in atmospheric chemistry. Microbially mediated anaerobic oxidation of

methane (AOM) reduces concentrations of dissolved methane in open ocean water and freshwater environments (for reviews see refs (22, 23)).

Second, the mechanism and microbial communities responsible for activating these initial oxidation reactions are not fully known. The data generated would be original geometries, energy values, and rates which represent the potential energy requirements for the conversion of methane, ethane, propane and butane via a potential reaction mechanism. The resulting PESs would provide original lines evidence that the oxidation of these substrates could proceed by the fumarate addition mechanism, and provide insight into substrate preferences of glycyl radical-containing enzymes. The resulting rates would provide tools for remediation strategies as well as information to characterize natural gas formation and degradation.

Third, the proposed calculations provide additional benchmarks for the work completed in Chapter 3. A comparison of energetic barriers and potential energy gains of methane and ethane to substrates that have been shown to undergo fumarate addition in laboratory experiments (i.e., propane and butane) would provide further insight into whether 25 kcal/mol is a realistic barrier to overcome and what sort of growth can be expected from an overall energy gain of 11.2 kcal/mol (see the results section of Chapter 3). In addition, the molecular stability and low aqueous solubility of all four compounds make them ideal model substrates in efforts to define the limits of energy barriers and minimal energy requirements for growth in reactions activated by glycyl radical-containing enzymes.

Fourth, studying fumarate addition to these small alkanes is also of significance because this mechanism represents a unique strategy by which microorganisms convert

inert substrates in the absence of oxygen. The application of the computational calculations described above to biological processes occurring in energy-limited environments contributes to the understanding of how small the amount of energy available to microorganisms can be. Determining the energy required to perform these conversions or catalyze these reactions is critical to learning more about the unique strategies microorganisms use to survive in energy-limited environments (for examples of these strategies see refs (24, 25)).

Finally, this work contributes information about the substrate range of fumarate addition, a major mechanism of anaerobic hydrocarbon biodegradation. The mechanism is of great environmental significance due to the fact that it is responsible for the attenuation of various hydrocarbons in anaerobic environments (as discussed in Chapter 1). Like the work presented in Chapters 2, 3 and Appendix A, the proposed work would improve predictive capabilities and further our understanding of metabolic processes.

Literature Cited

(1) Boethling, R. S.; Costanza, J. Domain of EPI suite biotransformation models. *SAR and QSAR in Environmental Research* **2010,** *21* (5-6), 415-443.

(2) Cramer, C. J. *Essentials of computational chemistry: theories and models*. 2nd ed.; John Wiley and Sons: West Sussex, England, Ltd, 2004; pp 596.

(3) Kniemeyer, O.; Musat, F.; Sievert, S. M.; Knittel, K.; Wilkes, H.; Blumenberg, M.; Michaelis, W.; Classen, A.; Bolm, C.; Joye, S. B.; Widdel, F. Anaerobic oxidation of short-chain hydrocarbons by marine sulphate-reducing bacteria. *Nature* **2007,** *449*, 898-U10.

(4) Duncan, K. E.; Gieg, L. M.; Parisi, V. A.; Tanner, R. S.; Green Tringe, S.; Bristow, J.; Suflita, J. M. Biocorrosive Thermophilic Microbial Communities in Alaskan North Slope Oil Facilities. *Environmental Science & Technology* **2009,** *43* (20), 7977-7984.

(5) Hratchian, H. P.; Schlegel, H. B. Finding minima, transition states, and following reaction pathways on ab initio potential energy surfaces. In *Theory and*

applications of computational chemistry: the first forty years, 1st ed.; Dykstra, C. E.; Frenking, G.; Kim, K.; Scuseria, G., Eds. Elsevier B.V.: Amsterdam, The Netherlands, 2005.

(6) Savage, K. N.; Krumholz, L. R.; Gieg, L. M.; Parisi, V. A.; Suflita, J. M.; Allen, J.; Philp, R. P.; Elshahed, M. S. Biodegradation of low-molecular-weight alkanes under mesophilic, sulfate-reducing conditions: metabolic intermediates and community patterns. *Fems Microbiology Ecology* **2010,** *72* (3), 485-495.

(7) Himo, F. C-C bond formation and cleavage in radical enzymes, a theoretical perspective. *Biochimica Et Biophysica Acta-Bioenergetics* **2005,** *1707* (1), 24-33.

(8) Bhat, K. L.; Brendley, W. H.; Bock, C. W. Thermodynamics and kinetics of MTBE degradation: A density functional theory study. *Soil & Sediment Contamination* **2004,** *13* (3), 267-281.

(9) Librando, V.; Alparone, A. Electronic polarizability as a predictor of biodegradation rates of dimethylnaphthalenes. An ab initio and density functional theory study. *Environmental Science & Technology* **2007,** *41* (5), 1646-1652.

(10) Levine, I. N. *Quantum Chemistry*. 5th ed.; Prentice Hall: Upper Saddle River, NJ, 2000; pp 739.

(11) Foresman, J. B.; Frisch, A. *Exploring chemistry with electronic structure methods*. 2nd ed.; Gaussian, Inc.: Pittsburgh, PA, 1993; p 296.

(12) Himo, F.; Siegbahn, P. E. M. Quantum chemical studies of radical-containing enzymes. *Chemical Reviews* **2003,** *103* (6), 2421-2456.

(13) Tirado-Rives, J.; Jorgensen, W. L. Performance of B3LYP density functional methods for a large set of organic molecules. *Journal of Chemical Theory and Computation* **2008,** *4* (2), 297-306.

(14) Himo, F. Catalytic mechanism of benzylsuccinate synthase, a theoretical study. *Journal of Physical Chemistry B* **2002,** *106* (31), 7688-7692.

(15) Himo, F.; Eriksson, L. A. Catalytic mechanism of pyruvate formate-lyase (PFL). A theoretical study. *Journal of the American Chemical Society* **1998,** *120* (44), 11449-11455.

(16) Gill, P. M. W.; Johnson, B. G.; Pople, J. A.; Frisch, M. J. The Performance of the Becke-Lee-Yang-Parr (B-LYP) Density Functional Theory with Various Basis Sets. *Chemical Physics Letters* **1992,** *197* (4-5), 499-505.

(17) Koch, W.; Holthansen, M. C. *A Chemist Guide to Density Functional Theory*. 2nd ed.; Wiley-VCH: Weinheim, Federal Republic of Germany, 2001.

(18) Bock, C. W.; Brendley, W. H.; Hamann, H.; Bhat, K. L. Formation of bis (chloromethyl) ether in the vapor phase: a computational investigation. *Journal of Molecular Structure-Theochem* **2002,** *619*, 207-228.

(19) Frisch, M. J. T., G. W.; Schlegel, H. B.; Scuseria, G. E.; Robb, M. A.; Cheeseman, J. R.; Scalmani, G.; Barone, V.; Mennucci, B.; Petersson, G. A.; Nakatsuji, H.; Caricato, M.; Li, X.; Hratchian, H. P.; Izmaylov, A. F.; Bloino, J.; Zheng, G.; Sonnenberg, J. L.; Hada, M.; Ehara, M.; Toyota, K.; Fukuda, R.; Hasegawa, J.; Ishida, M.; Nakajima, T.; Honda, Y.; Kitao, O.; Nakai, H.; Vreven, T.; Montgomery, Jr., J. A.; Peralta, J. E.; Ogliaro, F.; Bearpark, M.; Heyd, J. J.; Brothers, E.; Kudin, K. N.; Staroverov, V. N.; Kobayashi, R.; Normand, J.; Raghavachari, K.; Rendell, A.; Burant, J. C.; Iyengar, S. S.; Tomasi, J.; Cossi, M.; Rega, N.; Millam, N. J.; Klene, M.; Knox, J. E.; Cross, J. B.; Bakken, V.; Adamo, C.; Jaramillo, J.; Gomperts, R.; Stratmann, R. E.; Yazyev, O.; Austin, A. J.; Cammi, R.; Pomelli, C.; Ochterski, J. W.; Martin, R. L.; Morokuma, K.; Zakrzewski, V. G.; Voth, G. A.; Salvador, P.; Dannenberg, J. J.; Dapprich, S.; Daniels, A. D.; Farkas, Ö.; Foresman, J. B.; Ortiz, J. V.; Cioslowski, J.; Fox, D. J. *Gaussian 09, Revision A.1*, Gaussian, Inc.: Wallingford, CT, 2009.

(20) Irikura, K. K.; Johnson III, R. D.; Kacker, R. N.; Kessel, R. Uncertainties in scaling factors for ab initio vibrational zero-point energies. *Journal of Chemical Physics* **2009,** *130* (11), 114102-1-11.

(21) Olah, G. A.; Molnár, Á. *Hydrocarbon Chemistry*. 2nd ed.; Wiley-Interscience: 2003; pp 871.

(22) Reeburgh, W. S. Oceanic Methane Biogeochemistry. *Chemical Reviews* **2007,** *107* (2), 486-513.

(23) Caldwell, S. L.; Laidler, J. R.; Brewer, E. A.; Eberly, J. O.; Sandborgh, S. C.; Colwell, F. S. Anaerobic oxidation of methane: Mechanisms, bioenergetics, and the ecology of associated microorganisms. *Environmental Science & Technology* **2008,** *42* (18), 6791-6799.

(24) Schink, B. Energetics of syntrophic cooperation in methanogenic degradation. *Microbiology and Molecular Biology Reviews* **1997,** *61* (2), 262-280.

(25) Jackson, B. E.; McInerney, M. J. Anaerobic microbial metabolism can proceed close to thermodynamic limits. *Nature* **2002,** *415* (6870), 454-456.

Appendix A

Biodegradation Rate Determination by Direct Analysis of Sacrificed Microcosms

Abstract

Biodegradation rate measurements were collected from microcosms created in 40 mL volatile organics analysis (VOA) vials and 120 mL serum bottles. VOA vials were selected in order to streamline hydrocarbon measurements by purge and trap GC-MS analysis. Anaerobic conditions were maintained in the 40 mL VOA vials, containing only 2.5 g of sediment. Additionally, the use of 1,1,3-trimethylcyclohexane as a conserved marker in these systems was successful. Therefore, small systems such as those created in the 40 mL VOA vials may be a successful design strategy for studies focusing on non-volatile hydrocarbon concentrations in environmental samples. However, the experimental approach was not a successful method for the measurement of attenuation rates of aromatic compounds. The automation allowed by the use of 40 mL VOA vials did improve ease of analysis of hydrocarbon concentrations. However, the initial set up was time intensive as more vials need to be produced because the systems were sacrificed at each time point. In addition, reproducibility among the 40 mL VOA vials was not successful when dealing with such small measurements. The difficulties in obtaining refined and consistent data prevented the use of these results for model validation presented in Chapter 2. The 120 mL serum bottle microcosms served as comparisons for the output of the 40 mL VOA vial experiment. The demonstrated relationships between sulfate and substrate loss in the 120 mL serum bottle microcosms suggest that the depletion observed was a result of biological transformations.

Introduction

As discussed in Chapter 1, the presence of hydrocarbons in the environment is of concern for human and ecosystem health reasons (for recent examples see references (1, 2)). Anaerobic biodegradation of hydrocarbons has been demonstrated as a means of successfully mitigating contamination in natural environments (3-6). In favorable environments, intrinsic bioremediation can be faster, safer, and cheaper than traditional remediation strategies (7). Anaerobic biodegradation of hydrocarbons has also been shown to alter the chemical composition of fossil fuels, thereby decreasing the value of fuel sources (8-11). A great deal of characterization of the organisms and mechanisms capable of anaerobic hydrocarbon metabolism has been produced over the last 25 years (3, 4, 12-16). However, there is still a great need for reproducible, refined rate data to support this information.

Rate data are used to establish fate and transport models of chemicals in the environment. For example, the rate at which benzene, toluene, ethylbenzene and xylenes are attenuated in situ is of interest because of their toxicity (17). The rate at which anaerobic metabolism attenuates the concentrations of these priority pollutants affects the concentrations in aquifers and sediment and how far they migrate.

Rate data can also be used to demonstrate relationships between different types of data observed. For example, substrate loss rates can be correlated with terminal electron acceptor depletion rates, metabolite formation rates, and/or end product formation rates. The correlation of these values provides another line of evidence that biological processes are proceeding as predicted. On the other hand, when rates are not consistent, they

provide evidence of multiple pathways, confounding factors, or cometabolic activity. Confirming consistencies in rates is critical to elucidating biodegradation pathways (18).

This work in this appendix addresses the concerns associated with collecting rate data, by exploring if it is possible to improve the ease of collecting substrate loss measurements for multiple hydrocarbons. The research question addressed is: how can we design an experimental approach to help improve acquisition of rate data? In response to that question an experimental approach was designed using incubations for time series analysis that could be measured directly, and then sacrificed at each time point. The design makes use of an established automated method that measures hydrocarbon concentrations in sediment samples from microcosms, the purge and trap system (19, 20). Previously, samples for analysis were taken from incubations in 160 mL serum bottles. The bottles were frozen at the time point of interest and then thawed for analysis. A portion of the sediments were then transferred to a 40 mL VOA vial that was then placed in the automatic sample for purge and trap sample extraction and GC-MS analysis (20).

The smaller incubations used in this study were created directly in glass volatile organics analysis (VOA) vials and thus are referenced in this document as "40 mL VOA vial microcosms". The use of VOA vials as the container in which the microorganisms are established allows for automatic and direct analysis of the incubation. Eliminating the need to transfer sample reduces the time spent preparing for analysis, thus allowing the collection of more time points in a given period of time while using less sample and leaving less opportunity for hydrocarbon loss.

Another goal of this work is to establish a dataset with many time points to serve as a basis for developing and confirming rate models. In general, producing rate data for many substrates could provide a basis for decision making, model development, and helping understand general ideas about how these physical systems work. This work is specifically designed to validate the model presented in Chapter 2. To provide data for this purpose, and to validate the results generated from the 40 mL VOA vial microcosms, microcosms were also created using ten times more sediment than in the smaller systems. These microcosms are referred to in this document as "120 mL serum bottle microcosms". This amount is more consistent with traditional methods of collecting hydrocarbon loss data (e.g., references (20) and (19) use 50 g of sediment) and would therefore serve as a benchmark for the more novel approach.

The sediments studied in both sets of microcosms are taken from a site on which fumarate addition has been established as a potential mechanism of biodegradation through metabolite analysis during onsite push-pull studies (6, 21), onsite push-pull studies using deuterated substrates (22), and in bench-scale microcosms developed with site sediments (19, 21, 23). Site characteristics are discussed in reference (6). Knowing the potential mechanism of alkylbenzene biodegradation occurring in the sediments makes the rate data more useful as a validation dataset for the model presented in Chapter 2.

The objective of the first experiment is to collect biodegradation rate measurements from 40 mL VOA vial microcosms. Two types of freshwater media are examined to determine any difference in their effects on biodegradation rates. The objectives of the 120 mL serum bottle portion of the study is to provide a comparison to the output of the

40 mL VOA vial experiment and to serve as a potential source for metabolite analysis in future experiments (as a larger volume of supernatant than is provided in 40 mL VOA vials is required for metabolite analysis). In these larger microcosms, rates of biodegradation were collected for nine compounds including methyl-, ethyl-, and propylbenzenes.

Materials and Methods

40 mL VOA vial microcosms. Ft. Lupton, CO gas condensate-contaminated sediment was collected from a shallow aquifer overlying a natural gas field (site previously described by ref (6)). Collection procedures are described previously (20). An initial analysis revealed that 5 g of sediment in a 40 mL VOA vial resulted in hydrocarbon concentrations too high for the purge and trap GC-MS analysis; therefore, the 40 mL VOA vials used in this study contained 2.5 g of sediment and 7 mL of medium. Microcosms were prepared in a glove bag under an N_2/H_2 atmosphere. The sediment was well mixed prior to distribution into the vials. After preparation the headspace was exchanged (about 30 mL) to N_2/CO_2 (80:20) and was kept at an overpressure of 10-15 kPa**.** Treatments included the addition of 0.25 µL gasoline (American Petroleum Institute separator gasoline) and 1% Bushnell Haas broth (Fisher Scientific). For those VOA vials being treated with additional nitrate, 1g of Bushnell Haas per 100 mL was added (Bushnell Haas contains 0.2 g/L $MgSO_4$. 0.02 g/L $CaCl_2$, 1.0 g/L KH_2PO_4, 1.0 g/L K_2HPO_4, 1.0 g/L NH_4NO_3, 0.05 g/L $FeCl_3$). Controls contained no gasoline and general (freshwater) sulfate reducing bacteria (SRB) medium. SRB medium (per 100 mL) contained: 5 mL Pfennig I (10 g/L K_2HPO_4), 5 mL Pfennig II (6.6 g/L $MgCl_2$; 8.0 g/L NaCl; 8.0 g/L NH_4Cl; 1.0 g L $CaCl_2 \cdot 2H_2O$), 1 mL Wolin metals (0.5 g/L EDTA; 3.0 g/L

$MgSO_4 \cdot 6H_2O$; 0.5 g/L $MnSO_4 \cdot H_2O$; 1.0 g/L NaCl; 0.1 g/L $CaCl_2 \cdot 2H_2O$; 0.1 g/L $ZnSO_4 \cdot 7H_2O$; 0.1 g/L $FeSO_4 \cdot 7H_2O$; 0.01 g/L $CuSO_4 \cdot 7H_2O$; 0.01g/L $Na_2MoO_4 \cdot 2H_2O$; 0.01 g/L H_3BO_3, 0.005 g/L Na_2SeO_4; 0.003 g/L $NiCl_2 \cdot 6H_2O$), 1 mL Balch vitamins (2.0 mg/L biotin; 2.0 mg/L folic acid; 10.0 mg/L pyridoxine–HCl; 5.0 mg/L thiamine–HCl; 5.0 mg/L riboflavin; 5.0 mg/L nicotinic acid; 5.0 mg/L DL-calcium pantothenate; 0.1 mg/L vitamin B12; 5.0 mg/L p-aminobenzoic acid (PABA); 5.0 mg/L lipoic acid mercaptoethane; 5.0 mg/L methyl ester sulfonic acid (MESA)), 0.1 mL 0.1% resazurin, 0.35 g $NaHCO_3$, 2 mL of 2.5% cysteine sulfide ((24) and references therein).

Sterile controls (vials that were autoclaved) for each combination of these treatments were also tested. All incubations were maintained in the dark at room temperature. One vial was created for each type of analysis, at each time point, for each treatment, resulting in the creation of approximately 140 vials.

The vials prepared for hydrocarbon loss analysis were shipped to Roger C. Prince, ExxonMobil Biomedical Sciences Inc., in Annandale, NJ where the analysis was performed. Prior to shipment, all samples were preserved with hydrochloric acid to bring the system pH to 2. Hydrocarbons were analyzed at three time points: 0, 14, and 24 days. Hydrocarbon compounds were analyzed by purge and trap extraction and gas chromatography (Supelco Petrocol DH octyl column, 100 m x 0.25 mm ID fused silica) (20). The vials were loaded directly onto an OI Analytical 4552 water/soil autosampler. Pressurized inert gas injected directly into the microcosm mobilized the hydrocarbons, after which they were collected in a heated trap and directed to the gas chromatograph (25). Loss of hydrocarbon was measured in reference to a conserved internal marker, 1,1,3-trimethylcyclohexane (25).

Analyses of methane and sulfate concentrations were performed at each time point by gas chromatography and ion chromatography, respectively. Sulfate and methane concentrations were analyzed at four time points: 0, 15, 24 and 57 days. These methods are described by Townsend et al. (2003) (5).

120 mL Serum bottle microcosms. Incubations were prepared in a glove bag as described above with the following exceptions. These microcosms were prepared in 120 mL serum bottles with 25 g of Ft. Lupton sediment and 38 mL of general sulfate-reducing bacteria medium (10 mM sodium sulfate). There was no treatment with Bushnell Haas broth in these bottles. All bottles were prepared in triplicate with duplicate sterile controls. Four unamended microcosms were prepared, otherwise the bottles were amended with 2 μL of one of the following substrates: toluene, ethylbenzene, propylbenzene, m-xylene, o-xylene, p-xylene, 1,3,5-trimethylbenzene, 1,2,4-trimethylbenzene, or 1-ethyl-3-methylbenzene. Changes in sulfate and hydrocarbon concentrations were monitored on days 0, 14, 50, and 100 by ion chromatography (5) and GC–MS analysis, respectively (21).

All bottles and vials were amended with resazurin (0.1% by volume) which was used as an indicator of redox conditions.

Results and Discussion

40 mL VOA vial microcosms. Results from the Ft. Lupton 40 mL VOA vial sediment biodegradation studies are shown in Figures A.1 through A.5. Figures A.1 and A.2 show the levels of sulfate and methane monitored in the systems, respectively. Two types of freshwater media were examined to determine any difference in their effects on biodegradation rates. All microcosms with viable microorganisms and no Bushnell Haas

medium showed production of methane over time, with or without the gasoline amendment. It is likely that the high concentrations of nitrate in Bushnell Haas inhibit methanogenic activity, and that sulfate-reducing activity was inhibited by low levels of sulfate.

Therefore, while this method of setting up incubations may work for analysis of non-volatile compounds or for analysis of very uniform sediment with large amounts of

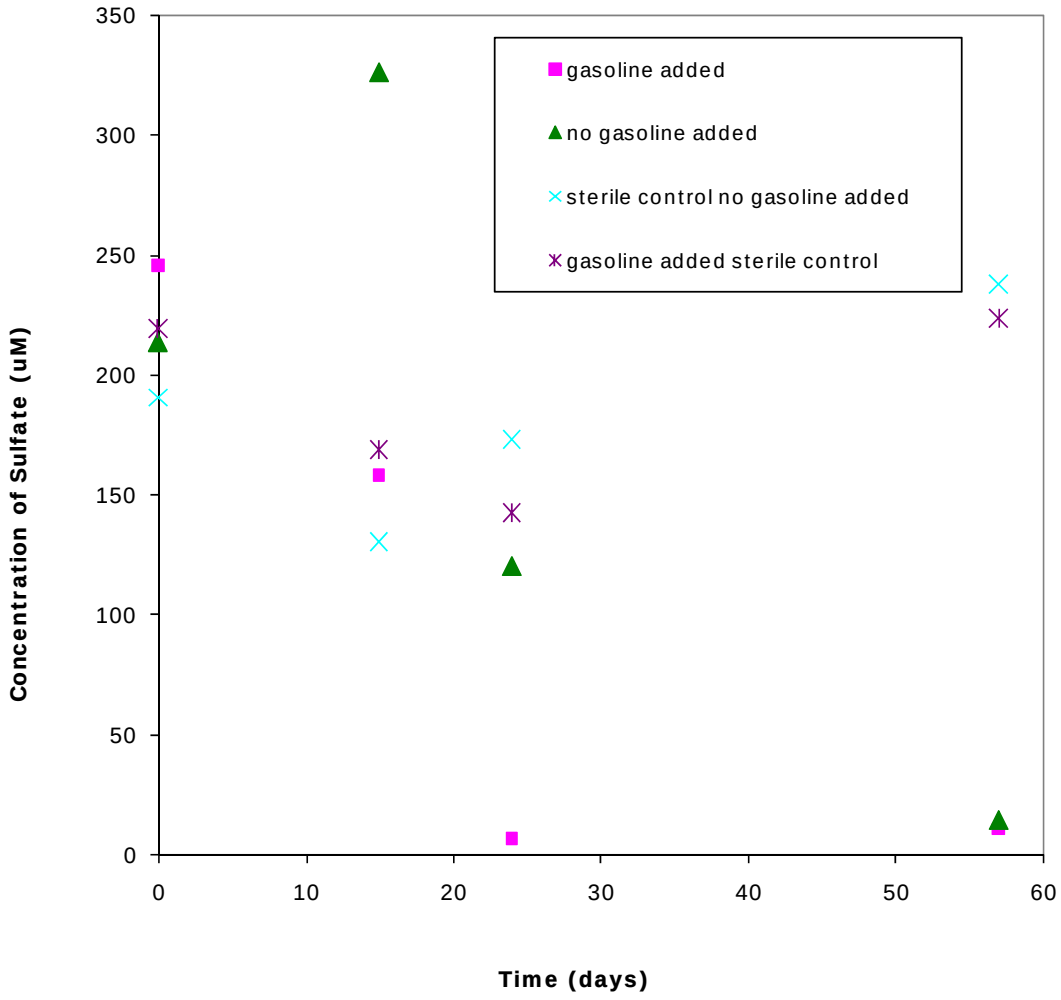

Figure A.1 Concentrations of sulfate (µM) over time in 40 mL VOA vial microcosms containing general SRB freshwater medium (± 0.25 µL gasoline).

associated groundwater; this was not an ideal set up for analysis of aromatic compounds with sediments alone. Concentrations of aromatic compounds varied greatly from one vial to another, likely as a result of the small sample size and the volatility of the substrates in the sediment. Some of the vials did not contain aromatic compounds in concentrations higher than detection limits on day 0, even those that were supposed to contain gasoline amendments. This point also demonstrates the difficulty of amending the VOA vials with only 0.25 µL of gasoline. It is unlikely that the vials received equal

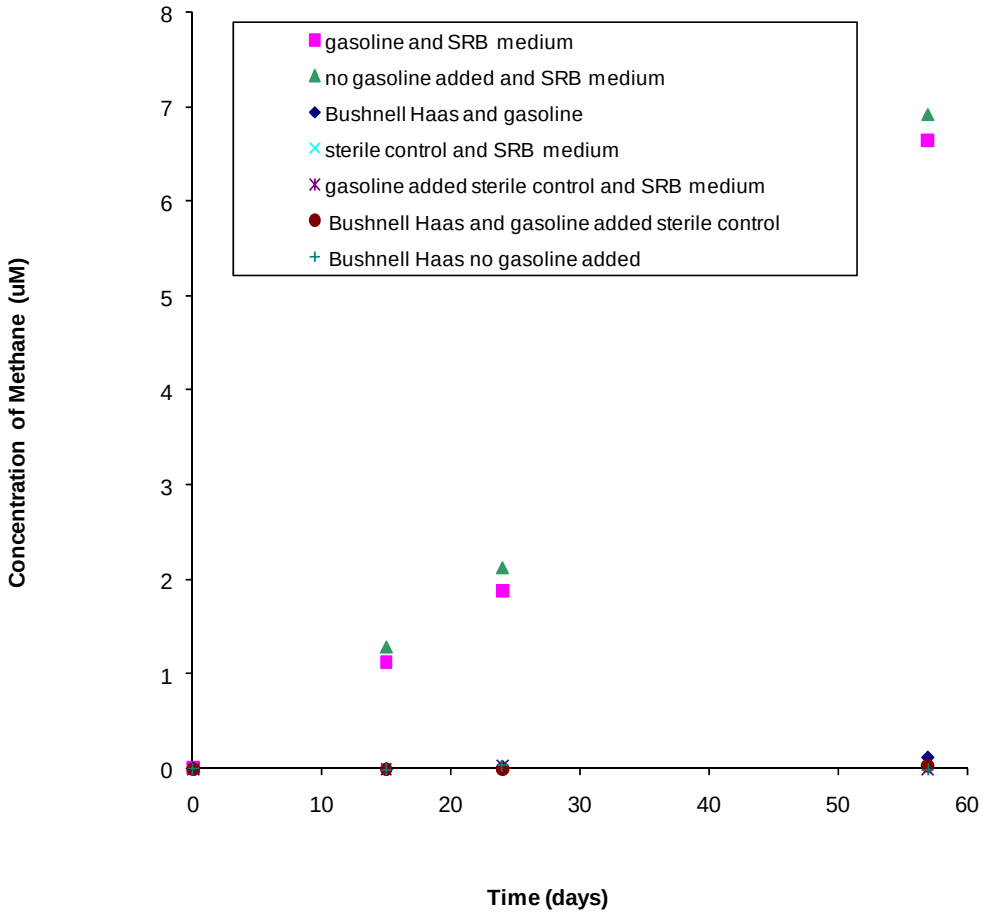

Figure A.2 Concentrations of methane (µM) over time in 40 mL VOA vial microcosms containing Bushnell Haas medium and general SRB freshwater medium (± 0.25 µL gasoline).

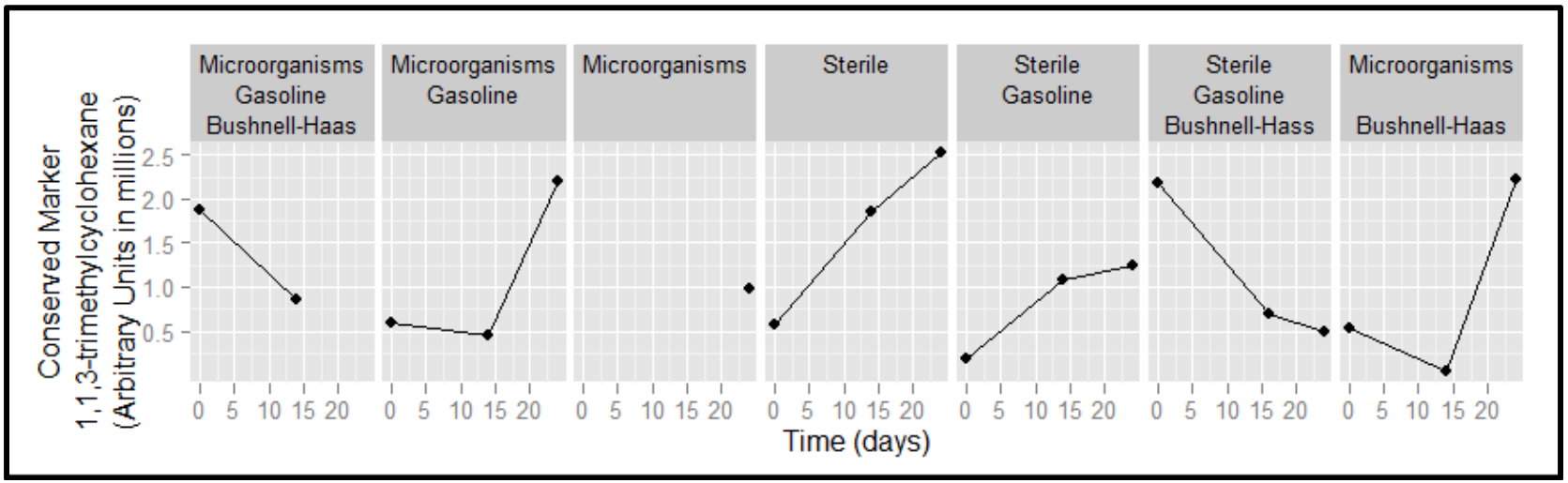

Figure A.3 Amounts of conserved marker (1,1,3-trimethylcyclohexane) in the VOA vial microcosms for days 0, 14 and 24.

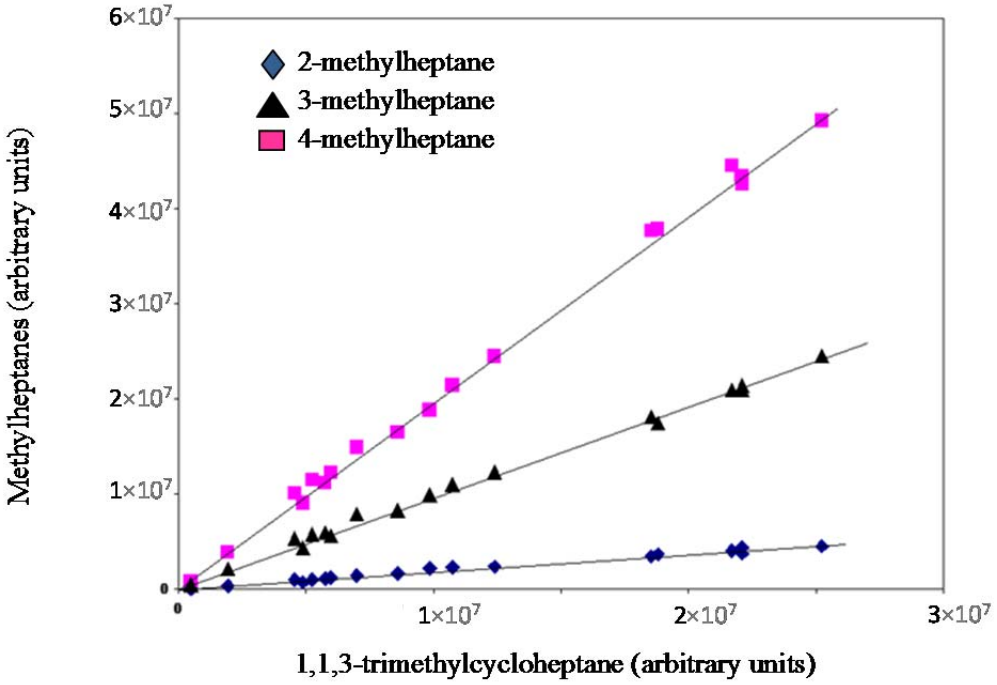

Figure A.4 Relationship between amounts of the conserved marker and methylheptanes in the VOA vial microcosms for days 0, 14 and 24 (created by Roger Prince).

amounts of gasoline amendments; however, using a higher concentration was not an option as it would likely have been toxic to the microorganisms.

Microorganisms in the sediment were likely converting substrates via sulfate-reduction and methanogenesis in vials with viable cultures, as was evident from the measurements of each. The color of the solution in the vials (and the serum bottles) remained clear throughout the experiments, not showing any signs that the resasurin had been significantly oxidized. However, which hydrocarbons were undergoing biodegradation could not be determined. Because of the challenges of replicating the experimental conditions in each microcosm (i.e., in 40 mL VOA vials) and the loss of some data from vials that were discarded by the machine, the data were not used to

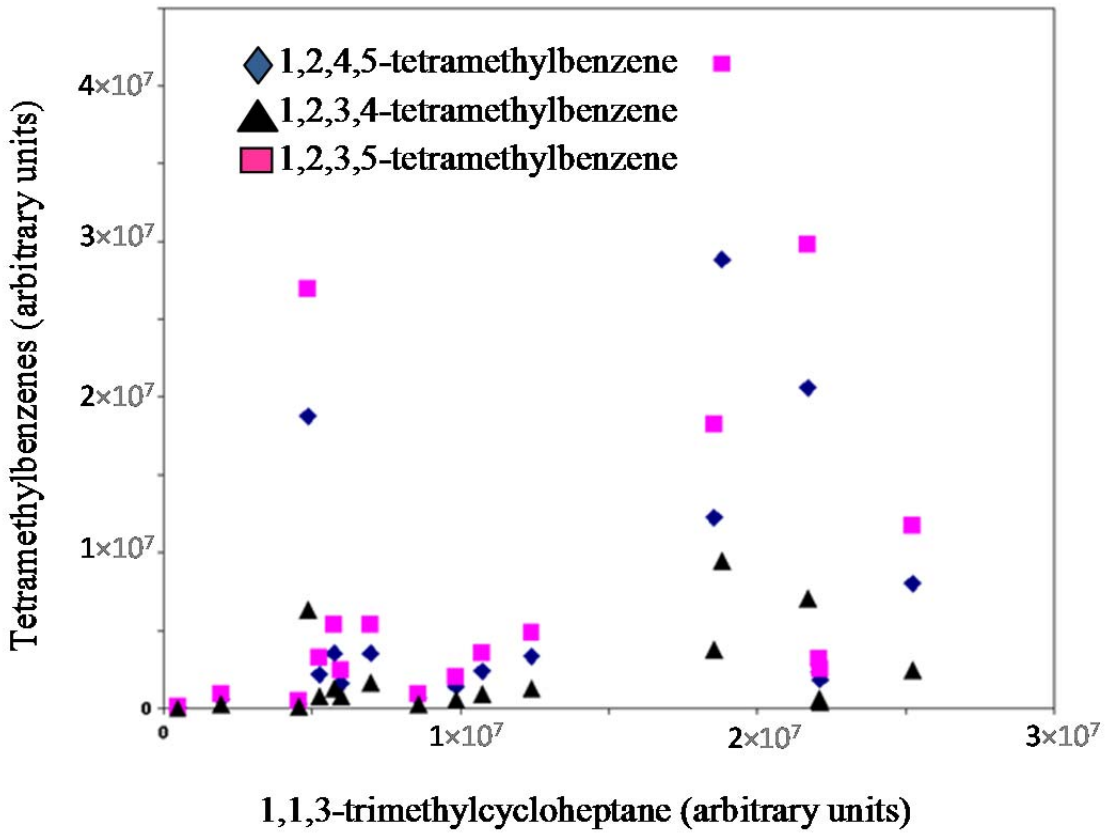

Figure A.5 Relationship between amounts of the conserved marker and tetramethylbenzenes in the VOA vial microcosms for days 0, 14 and 24 (created by Roger Prince).

validate any models. The validation dataset needed to be based on data collected from systems that could be more reliably replicated, and scaling down to such a small size resulted in high variability and low reproducibility. Since the experimental design did not work as planned, hydrocarbon analysis of the samples at day 54 was not completed.

120 mL Serum bottle microcosms. Sulfate and substrate loss values from the 120 mL serum bottle microcosms are shown in Figures A.6 and A.7, respectively. Sulfate concentrations in incubations containing toluene and m-xylene decreased an average of 36% and 30%, respectively, after 54 days (see Figure A.6). The results presented in Figure A.7 show that after approximately 50 days, toluene and m-xylene concentrations

decreased to values below detection limits while the concentrations in the sterile controls had not altered significantly. Figure A.7 also shows that the same is true for 1,3,5-trimethylbenzene and o-xylene after approximately 100 days.

The results of the analyses demonstrate that hydrocarbons degraded in an order consistent with that observed in the Prince and Suflita (2007) analysis (20), however at a slower rate. This could be due to the fact that the sediments had been stored (at approximately 4 degrees C) in the time between studies rather than being freshly obtained. Or, because these systems contained half of the amount of sediment that was used in the previous study.

By day 52, toluene and m-xylene were not detected in the microcosms. Sulfate loss was calculated and adjusted for loss in sterile controls. A stoichiometric comparison of these values suggests that up to 74% of toluene depletion and 79% of m-xylene depletion could be attributed to sulfate loss. Calculations were based on a total volume of liquid (in the microcosm) of 38 mL. The total sample volume of the sulfate samples was 0.5 mL(consisting of 10 μL supernatant and 490 μL of nano pure water). Some sulfate could have been incorporated as biomass, therefore it was not expected that hydrocarbon loss would account for 100% of the sulfate loss. The results show clear evidence of substrate loss in correlation with sulfate depletion. Because of this evidence, these microcosms have the potential to be used for metabolite analysis in the future.

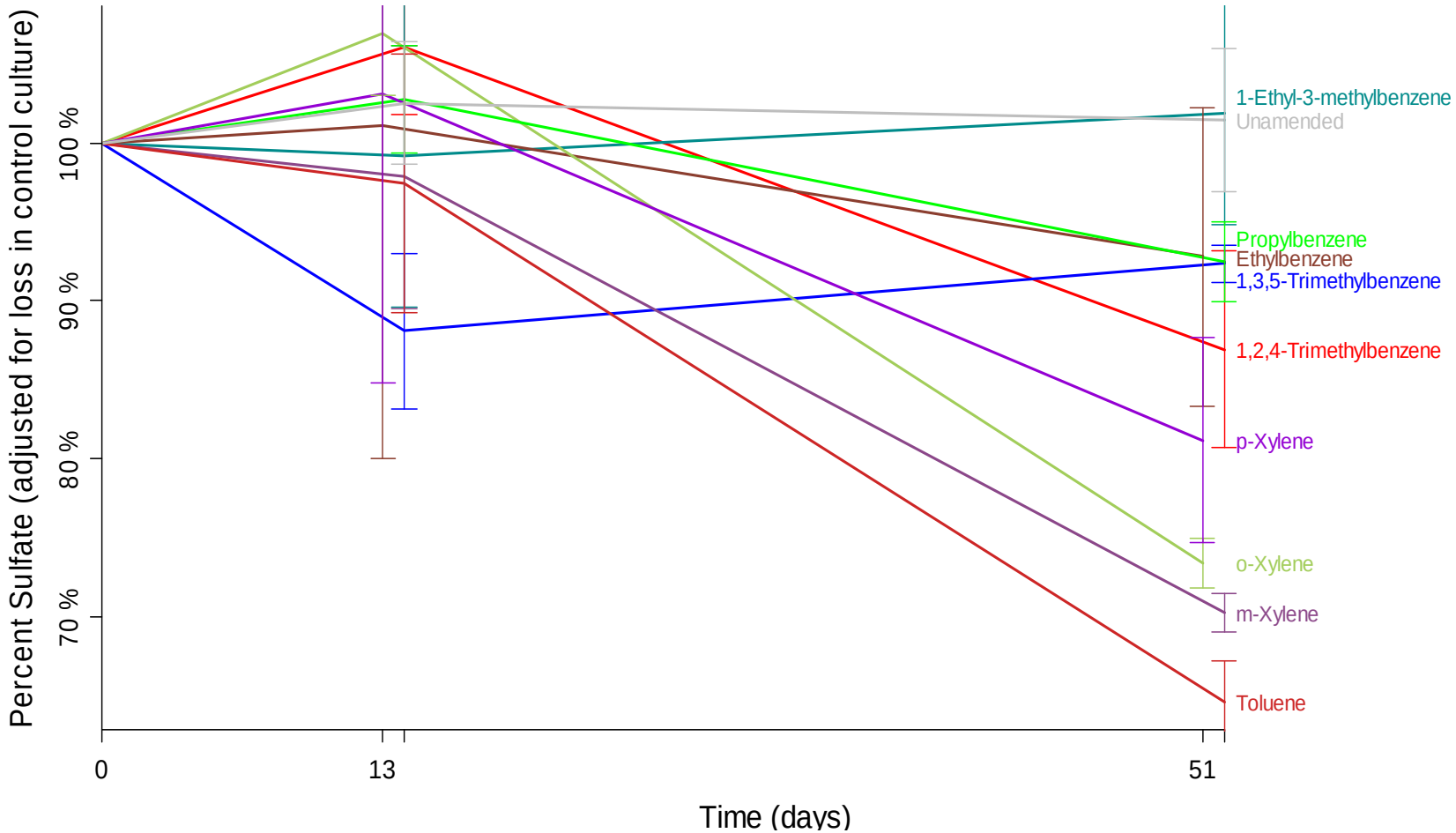

Figure A.6 Percent sulfate in Ft. Lupton sediment microcosms (120 mL serum bottles) over time. Bottles were amended with 2 µL of the substrate shown. Values are averages of triplicate systems and are corrected for any sulfate loss in sterile controls.

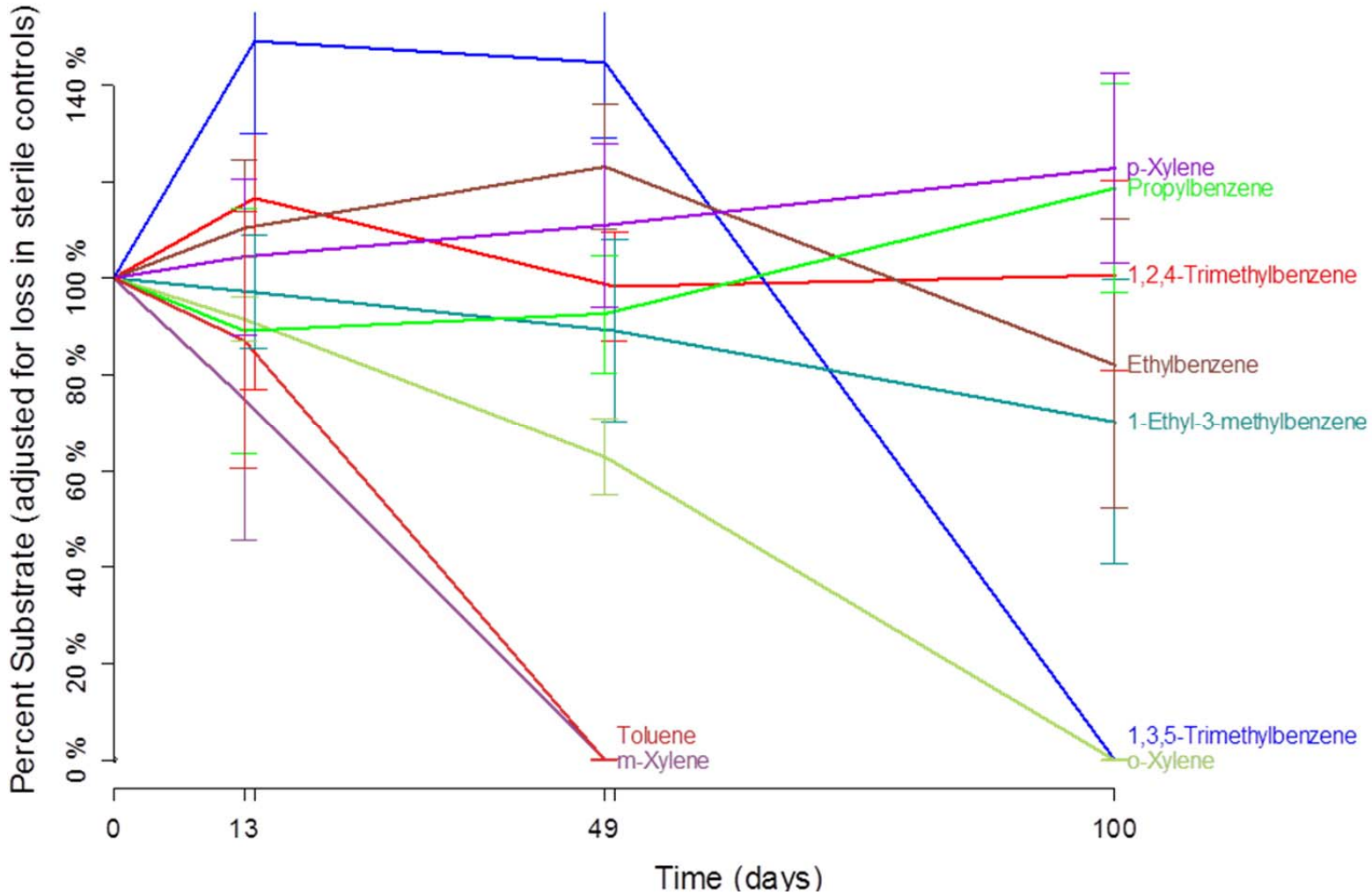

Figure A.7 Percent substrate in Ft. Lupton sediment microcosms (120 mL serum bottles) over time. Bottles were amended with 2 µL of the substrate shown. Values are averages of triplicate systems and are corrected for any sulfate loss in sterile controls.

In conclusion, the difficulties in obtaining refined and consistent data prevented the use of these results for model validation presented in Chapter 2. However, the results suggest that there are some applications in which there is a potential for using this method in the acquisition of reproducible, refined rate data. Even though the quantification of hydrocarbon loss was difficult, there was clear evidence that anaerobic metabolism was occurring in the vials. Thus, anaerobic conditions were able to be maintained in the 40 mL VOA vials, containing only 2.5 g of sediment. Additionally, the use of 1,1,3-trimethylcyclohexane as a conserved marker in these systems showed potential (see Figure A.4). Therefore, small systems such as those created in the 40 mL VOA vials may be a successful design strategy for studies focusing on non-volatile hydrocarbon concentrations in environmental samples. This method may also be a successful means of quickly obtaining refined rate measurements of attenuation in situ.

Literature Cited

(1) Committee on the Effects of the Deepwater Horizon Mississippi Canyon-252 Oil Spill on Ecosystem Services in the Gulf of, M.; National Research, C., *Approaches for Ecosystem Services Valuation for the Gulf of Mexico After the Deepwater Horizon Oil Spill: Interim Report*. The National Academies Press: 2012.

(2) Institute of Medicine, *Assessing the Effects of the Gulf of Mexico Oil Spill on Human Health: A Summary of the June 2010 Workshop*. The National Academies Press: 2010.

(3) Widdel, F.; Rabus, R. Anaerobic biodegradation of saturated and aromatic hydrocarbons. *Current Opinion in Biotechnology* **2001,** *12* (3), 259-276.

(4) Suflita, J. M.; Davidova, I. A.; Gieg, L. M.; Nanny, M.; Prince, R. C. Anaerobic hydrocarbon biodegradation and the prospects for microbial enhanced energy production. In *Petroleum Biotechnology: Developments and Perspectives*, 2004; Vol. 151, pp 283-305.

(5) Townsend, G. T.; Prince, R. C.; Suflita, J. M. Anaerobic oxidation of crude oil hydrocarbons by the resident microorganisms of a contaminated anoxic aquifer. *Environmental Science & Technology* **2003,** *37* (22), 5213-5218.

(6) Gieg, L. M.; Kolhatkar, R. V.; McInerney, M. J.; Tanner, R. S.; Harris, S. H.; Sublette, K. L.; Suflita, J. M. Intrinsic bioremediation of petroleum hydrocarbons in a gas condensate-contaminate aquifer. *Environmental Science & Technology* **1999,** *33* (15), 2550-2560.

(7) Committee on In Situ, Bioremediation, National Research Council, *In Situ Bioremediation:When Does it Work?* The National Academies Press: 1993.

(8) Head, I. M.; Jones, D. M.; Larter, S. R. Biological activity in the deep subsurface and the origin of heavy oil. *Nature* **2003,** *426* (6964), 344-352.

(9) Aitken, C. M.; Jones, D. M.; Larter, S. R. Anaerobic hydrocarbon biodegradation in deep subsurface oil reservoirs. *Nature* **2004,** *431* (7006), 291-294.

(10) Rabus, R.; Wilkes, H.; Aeckersberg, F.; Zengler, K.; Willsch, H.; Widdel, F. Anaerobic degradation of alkylbenzenes in crude oil .1. Isolation and characterization of alkylbenzene-degrading sulfate-reducing and denitrifying bacteria. *Abstracts of Papers of the American Chemical Society* **1996,** *211*, 5-GEOC.

(11) Wilkes, H.; Rabus, R.; Willsch, H.; Aeckersberg, F.; Zengler, K.; Widdel, F. Anaerobic degradation of alkylbenzenes in crude oil .2. Changes of oil composition upon incubation with sulfate-reducing and denitrifying bacteria. *Abstracts of Papers of the American Chemical Society* **1996,** *211*, 6-GEOC.

(12) Spormann, A. M.; Widdel, F. Metabolism of alkylbenzenes, alkanes, and other hydrocarbons in anaerobic bacteria. *Biodegradation* **2000,** *11* (2-3), 85-105.

(13) Heider, J. Adding handles to unhandy substrates: anaerobic hydrocarbon activation mechanisms. *Current Opinion in Chemical Biology* **2007,** *11* (2), 188-194.

(14) Gieg, L. M.; Suflita, J. M. Metabolic indicators of anaerobic hydrocarbon biodegradation in petroleum-laden environments. In *Petroleum Microbiology*, 2005; pp 337-356.

(15) Mbadinga, S. M.; Li-Ying, W.; Lei, Z.; Jin-Feng, L.; Ji-Dong, G.; Bo-Zhong, M. Microbial communities involved in anaerobic degradation of alkanes. *International Biodeterioration & Biodegradation* **2011,** *65* (1), 1-13.

(16) Rabus, R. F. Biodegradation of hydrocarbons under anoxic conditions. *Petroleum Microbiology* **2005**, 277-299.

(17) U.S. Environmental Protection Agency Drinking Water Contaminants. http://water.epa.gov/drink/contaminants/index.cfm#Organic (accessed March 2012).

(18) Wackett, L. P.; Hershberger, C. D. *Biocatalysis and biodegradation: microbial transformation of organic compounds*. ASM Press: Washington, DC, 2001.

(19) Townsend, G. T.; Prince, R. C.; Suflita, J. M. Anaerobic biodegradation of alicyclic constituents of gasoline and natural gas condensate by bacteria from an anoxic aquifer. *Fems Microbiology Ecology* **2004,** *49* (1), 129-135.

(20) Prince, R. C.; Suflita, J. M. Anaerobic biodegradation of natural gas condensate can be stimulated by the addition of gasoline. *Biodegradation* **2007,** *18* (4), 515-523.

(21) Elshahed, M. S.; Gieg, L. M.; McInerney, M. J.; Suflita, J. M. Signature metabolites attesting to the in situ attenuation of alkylbenzenes in anaerobic environments. *Environmental Science & Technology* **2001,** *35* (4), 682-689.

(22) Gieg, L. M.; Alumbaugh, R. E.; Field, J. A.; Jones, J.; Istok, J. D.; Suflita, J. M. Assessing *in situ* rates of anaerobic hydrocarbon bioremediation. *Microbial Biotechnology* **2009,** 2, 222-233.

(23) Rios-Hernandez, L. A.; Gieg, L. M.; Suflita, J. M. Biodegradation of an alicyclic hydrocarbon by a sulfate-reducing enrichment from a gas condensate-contaminated aquifer. *Applied and Environmental Microbiology* **2003,** *69* (1), 434-443.

(24) Golby, S.; Ceri, H.; Gieg, L. M.; Chatterjee, I.; Marques, L. L. R.; Turner, R. J. Evaluation of microbial biofilm communities from an Alberta oil sands tailings pond. *Fems Microbial Ecology* 2012, 29 (1), 240-250.

(25) Prince, R. C.; Douglas, G. S. Quantification of hydrocarbon biodegradation using internal markers. In *Manual of Soil Analysis : Monitoring and Assessing Soil Bioremediation*, Margesin, R.; Schinner, F., Eds. Springer-Verlag: Berlin, Germany, 2005; pp 179-188.

Appendix B

Definitions of Computational Methods Used or Proposed for Use in this Dissertation

Summary

Work in presented in Chapters 2 and 3 used density functional theory to located peaks, saddle points and reaction paths of interest to the fumarate addition mechanism on the potential energy surface. Table B.1 includes the definitions of the terms associated with these methods.

Table B.1 Definitions of Computational Methods Used or Proposed for Use in this Dissertation.

Symbol or Notation	Name	Definition and References	References
B3LYP	Becke-style 3-parameter density functional theory using the Yee, Lang, and Parr correlation functional	A hybrid functional "…which define[s] the exchange functional as a linear combination of Hartree-Fock, local and gradient-corrected exchange terms" (Foresman and Frisch 1993, page 119 (1); operationally defined in Cramer 2004, Page 267 (2)).	(2-5)
6-31G	Double split valence basis set 6-31G	"…[M]athematical representation of the molecular orbitals within a molecule. The larger basis sets impose fewer constraints on electrons and more accurately approximate exact molecular orbitals." Foresman and Frisch 1993, Page 9 (1).	(1, 6)
6-311G	Triple split valence basis set 6-311G	"..[U]se three sizes of contracted functions for each orbital-type" rather than two. (Foresman and Frisch 1993, page 98 (1))	(1, 6)
+	Diffuse function	Diffuse functions are "…large-size versions of s- and p-type functions[…]They allow orbitals to occupy a larger region of space. Basis sets with diffuse functions are important for systems where electrons are relatively far from the nucleus…" (Foresman and Frisch 1993, page 99 (1))	(2, 3)

Symbol or Notation	Name	Definition and References	References
d,p	Polarized basis set	Adds "…orbitals with angular momentum beyond what is required for the ground state to the description of each atom." (d,p) specifically"...[A]dds p functions to hydrogen atoms in addition to the d functions on heavier atoms" (Foresman and Frisch, page 98 (1))	(1-3)
U	Unrestricted	Indicated the use of open shell model calculations. These are used when modeling systems with unequal numbers of spin up and spin down electrons. This option is required for modeling homolytic atom abstraction (Foresman 1993, page 10 (1))	(1)
IRC	Intrinsic reaction coordinate	Intrinsic reaction coordinate calculations generate a path on the PES following the "…steepest descent downhill from the [transition state structures] to reactant and product PES minima." (Hratchian and Schlegel 2005, page 230 (7)). "…Following the [IRC] will lead, in each direction, to the ultimate minimum energy structures connected by the TS structure." (Cramer 2004, page 523 (2)). Units: "…mass-weighted Cartesian coordinates are simply the Cartesian coordinates scaled by the square root of the atomic mass. When IRC is in mass-weighted coordinates,"…the [IRC] is also the path that follows the steepest gradient at every point." (Cramer 2004, page 522 (2)).	(2, 7)
QST3	quadratic synchronous transit calculation with three staring geometries entered in the input, the reactants, the products, and an initial guess for the transition state structure	"[An] interpolation method using structural information from the reactant and product minima…" to locate a saddle point (Hratchian and Schlegel 2005, page 221(7)).. "The maximum point on the QST pathway is located and serves as the QST estimate for the TS." (Hratchian and Schlegel 2005, page 222(7)).	(1, 7)

Literature Cited

(1) Foresman, J. B.; Frisch, A. *Exploring chemistry with electronic structure methods*. 2nd ed.; Gaussian, Inc.: Pittsburgh, PA, 1993; pp 296.

(2) Cramer, C. J. *Essentials of computational chemistry: theories and models*. 2nd ed.; John Wiley and Sons: West Sussex, England, Ltd, 2004; pp 596.

(3) Levine, I. N. *Quantum Chemistry*. 5th ed.; Prentice Hall: Upper Saddle River, NJ, 2000; pp 739.

(4) Becke, A. D. Density-functional thermochemistry. III. The role of exact exchange. *Journal of Chemical Physics* **1993,** *98* (7), 5648-5652.

(5) Becke, A. D. A new mixing of Hartree-Fock and local density-functional theories. *Journal of Chemical Physics* **1993,** *98* (2), 1372-1377.

(6) Hehre, W. J.; Random, L.; Schleyer, P. v. R.; Pople, J. A. *Ab Initio Molecular Orbital Theory*. 2nd ed.; Wiley: New York, 1986; pp 548.

(7) Hratchian, H. P.; Schlegel, H. B. Finding minima, transition states, and following reaction pathways on ab initio potential energy surfaces. In *Theory and applications of computational chemistry: the first forty years*, 1st ed.; Dykstra, C. E.; Frenking, G.; Kim, K.; Scuseria, G., Eds. Elsevier B.V.: Amsterdam, The Netherlands, 2005.

Appendix C

Definitions of Computational Methods Used or Proposed for Use in this Dissertation

Table C.1 Strategy for locating transition state structures.

Activity	Purpose
Guess or use another program to find an initial structure (e.g., QST, molecular mechanics, scans)	To get a starting geometry
Run frequency calculations on Gaussian DFT uB3LYP/6-31+g(d,p)	To check that converges properly; one imaginary frequency
Reaction path following (IRC)	To be sure transition state is connecting the correct reactants and products

Table C.2 Computational chemistry software and their uses.

Software	Use
Gaussian	Computational software
GaussView	Geometry and results visualization software
WinSCP	For transferring files from OSCER supercomputers and local machines
Putty	Software used to interface with the OSCER supercomputers

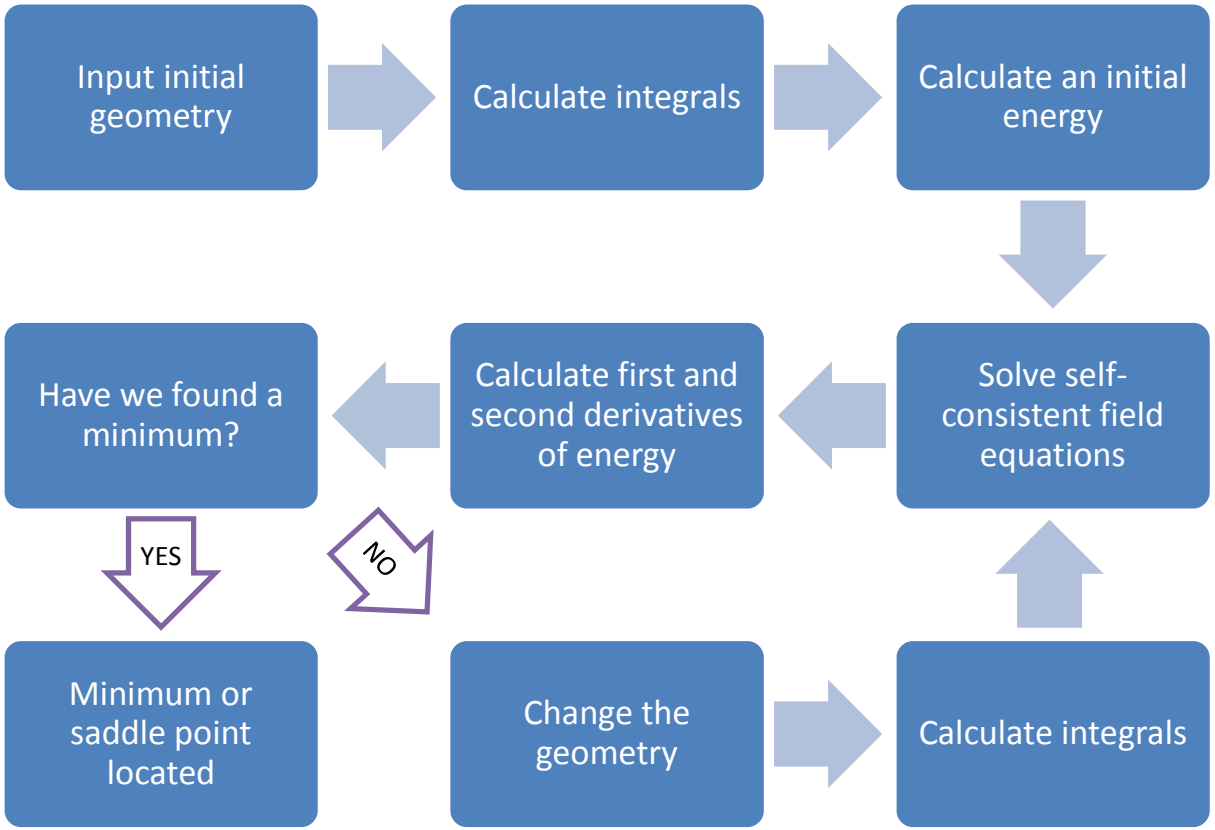

Figure C.1 Flow chart of the optimization procedure for locating equilibrium geometries of minima and transition states, adapted from SHODOR resources (1).

Table C.3 Specific details of how each calculation type was performed in this dissertation. Further information about options can be found in Foresman and Frisch, 1993 (2).

Calculation Type	Example Route Section Input	Notes
Geometry optimization	# opt ub3lyp/6-31+g(d,p) geom=connectivity	
Frequency calculation	# freq ub3lyp/6-31+g(d,p) geom=connectivity	Optimization and frequency calculations can be combined as shown in the next row.
Spin Density	# opt freq ub3lyp/6-31+g(d,p) geom=connectivity density=current	'density=current' signals that the spin density should be calculated using the specified method rather than the default.
QST2	# opt=(calcall,qst2) freq ub3lyp/6-31+g(d,p) geom=connectivity	Requires two input structures. QST3 requires 3 input structures.
TS	# opt=(calcall,ts,verytight,maxcycle=1000) freq ub3lyp/6-31+g(d,p) geom=connectivity int=ultrafine	
IRC	#irc=(maxpoints=40,calcfc,stepsize=1) ub3lyp/6-31+g(d,p) geom=connectivity int=ultrafine	

Literature Cited

(1) Choice of Theoretical Method. http://www.shodor.org/ncsi-1.0/ccce/Lesson3/3_Choice_Lectures.pdf (accessed March 2012).

(2) Foresman, J. B.; Frisch, A. *Exploring chemistry with electronic structure methods*. 2nd ed.; Gaussian, Inc.: Pittsburgh, PA, 1993; pp 296.